



MINISTÉRIO DA EDUCAÇÃO
Universidade Federal de Alfenas. Unifal-MG
Rua Gabriel Monteiro da Silva, 714 – Alfenas/MG – CEP 37130-000
Fone: (35) 3299-1000. Fax: (35) 3299-1063



**Biomarkers of anti-inflammatory and neuroprotective activity investigated by
untargeted UPLC-ESI-QTOF-MS metabolomics analyses**

Post-graduate: Albert Katchborian Neto

Advisor: PhD. Daniela Aparecida Chagas de Paula

Co-advisor: PhD. Ana Cláudia Chagas de Paula Ladvoat

Alfenas/MG

2020

ALBERT KATCHBORIAN NETO

**Biomarkers of anti-inflammatory and neuroprotective activity investigated by
untargeted UPLC-ESI-QTOF-MS metabolomics analyses**

The dissertation as part of the requirements for
obtaining a master's degree in Chemistry by the
Federal University of Minas Gerais.

Area of concentration: Organic Chemistry

Advisor: PhD. Daniela A. Chagas de Paula

Co-advisor: PhD. Ana Cláudia C. P. Ladvocat

Alfenas/MG

2020

Dados Internacionais de Catalogação-na-Publicação
(CIP) Sistema de Bibliotecas da Universidade Federal de
Alfenas

Katchborian Neto, Albert.

K19b Biomarkers of anti-inflammatory and neuroprotective activity investigated by untargeted UPLC-ESI-QTOF-MS metabolomics analyses/ Albert Katchborian Neto -- Alfenas/MG, 2020.

123f. il. --

Orientadora: Daniela A. Chagas de Paula.

Dissertação (Mestrado em Química) - Universidade Federal de Alfenas, 2020.

Bibliografia.

1. Ocotea. 2. Banisteriopsis. 3. Doença de Parkinson. 4. Receptores de Lipopolissacarídeos. 5. Prostaglandinas e Sintéticas.
I. Paula, Daniela A. Chagas de. II. Título.

CDD-547

Ficha Catalográfica elaborada por Fátima dos Reis
Goiatá Bibliotecária-Documentalista CRB/6-425

ALBERT KATCHBORIAN NETO

**Biomarkers of anti-inflammatory and neuroprotective activity by untargeted
UPLC-ESI-QTOF-MS metabolomic analyses**

A Banca examinadora abaixo-assinada aprova a Dissertação apresentada como parte dos requisitos para a obtenção do título de Mestre em Química pela Universidade Federal de Alfenas. Área de concentração: Química Orgânica.

Aprovado em: 15 de maio de 2020

Profa. Dra. Daniela Aparecida Chagas de Paula
Instituição: Universidade Federal de Alfenas

Profa. Dra. Maria Elvira Poleti Martucci
Instituição: Universidade Federal de Ouro Preto

Profa. Dra. Rejane Barbosa de Oliveira
Instituição: Universidade Tecnológica Federal do Paraná



Documento assinado eletronicamente por **Daniela Aparecida Chagas de Paula, Professor do Magistério Superior**, em 15/05/2020, às 17:18, conforme horário oficial de Brasília, com fundamento no art. 6º, § 1º, do



[Decreto nº 8.539, de 8 de outubro de 2015.](#)

Documento assinado eletronicamente por **Rejane Barbosa de Oliveira, Usuário Externo**, em 15/05/2020, às 17:30, conforme horário oficial de Brasília, com fundamento no art. 6º, § 1º, do [Decreto nº 8.539, de 8 de outubro de 2015.](#)



Documento assinado eletronicamente por **Maria Elvira Poleti Martucci, Usuário Externo**, em 15/05/2020, às 17:30, conforme horário oficial de Brasília, com fundamento no art. 6º, § 1º, do [Decreto nº 8.539, de 8 de outubro de 2015.](#)



A autenticidade deste documento pode ser conferida no site <https://sei.unifal->

mg.edu.br/sei/controlador_externo.php?acao=documento_conferir&id_orgao_acesso_externo=0, informando o código verificador **0298947** e o código CRC **4B8DEB14**.

ACKNOWLEDGEMENT

Firstly, I want to thank God and the universe to put myself on a privilege position in this world. I want to thank so much my parents (Francisca and João Katchborian) for all the care, love and effort they have given to make possible to me reach this post-graduate academic stage. Also, I am so thank-full for still having my grandad among us, which gave me power and motivation for going forward. I would like to give a special thanks for my girlfriend (Bruna Pereira Matos) for always giving me the support, the love and the encouragement that I needed through these days of work.

I want to thank so much the professors of the LFQM, PhD. Marisi Gomes Soares and PhD. Danielle Ferreira Dias for all the care, knowledge and friendship built and transmitted. I want to also thank Jonas Cruz, besides the long friendship, the support in the quantitative analyses of PGE2 in this work. Also, I want to thanks all my colleagues from the LFQM for being available to help me out always when I needed. Especially the PhD. Karen Nicácio for the collaborations and classes along the year, and also my friends, Luiz Paulo Belchior and Miller Ferreira for the friendship built, the moments shared, and all empathy developed, together with all other friends from the Lab. Moreover, I want to thanks all friend out of the Lab that was essential to complement not only academic but personal knowledge as a human being.

I want to thanks also the Federal University of Alfenas for allowing me to grow as a researcher and all the teachers of the PPGQ that somehow were accurate in their mission of transmitting knowledge. Also, I want to thank so much the employees of the UNIFAL that are less seen but are so important for our work to be in a clean and comfortable place. Furthermore, I thank the FINEP and the funding agencies, CAPES, CNPq and FAPEMIG for financial support for always keeping the scholarship on time, which is so important to keep the calmness and the necessary focus on the academic research. As this work was supported by the CAPES - Finance Code 001, CNPq - Grant number 427497/2018-3 and FAPEMIG - Grants numbers: APQ-02353-17, APQ-00443-18, APQ-01954-18 and APQ 03701-17. Additional, I am grateful to J.R. Nicolai and W. Dias from the Santo Daime Church for the generous donation of the typical Ayahuasca beverage. And also thanks C.M.C. Maranduba for his valuable contribution, and PhD. F. B. Da Costa (AsterBioChem) for access to SIMCA P⁺ software.

Special thanks to the Herbariums CESJ herbarium – Federal University of Juiz de Fora (UFJF) and OUPR herbarium from Federal University of Ouro Preto (UFOP) and their respective curators. They make possible to study several *Ocotea* species properly identified and

preserved. I would like to thank as well the UALF herbarium - Federal University of Alfenas and its curator, PhD. Marina, always available to help.

Moreover, I want to give special thanks for the PhD. M. Murgu from Waters Company that has amazingly assisted me with all the MS experiments and data to get the success of the metabolomics analyses developed. Besides, I would like to thank the Idehia Institute, especially C. Pinto and PhD. A.P Almeida and PhD. Also, thanks to A. Kijoa from the University of Porto – Portugal for the academic exchange in Natural Products research.

At last, but not less important, a very special thanks to my advisor, PhD. Daniela Aparecida Chagas de Paula for all the support and for being my inspiration along these almost two years, what already became 4 years, since scientific initiation times. So, thank you so much for everything Dani, apart from the friendship we made stronger, you were much more than just a Professor and Mentor, but a real instrument that made me see further and makes me seek a more enthusiastic future into the academic research field. Thank you for always caring, teaching, guiding, warning and showing that you can live on what you like best. Also, I would like to thank PhD. Dr Ivo Caldas, for all the availability, support and collaboration when necessary. And finally, my co-advisor PhD. Ana Chagas for the availability, and the substantial support on my research, my first publication, my qualification stage and all the care along these two years

Thank you all so much! From the deep heart! Everyone in its own way made this dream possible !

"If I have seen further it is by standing on the shoulders of Giants."

Isaac Newton, 05/02/1676

ABSTRACT

Screening for bioactive metabolites is frequently carried out in pharmaceutical drug discovery, and metabolomics arises as a modernized tool applied in the Natural Products (NP) research field for accessing plant metabolites through faster real-time analyses. Thus, this research aimed to perform a comprehensive LC/MS-based metabolomics study to investigate the anti-inflammatory potential of *Ocotea* (Lauraceae) species as well as the neuroprotective activity of the popularly known Ayahuasca beverage and its matrix plants. It is well known the chief role of PGE₂ in acute inflammatory diseases, and recent publications have also indicated that higher COX 2 expression and increased circulating PGE₂ levels play a significant role in cancer progression through lymphangiogenic growth. On the other hand, neural damage is involved in Parkinson disease (PD) progression and in other neurodegenerative diseases, and neuroprotective candidates for medical treatment are utterly needed to develop therapies that can prevent the natural progression of the disease. Thus, new drugs able to elicit neuroprotective activity or to inhibit PGE₂ release are potential targets for drug discovery and development. Formerly, 60 different *Ocotea* species and the matrix plants of Ayahuasca beverage were extracted following current metabolomics extraction protocol. For biological activity, an *ex-vivo* anti-inflammatory screening was realised using human blood LPS-induced inflammation for quantitative PGE₂ determination in plasma by UPLC-MS/MS. The dexamethasone and indomethacin were used as positive controls. For the neuroprotective evaluation, the Ayahuasca beverage, the extracts from its matrix plants (*Banisteriopsis caapi* and *Psychotria viridis*), its fractions and its main alkaloids were evaluated on the viability of SH-SY5Y neuroblastoma cells in an *in vitro* PD model. For the metabolomics analyses, quality control samples were prepared and all samples were subjected to UPLC-ESI-TOF-MS. The MS^E data acquisition and treatment were performed and the dereplication was done using the *in-house* together with the UNIFI software databases (Waters[®]) and the Dictionary of Natural Products (DNP) for MS¹ and molecular formula match. The level 2 identification was performed for the *Ocotea* study by the obtained MS^E product ions, which were compared with a spectral library in the literature for tentative compound identification. The Ayahuasca study was performed via level 3 according to current metabolomics standards. The treated data were analysed by multivariate statistical analysis for biomarkers investigation. The metabolic fingerprints generated allowed the dereplication of the majority of the extracted compounds found on the evaluated extracts. Under the *Ocotea* metabolomics study, it was observed quantitatively more aporphine alkaloids and glycosylated flavonoids in most of the *Ocotea* extracts. Moreover, 12 out of 60 *Ocotea* spp. evaluated have exhibited high satisfactory PGE₂ inhibition. Regarding the neuroprotective evaluation, the lower doses of the active samples from Ayahuasca and its base plants showed to be able to stimulate neuronal cell proliferation and/or display the most efficacious neuroprotection profile. Intriguingly, the hydroalcoholic fractions exhibited enhanced neuroprotective effects when compared to other samples and isolated alkaloids. The general metabolomic analysis allowed determining the biomarkers of anti-inflammatory and neuroprotective activity, besides possibly new compounds with no hits in chemical databases. The biomarkers findings of this research might be potential neuroprotective or anti-inflammatory lead-structures. In addition, this is the first report regarding the chemical composition and bioactivity of several endemic *Ocotea* spp. of the Brazilian territory. And also, this work found that the Ayahuasca beverage and its base plants have potential applicability for PD treatment and other neurodegenerative diseases.

Keywords: *Ocotea*. Ayahuasca. Parkinson's disease. LPS-induced PGE₂ inhibition.

RESUMO

A triagem de metabólitos bioativos é frequentemente realizada na descoberta de medicamentos, e a metabolômica surge como uma ferramenta moderna aplicada no campo de pesquisa de Produtos Naturais (NP) para acessar os metabólitos de plantas por meio de análises mais rápidas em tempo real. Assim, esta pesquisa teve como objetivo realizar um estudo abrangente de metabolômica baseada em LC / MS para investigar o potencial anti-inflamatório de espécies de *Ocotea* (Lauraceae), bem como a atividade neuroprotetora da bebida conhecida popularmente por Ayahuasca e de suas plantas matrizes. É bem conhecido o papel principal da PGE2 em doenças inflamatórias agudas, e publicações recentes também indicaram que uma expressão mais alta de COX 2 e níveis aumentados de PGE2 circulantes desempenham um papel significativo na progressão do câncer através do crescimento linfangiogênico. Por outro lado, o dano neural está envolvido na progressão da doença de Parkinson (DP) e em outras doenças neurodegenerativas, e os candidatos neuroprotetores ao tratamento médico são absolutamente necessários para desenvolver terapias que possam impedir a progressão natural da doença. Assim, novos fármacos capazes de desencadear atividade neuroprotetora ou inibir a liberação de PGE2 são alvos potenciais para a descoberta e desenvolvimento de fármacos. Um total de 60 espécies diferentes de *Ocotea* e as plantas matrizes da bebida Ayahuasca foram extraídas seguindo o atual protocolo de extração metabolômica. Para atividade biológica, uma triagem anti-inflamatória *ex vivo* foi realizada usando inflamação induzida por LPS no sangue humano para determinação quantitativa de PGE2 no plasma por UPLC-MS / MS. A dexametasona e a indometacina foram usadas como controles positivos. Para a avaliação neuroprotetora, a bebida Ayahuasca, os extratos de suas plantas matriciais (*Banisteriopsis caapi* e *Psychotria viridis*), suas frações e seus principais alcaloides foram avaliados quanto à viabilidade das células do neuroblastoma SH-SY5Y em modelo PD *in vitro*. Para as análises metabolômicas, foram preparadas amostras de controle de qualidade e todas as amostras foram submetidas a UPLC-ESI-TOF-MS. A aquisição e o tratamento dos dados obtidos por MS^E foram realizados, juntamente com os bancos de dados do software UNIFI (Waters®) e o Dictionary of Natural Products (DNP) para MS¹ e correspondência de fórmula molecular. A identificação do nível 2 foi realizada pelos íons produto MS^E obtidos, os quais foram comparados com uma biblioteca espectral na literatura para identificação experimental de compostos. O estudo da Ayahuasca foi realizado via nível 3, de acordo com os padrões atuais de metabolômica. Os dados tratados foram analisados por análise estatística multivariada para investigação de biomarcadores. As impressões digitais metabólicas geradas permitiram a desreplicação da maioria dos compostos extraídos encontrados nos extratos avaliados. No estudo da metabolômica de *Ocotea*, observou-se quantitativamente mais alcalóides de aporfina e flavonóides glicosilados na maioria dos extratos de *Ocotea*. Além disso, 12 de 60 *Ocotea* spp. avaliados exibiram alta inibição satisfatória da PGE2. Em relação à avaliação neuroprotetora, as doses mais baixas das amostras ativas da Ayahuasca e de suas plantas de base mostraram-se capazes de estimular a proliferação de células neuronais e / ou exibir o perfil de neuroproteção mais eficaz. Curiosamente, as frações hidroalcoólicas apresentaram efeitos neuroprotetores aprimorados quando comparadas a outras amostras e alcalóides isolados. A análise metabolômica geral permitiu determinar os biomarcadores da atividade anti-inflamatória e neuroprotetora, além de possivelmente novos compostos sem hits em bancos de dados químicos.. Além disso, este é o primeiro relatório sobre a composição química e a bioatividade de várias espécies endêmicas de *Ocotea* spp. do território brasileiro. E também, este trabalho descobriu que a bebida Ayahuasca e suas plantas de base têm potencial aplicabilidade para o tratamento da DP e outras doenças neurodegenerativas.

Palavras-chave: *Ocotea*. Ayahuasca. Doença de Parkinson. PGE2 induzida por LPS.

FIGURE LIST

Figure 1 - Schematic representation of the connection between the lymphangiogenic growth factors (VEGF-C and VEGF-D), PGE2 pathway and the cancer metastasis through lymphatic vessels regulated by enzyme 15-hydroxyprostaglandin dehydrogenase (pgdh) inactivation and COX-2 overexpression.....	26
Figure 2 - The map represents the distribution of species of the <i>Ocotea</i> genus worldwide. The yellow dots show that the <i>Ocotea</i> species are attending mainly the American continent, and also present in the Africa continent, in areas nearest to Madagascar island.....	29
Figure 3 - Biosynthetic pathway of benzyloquinoline and the alkaloid (<i>S</i>)-reticuline. A – (<i>S</i>)-reticuline via norcoclaurine. B- (<i>S</i>)-reticuline via norlaudanoline.....	31
Figure 4 - (<i>S</i>)-isoboldine, an aporphine alkaloid, is produced by phenolic oxidative coupling of the (<i>S</i>)-reticuline precursor	34
Figure 5 - The oxidation-reduction process through the intermediate 1,2-dehydroreticulinium cation to convert (<i>S</i>)-reticuline configuration in (<i>R</i>)-reticuline.....	35
Figure 6 - (1) benzyloquinoline, (2.1) aporphine, (2.2) dihydroaporphine (2.3) didehydroaporphine (2.4) C5- <i>O</i> -aporphine (2.5) C4- <i>O</i> -aporphine (3.1) oxo-aporphine (3.2) didehydroxo-aporphine, (4) pro-aporphine and (5) phenanthrene alkaloids from <i>Ocotea</i> spp.....	36
Figure 7 - C6C3 units of a phenylpropanoid and the difference between lignans and neolignans.....	37
Figure 8 - The summarized biosynthesis of flavonoids and the structural variation of the class...	39
Figure 9 - Molecular structure of metabolites annotated with high peak intensity levels identified within the QC ESI MS+ and MS- sample.....	49
Figure 10 - ESI MS metabolic fingerprint of the positive (above) and the negative (below) mode of the QC sample. TICs chromatograms are displayed as Based Peak Ion (BPI).....	52
Figure 11 - Structure of the aporphine alkaloids isomers with elemental composition C ₁₉ H ₂₁ NO ₄ , (1-boldine, 2-corytuberine, 3-isoboldine, 4- isocorytuberine, 10-laurotetanine, 11-norisocorydine 12-flavinantine, 13-pallidine, 14-sinoacutine and 15-isosinoacutine), the isomers with elemental composition C ₁₈ H ₁₉ NO ₃ (16-zenkerine and 17- tuduranine) and the isomers with elemental composition C ₁₈ H ₁₉ NO ₄ (6-laurelliptine, 18- laetanine and 19- laurolitsine).....	54

Figure 12 - QC ESI MS+ high energy channel evidencing the parent ion at m/z 328.154 and the MS ^E fragment ions of the isomers (1) – boldine, (2) – corytuberine, (3) – isoboldine, (4) isocorytuberine.....	55
Figure 13 - Structure of the aporphine alkaloids isomers with elemental composition C ₁₉ H ₂₃ NO ₄ (20- reticuline). C ₂₀ H ₂₃ NO ₄ (21- predicentrine, 22- lauroschooltzine, 23- corydine and 24- isocorydine). C ₂₀ H ₂₁ NO ₄ (5-dicentrine, 25- nantenine, 26- <i>N</i> -methyl isodomeesticine). C ₁₉ H ₁₉ NO ₂ (27- dehydronuciferine, 28- stephenanthrine). C ₁₉ H ₂₁ NO (29- nuciferine). C ₁₈ H ₁₉ NO ₂ (30- normuciferine). C ₂₂ H ₂₅ NO ₆ (31- leucoxylyonine).....	58
Figure 14 - The low energy and high-energy ESI MS- spectra of the glycosyl flavone (7) and the corresponding [M-146] ⁻ ion derived from the neutral loss of rhamnose residue (C ₆ H ₁₀ O ₄).....	62
Figure 15 - The high-energy QC ESI MS- spectra of the glycosyl flavone (8) kaempferol 3-(4"- <i>p</i> -coumarylrhamnoside and the (9) kaempferol 3-(2",4"-di-(E)- <i>p</i> -coumarylrhamnoside and the corresponding product ions derived from the loss of coumaryl/dicoumaryl rhamnose respectively.....	63
Figure 16 - Evaluation of 33 out the 60 <i>Ocotea</i> spp. with anti-inflammatory activity, 12 statistically similar to positive controls with high PGE2 inhibition ratio.....	69
Figure 17 - Score plot of Principal Component Analyses (PCA) of all samples, hotelling ellipse= 95%, for UPLC-ESI MS-, 4 components and R ² = 0.68. QC – Quality control; VI II- <i>Ocotea villosa</i> replicates.....	76
Figure 18 - Score plot 3D of Principal Component Analysis (PCA) of active anti-inflammatory samples, hotelling ellipse= 95%, 3 components and R ² = 0.77. QC – Quality control; VI II- <i>Ocotea villosa</i> replicates.....	76
Figure 19 - Score plot and loading plot of PLS-DA model indicating the discrimination of the active and inactive sample groups, normalized by UVar, 4 components, and the 8 variables (metabolites) and the responses (active and inactive), normalized by Pareto. 1- 521.20213_2.65; 2- 539.21349_2.98; 3- 551.21317_3.03; 4- 555.223362_2.88; 5- 395.15510_2.31; 6- 326.13901_2.00; 7- 591.26175_9.48; 8- 879.4965_7.76.....	79
Figure S1 - NU I - <i>Ocotea nutans</i> (UFOP), negative mode.....	116
Figure S2 - NU I - <i>Ocotea nutans</i> (UFOP), positive mode.....	116
Figure S3 - OD II - <i>Ocotea odorifera</i> (UFJF), positive mode.....	116

Figure S4 - OD II - <i>Ocotea odorifera</i> (UFJF), negative mode.....	116
Figure S5 - PC II 1- <i>Ocotea pulchella</i> (UFJF), negative mode.....	116
Figure S6 - PC II 1- <i>Ocotea pulchella</i> (UFJF), positive mode.....	116
Figure S7 - PR II - <i>Ocotea porosa</i> (UFJF), positive mode.....	117
Figure S8 - PR II - <i>Ocotea porosa</i> (UFJF), negative mode.....	117
Figure S9 - PT II - <i>Ocotea pretiosa</i> (UFJF), negative mode.....	117
Figure S10 - PT II - <i>Ocotea pretiosa</i> (UFJF), positive mode.....	117
Figure S11 - SP I - <i>Ocotea spectabilis</i> (UFOP), positive mode.....	117
Figure S12 - SP I - <i>Ocotea spectabilis</i> (UFOP), negative mode.....	118
Figure S13 - SX I - <i>Ocotea spixiana</i> (UFOP), positive mode.....	118
Figure S14 - SX I - <i>Ocotea spixiana</i> (UFOP), negative mode.....	118
Figure S15 - TE II 1 - <i>Ocotea tenuiflora</i> (UFOP), positive mode.....	118
Figure S16 - TE II 1 - <i>Ocotea tenuiflora</i> (UFOP), negative mode.....	118
Figure S17 - TR I - <i>Ocotea tristis</i> (UFOP), positive mode.....	118
Figure S18- TR I - <i>Ocotea tristis</i> (UFOP), negative mode.....	118
Figure S19 - VR I - <i>Ocotea variabilis</i> (UFOP), positive mode.....	119
Figure S20 - VR I - <i>Ocotea variabilis</i> (UFOP), negative mode.....	119
Figure S21 - VZ II 2- <i>Ocotea velloziana</i> (UFJF), positive mode.....	119
Figure S22 - VZ II 2- <i>Ocotea velloziana</i> (UFJF), negative mode.....	119
Figure S23 - VL II - <i>Ocotea velutina</i> (UFJF), positive mode.....	119
Figure S24 - VL II - <i>Ocotea velutina</i> (UFJF), negative mode.....	120
Figure S25- VI II - <i>Ocotea villosa</i> (UFJF), positive mode.....	120
Figure S26 - VI II - <i>Ocotea villosa</i> (UFJF), negative mode.....	120
Figure S27- The sample of <i>Ocotea diospyrifolia</i> , exsiccate #41173 from CESJ (Herbário Leopoldo Krieger- UFJF).....	121
Figure S28- The <i>Ocotea</i> extracts inside the speed vacuum during the drying stage.....	121
Figure S29- Waters mass spectrometer (UHPLC-TOF-MS/MS).....	122
Figure S30- Supelco (LC-18 Solid Phase Extraction -SPE 500mg, #57012).....	122
Graph S1- Calibration curve and equation of PGE2 quantification.....	123

TABLE LIST

Table 1 -	The SRM parameters for PGE2 and CAP. Q1 – Precursor ion SRM transition, CE- collision energy (eV), Q3- Fragment ion SRM transition negative mode..	46
Table 2 -	The putative identification of aporphine isomers at m/z 298, m/z 314 and m/z 328 by ESI-MS ^E	56
Table 3 -	The putative identification of aporphine isomers at m/z 282, m/z 294, m/z 296, m/z 340, m/z 342 and m/z 400 by ESI-MS ^E	59
Table 4 -	The putative identification of the compounds at m/z 183, m/z 246, m/z 274, m/z 359, m/z 373, m/z 387, m/z 415, m/z 593 and m/z 609 by ESI-MS ^E	61
Table 5 -	The putative identification of the compounds at m/z 287, m/z 431, m/z 433, m/z 447, m/z 463 and m/z 609 by ESI-MS ^E	64
Table 6 -	Percentage of PGE2 inhibition of the anti-inflammatory assay evaluated by SPE-UPLC-MS/MS PGE2 quantification method.....	67
Table 7 -	Summary of the ESI-MS ^E dereplication of active anti-inflammatory <i>Ocotea</i> spp. evidencing the highest peak areas of samples.....	73
Table 8 -	The list of potential biomarkers with the anti-inflammatory activity via PGE2 inhibition pathway. The sample column refers to the sample with the highest detector counts acquired for the biomarker. The detector counts (DC) is the intensity of the peak.....	80
Table 9 -	The list of unknown biomarkers with the anti-inflammatory activity via PGE2 inhibition pathway.....	81
Table S1 -	Vouchers from UFJF and UFOP and the <i>Ocotea</i> spp. details I.....	95
Table S2 -	Vouchers from UFJF and UFOP and the <i>Ocotea</i> spp. details II.....	99
Table S3 -	The <i>Ocotea</i> spp. extracts yield	103
Table S4 -	The unknown metabolites of the positive ionisation mode detected with the highest intensity counts (32 metabolites).....	104
Table S5 -	The VIP values > 1.5 referred to the putatively identified metabolites of <i>Ocotea</i> spp. in the ESI MS-.....	105
Table S6 -	PBS protocol (pH 7.2; 0.15 M chloride; 0.01 M phosphate).....	106
Table S7 -	The metabolites of the QC MS+ detected with the highest intensity counts dereplicated from the <i>in-house</i> database (82 annotated metabolites).....	107

Table S8 -	The metabolites of the QC MS- detected with the highest intensity counts dereplicated from the <i>in-house</i> database (21 annotated metabolites).....	113
------------	--	-----

ABBREVIATIONS LIST

ANOVA	- Variance Analyses – Standard Mean Error
AA	- Arachidonic Acid
CAP	- Chloramphenicol
COX	- Cyclooxygenase Enzyme
COX-2	- Cyclooxygenase Subtype II
CYP80G2	- Cytochrome P-450 80G2
MeCN	- Acetonitrile
DC	- Detector Counts
DEX	- Dexamethasone
DNP	- Dictionary of Natural Products
EP4	- Prostaglandin E2 receptor 4
ESI	- Electrospray Ionisation
MF	- Molecular Formula
HCA	- Hierarchical Cluster Analysis
HPLC	- High-Performance Liquid Chromatography
IL-1 β	- Interleukin 1 β
ID	- Identification Number
IND	- Indomethacin
LC-MS	- Liquid Chromatography hyphened with Mass Spectrometry
LFQM	- <i>Laboratório de Fitoquímica e Química Medicinal</i>

LPS	- Lipopolysaccharides
MAO	- Monoamine Oxidase Enzymes
MSA	- Multivariate Statistical Analyses
MS ^E	- Mass Spectrometry Fragment ion spectra - Data-independent analysis
NMR	- Nuclear Magnetic Resonance
NO	- Nitric oxide
NP	- Natural Products
NSAIDs	- Non-Steroidal Anti-Inflammatory Drugs
PCA	- Principal Component Analysis
PC	- Prostacyclin
PGs	- Prostaglandin
PGE ₂	- Prostaglandin E ₂
PGH ₂	- Prostaglandin H ₂
PLS-DA	- Partial Least Squares Regression – Discriminant Analyses
PTFE	- Polytetrafluoroethylene
Q ²	- Goodness of prediction
R ²	- Goodness of fit
SAIDs	- Steroidal Anti-Inflammatory Drugs
TNF- α	- Tumor Necrosis Factor
TX	- Thromboxanes

- UHPLC - Ultra-High-Performance Liquid Chromatography
- VEGF-C - Vascular Endothelial Growth Factor C
- VEGF-D - Vascular Endothelial Growth Factor D
- VIP - Variable Important in Projection
- X - Predicted variables

SUMMARY

1	INTRODUCTION.....	19
2	OBJECTIVES.....	22
2.1	General objective	22
2.2	Specified objectives	22
3	CHAPTER ONE - UNTARGETED UPLC-ESI-QTOF-MS METABOLOMIC STUDY OF <i>OCOTEA</i> GENUS (LAURACEAE) AND DETERMINATION OF LPS- INDUCED PGE2 INHIBITION BIOMARKERS OF ACTIVITY..	23
3.1	Theoretical reference	23
3.1.1	Inflammation and cancer	23
3.1.2	Lauraceae Jussieu family.....	27
3.1.3	<i>Ocotea</i> genus	28
3.1.4	<i>In-house</i> database, chemistry and biosynthesis of the <i>Ocotea</i> genus	30
3.1.5	Mechanism of action described for <i>Ocotea</i> metabolites and aporphine alkaloids ..	30
3.1.6	Computational chemical studies: a way forward in metabolomics analyses	39
3.2	Material and methods	42
3.2.1	Plant material (<i>Ocotea</i> spp.).....	42
3.2.2	Drugs and reactants.....	43
3.2.3	Metabolomics extracts preparation.....	43
3.2.4	An alytical UPLC-ESI-QTOF-MS metabolomics experiments	43
3.2.5	<i>Ex vivo</i> anti-inflammatory evaluation.....	44
3.2.5.1	<i>Prostaglandin E2 (PGE2) quantification by UPLC-MS/MS.....</i>	<i>45</i>
3.2.6	Metabolomic studies	47
3.2.6.1	<i>Data treatment and dereplication strategies</i>	<i>47</i>
3.2.6.2	<i>Multivariate Statistical Analyses (MSA)</i>	<i>48</i>
3.3	Results and discussion.....	48
3.3.1	<i>Ocotea</i> extracts and <i>in-house</i> database	48
3.3.2	Data treatment and QC metabolic fingerprint	50
3.3.3	Anti-inflammatory <i>ex vivo</i> evaluation (PGE2).....	65
3.3.4	Statistical analyses of the active anti-inflammatory samples	68
3.3.5	MS ^E dereplication of the highest intensity peaks of active <i>Ocotea</i> species.....	72
3.3.6	Metabolomics studies and biomarkers determination by MSA.....	75
3.3.6.1	<i>Principal Component Analyses (PCA).....</i>	<i>75</i>
3.3.6.2	<i>Partial Least Square – Discriminant Analyses (PLS-DA)</i>	<i>77</i>
3.4	Conclusion	83

4	CHAPTER TWO - NEUROPROTECTIVE POTENTIAL OF AYAHUASCA AND UNTARGETED METABOLOMICS ANALYSES: APPLICABILITY TO PARKINSON'S DISEASE.....	85
5	FINAL CONSIDERATIONS	86
	REFERENCES.....	87
	SUPPLEMENTAL MATERIAL.....	95

1 INTRODUCTION

The physiological inflammatory response can occur acutely or chronically, systemically or locally depending on the pathology which the inflammatory process is associated with, such as psoriasis, gout arthritis, acute inflammation, autoimmune diseases and also several types of cancer (LANDSKRON et al., 2014; MULTHOFF; MOLLS; RADONS, 2012). The inflammatory process is generally triggered by initial damage to living tissues which could be injured by the presence of a virus, bacteria, traumas, some type of neoplasias, toxins, heat, or any other cause that might elicit a physiological response in the body through the release of a series of chemical mediators, such as prostaglandins (PGs), growth factors, chemokines, and cytokines (COUSSENS; WERB, 2012; FIORUCCI et al., 2001; LANDSKRON et al., 2014). The PG such as PGE₂, which is one of the final mediators derived from the arachidonic acid (AA) inflammatory cascade, mediated mainly by cyclooxygenase (COX) and lipoxygenase (LOX) enzymes, and also by terminal synthases enzymes (CHAGAS-PAULA et al., 2015a; DING et al., 2018; FIORUCCI et al., 2001).

The cyclooxygenase subtype 2 (COX 2) is a key enzyme in the AA metabolism, which it is a 20-carbon polyunsaturated fatty acid that gives origin to metabolites known as eicosanoids, a primary constituent of cell membranes. The eicosanoids are substances derived from the AA inflammatory cascade, which are released from membrane phospholipids by phospholipases enzymes, predominantly by the type-IV cytosolic PLA₂ α throughout physiological stimulation due to initial damage in body tissues (BROUGHTON, II; JANIS; ATTINGER, 2006; MEIRER; STEINHILBER; PROSCHAK, 2014). This chemical mediator is metabolized via three pathways forming different classes of eicosanoids, which are substances that act in an autocrine and paracrine manner on target cells after its extracellular release. The COX is responsible for the catalyses that originate the PGs together with the thromboxanes (TX). Leukotrienes (LT) and lipoxins (LX) are produced by the lipoxygenase (LO) pathway. The cytochrome P450 enzymes (CYP) are important to produce the epoxyeicosatrienoic acids (EET) (COUSSENS; WERB, 2012; MEIRER; STEINHILBER; PROSCHAK, 2014).

Anti-inflammatory drugs are among the most worldwide used drug classes. However, when used in longtime treatments or chronic situations, the currently available drugs can have the ratio of the effectiveness-side effect highly decreased and a series of adverse drug reactions. In most of the times, these side effects occur due to lack of anti-inflammatory drug specificity what leads to non-selective PGE₂ inhibition. Thus, the continuous search for new

viable anti-inflammatory agents is indispensable, aiming at substances with less adverse drug reactions and enhanced effectivity (CHAGAS-PAULA et al., 2015b; DING et al., 2018; MEIRER; STEINHILBER; PROSCHAK, 2014). In this context, plants and microorganisms have been a source of biologically active samples giving rise to critical pharmaceutical agents in the drug discovery process. Particularly, NP research and secondary metabolites have been a significant source of inflammatory treatment in the last century (CHAGAS-PAULA et al., 2015a; GRAZIANI et al., 2018; ULLAH; AATIF, 2009).

A considerable number of scientific publications have shown that the presence and expression of COX-2 together with the inflammatory attendant PGE2 lipid mediator have a central role in the development of different types of epithelial cancers, such as breast cancer. More recently, studies in the literature evidenced that the cancer therapy associated with a COX-2 inhibitor has significantly decreased tumor growth, throughout tumor-associated angiogenesis and lymphangiogenesis inhibition pathways (KARNEZIS et al., 2012; LYONS et al., 2014; WANG; HONN; NIE, 2007). Cancer diseases became more deeply studied in the last past years, although the foremost description of cancer was earlier revealed in a papyrus from Ancient Egypt (BRUCHER et al., 2014). However, only in the 18th century, with the advent of the microscope, it was discovered that eventually, cancer could spread from the primary tumor location to other locations through the lymph nodes, and thus reach other sites in the human body. This phenomenon was named as metastasis (SEYFRIED; HUYSENTRUYT, 2013). In early 1863 the link between inflammation and cancer was first observed, and the role of inflammation in the development of certain types of cancer started to be investigated. The hypothesis that cancer diseases might arise from inflammatory sites were proposed as a result of the first biopsied tumor observations, concluding that inflammatory cells could infiltrate tumors (COUSSENS; WERB, 2012; LANDSKRON et al., 2014; MANTOVANI, 2018; MULTHOFF; MOLLS; RADONS, 2012).

Overall, the chemical mediators and cellular mechanisms involved in the process of inflammation are vital for the environment as well as the development of some type of malignant tumors (LANDSKRON et al., 2014). There are cancers, which the inflammatory conditions are indeed present even before the carcinogenesis process begins. Thus, there are varieties of cancer that might start to occur, triggered by specific inflammatory cascade conditions. Contrasting, in other types of cancer, it might arise due to oncogenic activation. However, the ongoing path leads to inflamed cell microenvironment that supports the development of the tumor, and therefore the inflammation process plays a dynamic role in cancer pathogenies (LANDSKRON et al., 2014; ULLAH; AATIF, 2009).

A high number of plant species around the world have demonstrated several medicinal applications for humans, and literature is filled with important anticancer and anti-inflammatory drugs. In this context, the Lauraceae family has shown high commercial and interesting pharmaceutical importance, such as the genus *Persea*, *Laurus*, *Cinnamomum* and *Ocotea*. One of the most abundant genera of the Lauraceae family is the *Ocotea*, with around 350 species, with variable morphology and secondary metabolite production. Among the plants of the family with therapeutic activity found in the literature, a large number belong to the *Ocotea* genus (BROTTO; CERVI; DOS SANTOS, 2013; MARQUES, 2001). For example, in Peru and Equator, *O. quixos* has demonstrated local anaesthetic and anti-bacterial and anti-diarrheic properties. In Brazil, *O. lancifolia* is known for anti-rheumatic properties, and a series of new biologically active sesquiterpenes have been isolated with pronounced pharmacological activity (BRUNI et al., 2004; PALOMINO et al., 1996; RAQUEL et al., 2010; SALLEH; AHMAD, 2017). Moreover, *O. odorifera* has demonstrated therapeutic properties, such as anti-inflammatory and antifungal potential (CASTRO; LIMA, 2011; MARQUES, 2001).

Furthermore, indigenous and mestizo communities of South America regularly use a beverage called as Ayahuasca to treat a wide range of medical conditions, which is often used by the indigenous people to engage into traditional spiritual healing rituals and also used to handle their social issues (ANTONIO et al., 2019; COE; MCKENNA, 2017; FABER; GROOT, 2007; FRECSKA; BOKOR; WINKELMAN, 2016; LABATE; CAVNAR, 2013). Scientifically, the beverage is recognised as an ethnomedicine to improve mood changes and treat physiological issues, such as mental illnesses (ANTONIO et al., 2019; DOMÍNGUEZ-CLAVÉ et al., 2016; SERRANO-DUEÑAS; CARDOZO-PELAEZ; SÁNCHEZ RAMOS, 2001). Currently, the beverage use garnered the attention of the academic community to study its pharmacological mechanisms and the therapeutical benefit (GAUJAC et al., 2012; LABATE CAIUBY; FEENEY, 2012; LUNA, 2011; MCKENNA, 2004; MCKENNA; TOWERS; ABBOTT, 1984; RAY; LASSITER, 2016; SCHENBERG et al., 2015). For example, research investigation regarding neurophysiologic stimulation, neuroprotection, and thus the therapeutic potential for the treatment of cognitive disabilities and mental disorders, such as benefit in Parkinsonism symptoms and other neurodegenerative diseases have been proposed (INABA-HASEGAWA et al., 2012; KATCHBORIAN-NETO et al., 2020; SAMOYLENKO et al., 2010).

In this tale, metabolomics based on liquid chromatography (LC) coupled with mass spectrometry (MS) arise as a modernized tool applied in the Natural Products (NP) research

field for accessing metabolites composition of different samples through faster real-time analyses (CRAGG; PEZZUTO, 2016; DEMAIN; VAISHNAV, 2011; KATAJAMAA; OREŠIČ, 2007; ROUX et al., 2011). Metabolomics can be defined as the systematic analyses of endogenous metabolites from biological specimens. Thus, the metabolome comprises all the chemical composition of low weight molecules from samples, which it is usually determined using a mix of analytical techniques, such as different methods of liquid chromatography coupled to mass spectrometry (LC-MS) to allow the evaluation of the maximum possible of the metabolome. This provides an overview of the chemical composition of the samples to determine active compounds that are common in bioactive samples and absent on inactive samples, among other applications. Metabolomics can be treated as an ally for the drug development process and as a comprehensive strategy that allows profiling complex mixtures of myriad chemical components in crude extracts (CHAGAS-PAULA et al., 2015a; VINAYAVEKHIN; SAGHATELIAN, 2010; WOLFENDER; MARTI; QUEIROZ, 2010; YULIANA et al., 2011). The MS-based metabolomics untargeted approach represents the latest omics technologies that have been applied with success in a wide range of science research areas for analysis of global metabolome of organisms (THEODORIDIS; GIKA; WILSON, 2011; VINAYAVEKHIN; SAGHATELIAN, 2010; WOLFENDER et al., 2019). Therefore, the untargeted metabolomics investigation of the anti-inflammatory effects of *Ocotea* species is described over the chapter I of this dissertation. Whereas, the neuroprotective potential of Ayahuasca, also investigated by metabolomics means is described over chapter II.

2 OBJECTIVES

2.1 General objective

The present work aims to perform an MS-based metabolomics study of *Ocotea* genus for shortening the time of finding new lead-structures candidates (biomarkers) in the drug discovery process of natural products with anti-inflammatory activity through inhibition of PGE2 release (chapter I). Besides, to find biomarkers and to evaluate the neuroprotective potential of the Ayahuasca beverage, the extracts from its matrix plants (*Banisteriopsis caapi* (Spru. ex Giseb) Morton and *Psychotria viridis* Ruiz & Pav), its fractions and its main alkaloids on the viability of SH-SY5Y neuroblastoma cells in an *in vitro* PD model (chapter II).

2.2 Specified objectives

The specific objective of the research are:

- a) to create an *in-house* database of metabolites from the *Ocotea* genus, *Banisteriopsis caapi* and *Psychotria viridis* species;
- b) to investigate the *Ocotea* samples by an *ex-vivo* anti-inflammatory assay SPE-UPLC-MS/MS for PGE2 quantification;
- c) to investigate the neuroproliferation and neuroprotective profile of Ayahuasca samples by a PD *in-vitro* assay;
- d) realize multivariate statistical analyses to determine the substances highly correlated with the activities;
- e) to investigate potential biomarkers by analytical UPLC-ESI-QTOF-MS and UPLC-ESI-TOF-MS plus dereplication of the compounds from the extracts;

3 CHAPTER ONE - UNTARGETED UPLC-ESI-QTOF-MS METABOLOMIC STUDY OF *OCOTEA* GENUS (LAURACEAE) AND DETERMINATION OF LPS- INDUCED PGE2 INHIBITION BIOMARKERS OF ACTIVITY

3.1 Theoretical reference

3.1.1 Inflammation and cancer

For several years, compounds able to cause inhibition on the AA inflammatory cascade pathway have been in the focus of pharmaceutical researches to develop safer treatments able to decrease inflammatory conditions. The lipid mediator PGE2 is a product of this cascade and it plays a major role in inflammatory diseases, and it is responsible for the classical inflammatory symptoms, such as pain, redness, increased heat, swelling and loss of cell function (FUNK, 2001; MEIRER; STEINHILBER; PROSCHAK, 2014). The COX enzymes are the most common drug target to reduce the inflammatory physiological response. While Steroidal anti-inflammatory drugs (SAIDs) is responsible to inhibit PLA2 α at the beginning of the cascade pathway, the Non-steroidal anti-inflammatory drugs (NSAIDs) are recognised as selective or non-selective direct inhibitors of the inflammatory enzymes COX-1 and COX-2. Thus, these drugs can lead to a decrease in PG secretion, and therefore reduce inflammation due to a meaningful decrease of the PGE2 in the inflammatory body sites (LESLIE, 2015; MEIRER; STEINHILBER; PROSCHAK, 2014).

Most of the available anti-inflammatory drugs in the market can evoke important adverse drug reactions. The corticosteroids (SAIDs) can cause mild or serious side effects, especially when used at higher doses or for extended periods, leading to high blood pressure, weight gain, fluid retention and others critical negative effects. The NSAIDs, in fact, can be safer and reduce aches and pain, however, it also displays unfavourable side effects mainly on the central nervous system and in the gastrointestinal tract (MEIRER; STEINHILBER; PROSCHAK, 2014; YANG et al., 2007). Recently, the enzyme Microsomal prostaglandin E synthase-1 (mPGES-1) has attracted great attention of the academic community as a new potential drug target for the next generation of anti-inflammatory drugs towards more selective PGE2 release inhibition with less adverse drug reactions (DING et al., 2018; MEIRER; STEINHILBER; PROSCHAK, 2014)

On the other hand, cancer represents a group of more than 100 different diseases that impair the worldwide population, and it is physiologically characterised by the loss of cellular function associated with an absence of differentiation, in addition to uncontrolled cell

proliferation (CAI et al., 2004; CRAGG; NEWMAN, 2005; SUBHASHINI; MAHIPAL; REDDANNA, 2005). Thus, cancer is considered a multifactorial disease with multistage characteristics, however, the process of inflammation is intimately associated with the cancer pathway (CLAVEL, 2007). Likewise, the presence and expression of COX 2, is significantly stimulated on the response of the progression and metastasis of a variety of cancers (NANDI et al., 2017; WANG; HONN; NIE, 2007).

Cancer and inflammation are associated in different levels, although they are more closely related upon lymphangiogenesis process. This phenomenon is involved in the spread of cancer cells by lymphatic metastasis, which consists of the development of new lymphatic capillaries in the body from already pre-existing lymphatic vessels (PADUCH, 2016). This negatively impacts patient health and it is a frequent manifestation in almost all epithelial cancers, including lungs, stomach, colon, breast, pharynx and larynx, uterine cervix, prostate and the ovary (NANDI et al., 2017; PADUCH, 2016). These inflammatory conditions are responsible for one of the first cancers route of spreads, which via the bloodstream, it can later metastasize from the lymph nodes and there to other organs in the body. Thus, researches are evidencing that newly formed lymphatics capillaries work as conduits for the entrance and spread of cancer cells to lymph nodes and then to other regions of the body (KARNEZIS et al., 2012; NANDI et al., 2017; PADUCH, 2016). It should be noted that depending on the stage of the tumor, metastasis can already occur in the existing lymphatic vessels, and thus the lymphangiogenesis is triggered as a late process. Therefore, tumor cells can enter the lymphatic system by invading pre-existing lymphatic vessels in the periphery of the tumor or causing lymphangiogenesis associated with tumor (NANDI et al., 2017; PADUCH, 2016).

Furthermore, lymphangiogenesis is a condition highly associated with breast cancer in women, which is characterised by abnormal COX 2 enzymes expression and thus more high levels of prostaglandin E2 (PGE2) in the tumors. The PGE receptor is highly expressed and activated in breast cancer and other types of cancers. Thus, it suggested that lipid-protein mediators, such as PGE2, plays a significant role in the inflammation course of cancer diseases and the COX-2 redeem an essential role in the promotion of lymphatic metastasis of several types of cancer (LYONS et al., 2014; NANDI et al., 2017). Therefore, the presence of PGE2 in the tumor micro-environment is a result of elevated COX-2 expression, and as this enzyme activation takes place cancer progression might start to occur by multiple mechanisms. Lymphangiogenesis is one of the mechanisms that several types of cancer rely on for its progression and development (LYONS et al., 2014; NANDI et al., 2017; PADUCH, 2016).

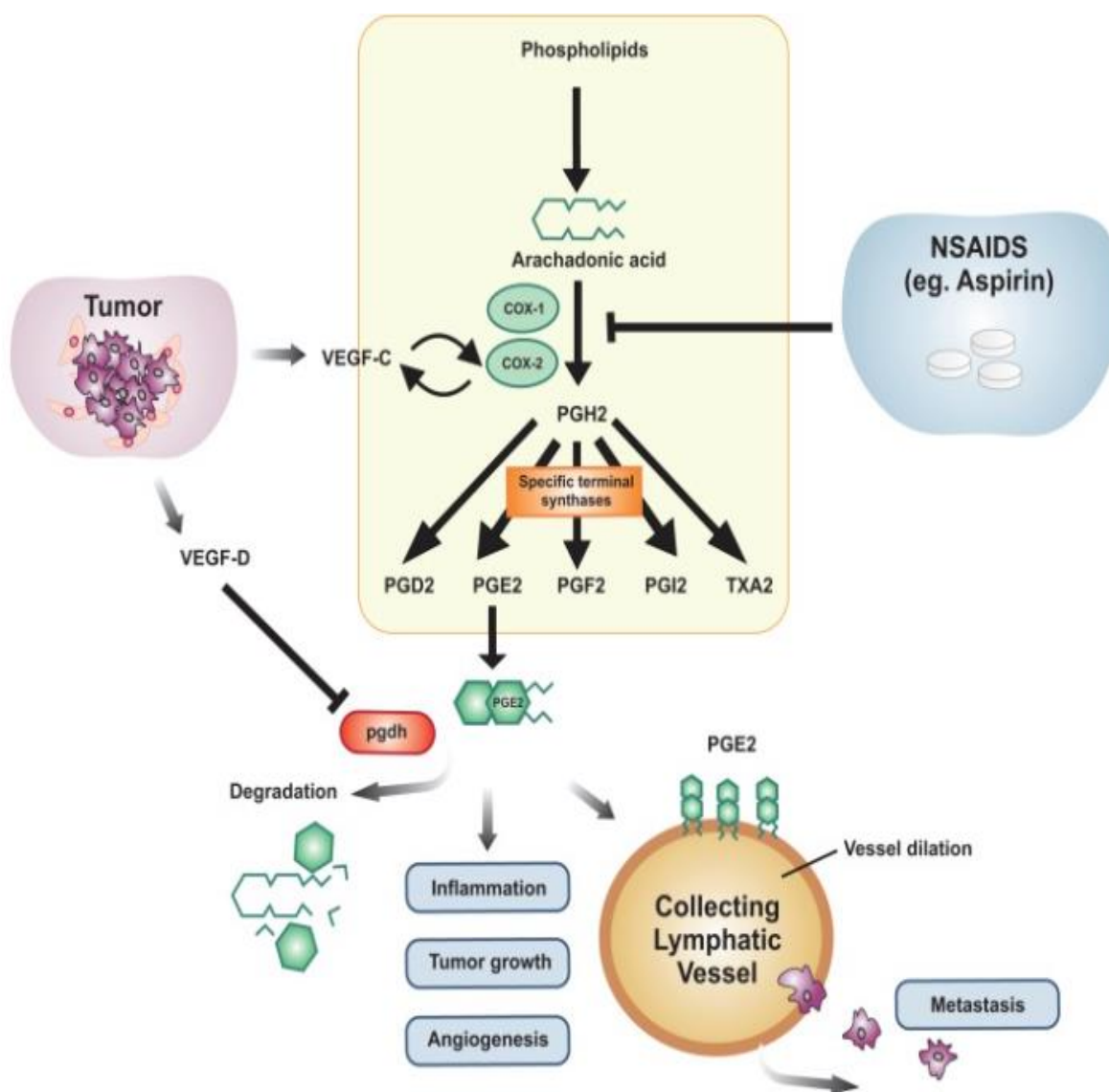
The main mechanisms involved in cancer proliferation via COX mediated activation and PGE₂ presence are the inactivation of host anti-tumor immune cells, stimulation of tumor cell migration and invasiveness, induction of stem-like cells (SLC), and the more recent academic research unfolded the main mechanism, which is related to an upregulation of lymphangiogenic growth factors VEGF-C or VEGF-D in tumor cells (NANDI et al., 2017; ROZIC; CHAKRABORTY; LALA, 2001).

The PGE₂ is the form of prostaglandin most associated with inflammation, tumor growth, angiogenesis and lymphangiogenesis. Physiologically the PGE₂ is degraded by the action of the enzyme 15-hydroxyprostaglandin dehydrogenase (pgdh). Thus, primary tumors can secrete VEGF-D which has the effect of negative regulation of the pgdh expression gene, inhibiting the degradation of PGE₂ from the extracellular medium. Therefore, it has been shown that VEGF-D is important for the tumor to increase EP4 receptor activation (Prostaglandin E2 receptor 4) and provide the dilation of lymphatic vessels, which leads to a significant increase in the number of metastases. The results of the blockage of PGE₂ degradation causes inflammation and tumor expansion and growth (KARNEZIS et al., 2012; NANDI et al., 2017).

Also, VEGF-C or VEGF-D secreted by tumor cells can increase vascular permeability or have important effects on the pressure of the tumor interstitial fluid, which can promote the entry of tumor cells into the lymph. Also, it has been reported that VEGF-C induces the expression of COX-2, which increases the conversion of arachidonic acid to PGH₂, and thus increasing the circulating PGE₂ levels. Therapeutically, this can be inhibited by COX pathway antagonists, which can reduce the amount of PGE₂ being synthesized. As well, as drugs that inhibit VEGF – C and D. In addition, studies are indicating that the therapy is not only with the COX-2 inhibitor, but also antagonists of the EP4 inhibited tumor growth by inhibiting lymphangiogenesis and preventing metastases to the lymph nodes (Figure 1) (KARNEZIS et al., 2012; MAJUMDER et al., 2014; NANDI et al., 2017).

Therefore, PGE₂ plays an essential role in cancer disease and makes it a therapeutic target to reduce the pathological response (MAJUMDER et al., 2014; NANDI et al., 2017) Besides, the current clinical data shows that some NSAIDs increase the survival of cancer patients by reducing metastases phenomena. Confirming the anticancer effects of anti-inflammatory agents through the inhibition of prostaglandin and VEGF signalling pathways (MAJUMDER et al., 2014; NANDI et al., 2017).

Figure 1 - Schematic representation of the connection between the lymphangiogenic growth factors (VEGF-C and VEGF-D), PGE2 pathway and the cancer metastasis through lymphatic vessels regulated by enzyme 15-hydroxyprostaglandin dehydrogenase (pgdh) inactivation and COX-2 overexpression



Source: KARNEZIS et al., 2012.

Since the continuous search for new viable anti-inflammatory agents is indispensable, aiming at substances with less adverse drug reactions and enhanced effect, and PGE2 has declared a key PG in cancer pathogenesis and reducing inflammation might represent a current valid strategy for cancer prevention and treatment. Thus, this work aimed to investigate samples of the *Ocotea* genus aiming to find compounds able to inhibit PGE2 production and thus to find biomarkers of this pharmacological activity by an untargeted metabolomics study approach.

3.1.2 Lauraceae Jussieu family

Antoine Laurent de Jussieu named the Lauraceae family in 1789 after years of botanical research. The Lauraceae family belongs to the order of Laurales, which is considered one of the most primitive families of the Magnoliophyta division and to the Plantae kingdom, that is represented by the organisms named as the flowering plants, scientifically known as the angiosperms. (CHASE et al., 2016).

Following the FLORA BRASIL 2020, to date, 46.732 species are belonging to the Plantae kingdom officially recognized for the Brazilian flora. However, there is an estimative that shows potential to possess around 400.000 plant species in the several phytogeographical domains of the country, corresponding to the most extensive plant genetic diversity in the world (SILVA et al., 2012). Moreover, Brazil has a significant record of ethnopharmacology use from a vast number of plant species, which were transmitted by popular knowledge through generations. The Brazil total land is extensive with many biomes and typical climates, as a result of different ecosystems with abundant natural resources. Thus, in each part of the country, there are different vegetal species, with unique characteristics (BREITBACH et al., 2013). The existing biomes in Brazil are the Amazon Forest, Cerrado, Pampas, Mata Atlântica, Caatinga, Pantanal, the transition bands and the Brazilian marine biome (IBAMA, 2017). Thus, Brazil is one of the richest sources of pharmacologically active compounds in worldwide, where most of them arise from the secondary metabolism of plants (PADILLA et al., 2018).

Regarding the botanical families of the Brazilian flora stands the Lauraceae Jussieu. It is a botanical family also popularly called laurel family, which has a natural distribution in all world tropical and subtropical regions, found mainly in Southeast Asia and South America. This family gather more than 2850 species distributed along 67 genera (CUSTÓDIO; VEIGA JUNIOR, 2014; YAMAGUCHI et al., 2011). Among the most known species of the family are laurel (*Laurus nobilis* L.), avocado (*Persea americana* Mill.), cinnamon (*Cinnamomum verum* J. Presl.) and camphor tree (*Cinnamomum camphor* Meisn.). The Lauraceae encompass a high diversity of utility for human, with broad economic input associated. Besides the use of these plants species in cooking, papermaking, carpentry and civil construction, several Lauraceae species are recognised as popular medicines, and the reputation of the production of its essential oil are well explored, for instance, arylpropanoids, terpenes and terpenoids, as

well as other non-volatile secondary metabolites, such as alkaloids, flavonoids and lignans constituents (GOTTLIEB, 1972; MARQUES, 2001).

There are 25 native genera and more than 400 species that have been registered in Brazil, but not necessarily endemic to the country land, occurring in other subtropical regions around the world. The Lauraceae genera found in Brazil are *Aiouea*, *Anaueria*, *Aniba*, *Beilschmiedia*, *Cassytha*, *Cinnamomum*, *Cryptocaria*, *Dicypellium*, *Endlicheria*, *Kubitzkia*, *Licaria*, *Mezilaurus*, *Misanteca*, *Nectandra*, *Ocotea*, *Paraia*, *Persea*, *Phoebe*, *Phyllostemonodaphne*, *Pleurothyrium*, *Rhodostemonodaphne*, *Sextonia*, *Systemonodaphne*, *Urbanodendron* and *Williamdendron*, besides, the *Laurus* and *Litsea* genera that are well established and grown in the country, although both were introduced to Brazil due to their economic importance (CUSTÓDIO; VEIGA JUNIOR, 2014; YAMAGUCHI et al., 2011).

3.1.3 *Ocotea* genus

The *Ocotea* is the largest genus of the Lauraceae family in the American continent and comprehends around 350 species widespread in world tropical and sub-tropical areas, such as the Central and South America, Southern Africa and Madagascar (CHAVERRI; CICCIO, 2005; SACCHETTI et al., 2006). In Brazil, there are 101 endemic *Ocotea* and around 160 species in total, which are significantly present in the Atlantic forest, covering the land of an elevated number of states in different parts of the country, but mainly south and central east. The *Ocotea* spp. are found in the states such as Paraná, Santa Catarina, São Paulo, Rio de Janeiro, Bahia and Alagoas (YAMAGUCHI et al., 2011; FLORABRASIL, 2018). The *Ocotea* distribution worldwide is detailed in Figure 2.

The *Ocotea* genus is represented mainly by aromatic trees which are fundamentally essential oil producers, rich in camphor and safrole (CHAVERRI; CICCIO, 2005; SALLEH; AHMAD, 2017). The genus arouses great economic interest, as a great aggregated value in the logging industry, such as the *O. porosa* or popularly known 'imbuia', and the wood from other species, for example, the *O. puberula* and *O. bullata*. The essential oils of the popularly known medicinal plant sassafras (*O. odorifera*), and others produced by *Ocotea* genus are present in the cosmetics and perfumery industry, also essential oils from other species, for example, *O. cymbarum*, *O. caudata*, *O. pretiosae*, *O. usambarensis*, *O. sassafras* and *O. brenessi*. Despite that, the *Ocotea* spp. is related to the potential pharmacological activity for a diverse spectrum of diseases (CHAVERRI; CICCIO, 2005; SACCHETTI et al., 2006).

Figure 2 - The map represents the distribution of species of the *Ocotea* genus worldwide. The yellow dots show that the *Ocotea* species are attending mainly the American continent, and also present in the Africa continent, in areas nearest to Madagascar island



Source: The Polistes Corporation/ <https://www.discoverlife.org>.

In popular medicine of native people from South America, some *Ocotea* species are recognised for valued medicinal properties, such as endowed with analgesic and anti-inflammatory properties that have shown several applications in natural products bioactivity evaluation tests (SALLEH; AHMAD, 2017). In Peru and Equator, native people traditionally use the *O. quixos* as a cinnamon substitute to aromatise food. However, it has demonstrated local anaesthetic and anti-diarrheic properties. In Brazil, *O. lancifolia*, is known for anti-rheumatic properties, and a series of new biologically active sesquiterpenes have been isolated together with aporphine alkaloids and other secondary metabolites (PALOMINO et al., 1996; RAQUEL et al., 2010). Moreover, in our research group, we have evidenced and confirmed anti-inflammatory properties from *O. odorifera* and *O. diospyrifolia*, which demonstrated potent anti-inflammatory effects with dual COX and lipoxygenase (LOX) inhibition by the plant crude extracts, and by the isolated benzyloquinoline alkaloid, the reticuline and also new aporphine alkaloid diospiriofoline (ALCÂNTARA, 2018; SILVA, 2019).

Moreover, the *O. caparrapi* has demonstrated cytotoxic effects and commonly is used to heal animal bites, such as insect or even snake; it also has been indicated for bronchitis (PALOMINO et al., 1996). Likewise, *O. leucoxydon* has potential to treat cancerous tumors, as its crude extracts exhibit Topoisomerase I inhibition in anti-proliferative assays (ZHOU et al., 2000). Chemically, the *Ocotea* genus revealed to possess several secondary metabolites, mainly aporphine and benzyloquinoline alkaloids, in addition to furans, lignans, bicyclo

octanes, neolignans, and sesquiterpenes (BATISTA et al., 2010; CAMARGO et al., 2013; LUDY CRISTINA; LUIS ENRIQUE, 2010).

The majority of the *Ocotea* evaluated in this research are endemic plants of Brazil where most have chemically or biologically never been evaluated before. This work aimed to study the anti-inflammatory activity of widespread *Ocotea* species in the Brazilian territory by metabolomics means.

3.1.4 *In-house* database, chemistry and biosynthesis of the *Ocotea* genus

First, as mentioned before the *Ocotea* genus is known as high oil producers plants, and their volatile compounds of several species are well described in the literature. Besides non-volatile compounds as alkaloids, furans, lignans, bicyclo octanes, neolignans, and sesquiterpenes are also reported (BATISTA et al., 2010; CAMARGO et al., 2013; LUDY CRISTINA; LUIS ENRIQUE, 2010). Thus, the *in-house* chemical database was built with non-volatile compounds to support the dereplication of the *Ocotea* extracts and accelerate the process of identification of the potential biomarkers in this research. This database included secondary metabolites from *Ocotea* spp. of different parts of the globe, to compel the maximum of the biosynthetic pathway produced by the genus.

The *Ocotea* genus generates one main class of non-volatile secondary metabolites, the alkaloids, more specifically from the class of benzyloisoquinoline and aporphine, which belongs to the class of isoquinoline alkaloids (SALLEH; AHMAD, 2017). The aporphine alkaloids have a natural isoquinoline skeleton condensed in a conjugated tetracyclic structure, which generally possesses multiple methoxys, methylenedioxy and hydroxy substituents attached to the aromatic cycles. These different substituents in different positions confer to the class an appreciable structural diversity and a broad variety of pharmacological activities (CARNEVALE NETO et al., 2019; SALLEH; AHMAD, 2017).

Aporphine alkaloids are common not only in the Lauraceae family but also occur in the Magnoliaceae, Menispermaceae, Papaveraceae, Ranunculaceae, Hernandiaceae, Annonaceae and others (COSTA et al., 2013; DEWICK, 2009). This class of alkaloids is one of the largest groups of the isoquinoline alkaloids, with more than 500 representatives known in the literature. The biosynthetic pathway of these compounds in plants is recognised by a great dependence on nitrogen sources, by mainly the amino acid tyrosine (L-Tyr). Other aromatic amino acids, such as tryptophan (L-Trp), lysine (L-Lys), ornithine (L-Orn) and histidine (L-His) are required to generate other alkaloids nuclei, for example, L-Trp is

responsible to form the indole alkaloids and the L-Orn the pyrrolidine and tropane alkaloids (DEWICK, 2009).

The secondary metabolites can be biosynthesized by a combination of several biosynthetic building blocks of the same type, or by a mixture of different building blocks, which represents different pathways in chemical biosynthesis. The isoquinoline derivatives alkaloid classes come from the mixture of the shikimate and pentose-erythrose-phosphate pathways. These pathways are also responsible to originate the aromatic amino acids L-Tyr, L-phenylalanine and L-tryptophan. This biosynthetic route is a combination of the phosphoenolpyruvate precursor with the erythrose 4-P. The former comes from the glycolysis pathway and the latter comes from the pentose-phosphate via, which is associated with the photosynthesis (DEWICK, 2009).

The enzyme tyrosine hydroxylase (E1) is responsible for the conversion of L-Tyr in L-DOPA by adding a second hydroxyl group in *ortho* position to the amino acid phenol group, and then it suffers decarboxylation by the activity of the DOPA decarboxylase (E2) leading the production of dopamine. In parallel, the L-Tyr also undergoes transamination by the activity of the tyrosine aminotransferase (E3) and PLP coenzyme giving rise to 4-hydroxyphenyl-pyruvic acid. This acid is also decarboxylated to the 4-hydroxyphenyl-acetaldehyde. Subsequently, mannich-like reaction takes place, which consists of an amino alkylation to gather both previous precursors to form the (*S*)-norcoclaurine, that is catalysed by norcoclaurine 6-*O*-methyltransferase (E4) and SAM (S-adenosyl methionine), a common cosubstrate involved in methyl group transfers reactions by S_N2-type nucleophilic substitution mechanism, to give rise to the (*S*)-coclaurine. This metabolite characterised by the presence of a methyl group at position 6 of the isoquinoline aromatic ring and is catalysed by (*RS*)-coclaurine N-methyltransferase (E5)/SAM to originate (*S*)-*N*-methylcoclaurine (DEWICK, 2009).

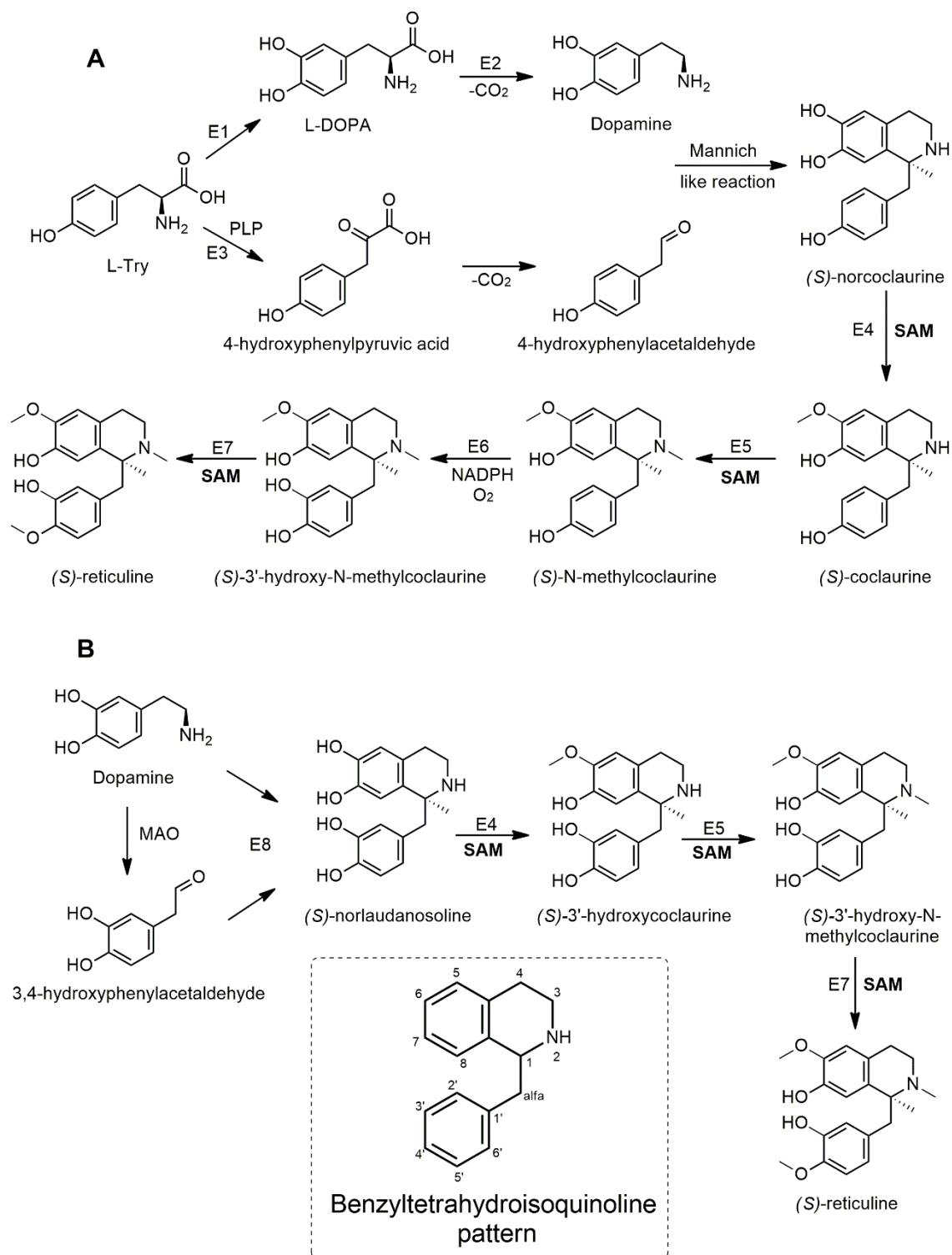
The (*S*)-*N*-methylcoclaurine precursor is reduced by the presence of a hydride-donating agent during the reduction reaction, the NADPH and by the activity of the enzyme (*S*)-*N*-methylcoclaurine 3'-hydroxylase (E6) to hydroxylate the position 3' of the benzil ring to form the tetrahydroxy substitution pattern and thus the (*S*)-3'-hydroxy-*N*-methylcoclaurine. Position 4' is after methylated by the action of (*RS*)-3'-hydroxy-*N*-methylcoclaurine-4'-*O*-methyltransferase (E7)/SAM to originate the alkaloid (*S*)-reticuline, as shown in Figure 3 (DEWICK, 2009)

In NP research the (*S*)-reticuline can also be obtained in a transgenic system by using genetic engineering to incorporate plant genes from *Coptis japonica* (Ranunculaceae) into

Escherichia coli host cells and also by incorporating bacterial gene encoding monoamine oxidase enzymes (MAO) which are important to convert the dopamine supplied to the culture into 3,4-dihydroxy phenyl-acetaldehyde. The *E. coli* host system naturally is responsible for the presence of the methylating agent SAM and the *C. japonica* for the enzymes of the biosynthetic pathways ongoing (E8: norcoclaurine synthases, E4: norcoclaurine 6-*O*-methyltransferase, E5: coclaurine N-methyltransferase and E7: 3'-hydroxy-N-methylcoclaurine 4'-*O*-methyltransferase) (DEWICK, 2009; MARINUS; LØBNER-OLESEN, 2014). Therefore, this is an alternative pathway to obtain (*S*)-reticuline via (*S*)-norlaudanoline formation, as is showed in Figure 3.

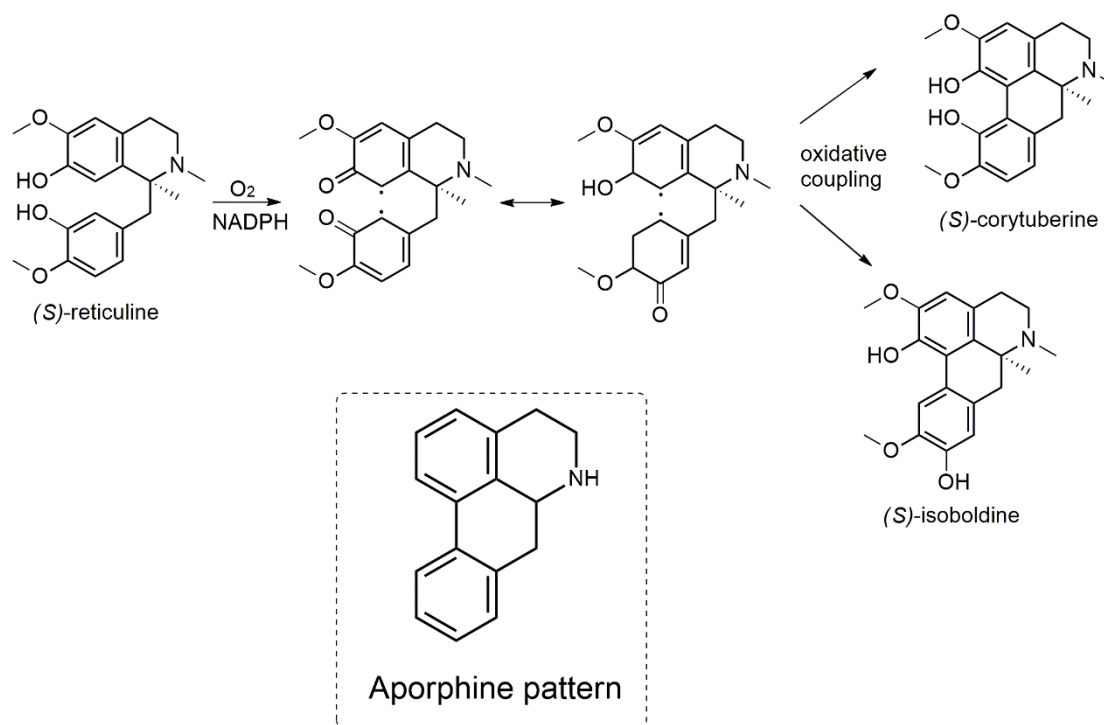
The (*S*)-reticuline precursor can undergo to phenolic oxidative coupling, which plays a significant role in modifying the basic benzyltetrahydroisoquinoline skeleton to originate several other types of alkaloids, such as the aporphines and morphinan derivatives structures (DEWICK, 2009). The isoboldine aporphine alkaloid is found in different species of the *Ocotea* genus, such as *O. caesia* and *O. lancifolia* and other species of the Lauraceae family (DEWICK, 2009; SALLEH; AHMAD, 2017). This aporphine is a product of the oxidative coupling *ortho* to the phenol group in the tetrahydroisoquinoline portion and *para* to the phenol of the benzyl substituent. The first reaction step consists of the reduction at the unprotected hydroxyl group of the aromatic rings through NADPH to form intermediate ketones. After electron oxidation leads to resonance-stabilized radicals, that causes the oxidative coupling at the position 8 of the aromatic ring of the isoquinoline structure and the position 2' of the benzyltetrahydroisoquinoline aromatic ring, as is showed in Figure 4. Furthermore, a cytochrome P-450-dependent enzyme is necessary for the catalysis of the (*S*)-reticuline oxidative coupling, for example, the CYP80G2 (DEWICK, 2009).

Figure 3 - Biosynthetic pathway of benzylisoquinoline and the alkaloid (*S*)-reticuline. A – (*S*)-reticuline produced via norcoclaurine. B- (*S*)-reticuline produced via norlaudanosoline



Source: From the author.

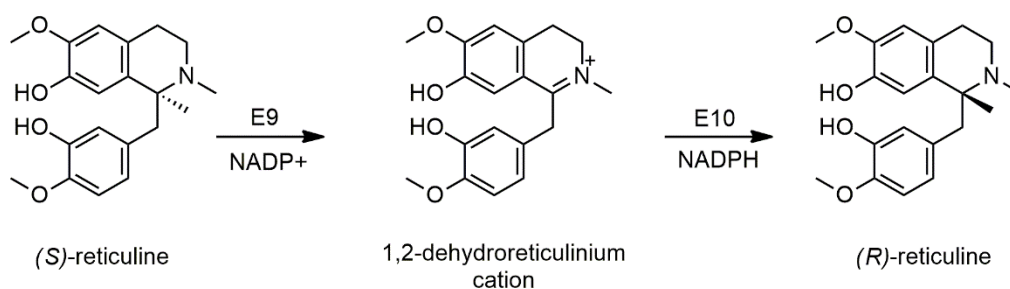
Figure 4 - (*S*)-isoboldine, an aporphine alkaloid, is produced by phenolic oxidative coupling of the (*S*)-reticuline precursor



Source: From the author.

However, some L-tyr derived alkaloids, such as opioid and morphinan alkaloids are biosynthetically elaborated from (*R*)-reticuline specimen rather than the first-formed (*S*)-isomer. Thus, the change in the absolute conFiguretion of theses alkaloids to the R enantiomeric conFiguretion is known to be achieved by an oxidation-reduction process through the intermediate 1,2-dehydroreticulinium cation. The initial oxidation turns up a planar iminium ion cation in the (*S*)-reticuline, which after reduction allows the change in the stereochemistry of the structure throughout the action of two coordinate enzymes. First, the 1,2-dehydroreticuline synthase (E9) / $NADP^+$ that causes first oxidation of the heterocyclic nitrogen and originates the 1,2-dehydroreticulinium cation, and the 1,2-dehydroreticuline reductase (E10) / $NADPH$ that causes reduction of the iminium ion to form the isomeric converted (*R*)-reticuline, as can be observed in Figure 5 (DEWICK, 2009).

Figure 5 - The oxidation-reduction process through the intermediate 1,2-dehydroreticulium cation to convert (*S*)-reticuline configuration in (*R*)-reticuline

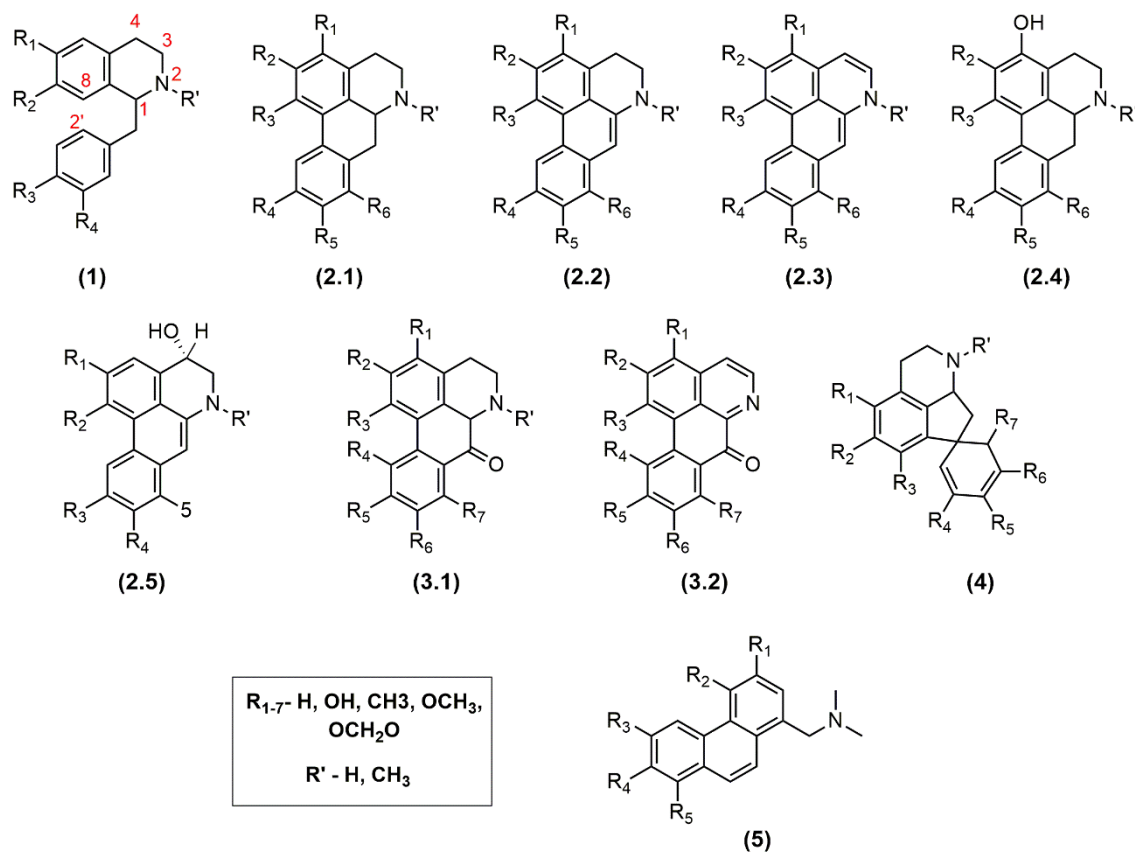


Source: From the author.

The most frequently occurring class of alkaloids in the *Ocotea* genus is the aporphines, and this alkaloid class has resulted of the modification on classic isoquinoline heterocycle, which is substituted at the C1 position by a benzyl group, to give rise to the benzylisoquinoline alkaloids, as demonstrated before by the biosynthesis pathways. Therefore, the aporphines occur when the C2' is attached to the C8 position, and thus several other derivatives are possible, such as different substituted aporphines and also oxo-aporphine, pro-aporphine, and phenanthrene alkaloids, which includes also others biosynthetic pathways (ZANIN; LORDELLO, 2007).

Thus, the aporphine alkaloids are a subgroup of heterocyclic aromatic alkaloids which have a significant physiological role in the plant kingdom and important for plant protection and resistance. However, these compounds exhibit a wide range of biological activities of interest to human health (CARNEVALE NETO et al., 2019; ZANIN; LORDELLO, 2007). The general alkaloids structure is shown in Figure 6. Particularly, a considerable number of aporphine alkaloids found in the genus *Ocotea* have notable bioactivity, such as nantenine (2.1- R₁-H, R₂/R₃-OCH₂O, R₄-OCH₃, R₅-OCH₃, R₆-H and R'-CH₃), which can act as muscle contraction blocker (Ca²⁺ translocation) and also as an α 1-adrenoreceptor antagonist. The coclaurine (1- R₁-OCH₃, R₂-OH, R₃-H, R₄-OH and R'-H) demonstrated high pronounced anti-HIV activity, and the glaucine (2.1- R₁-H, R₂-OCH₃, R₃-OCH₃, R₄-OCH₃, R₅-OCH₃, R₆-H and R'-CH₃), exhibited cytotoxicity. Moreover, the alkaloids dicentrine, which is an isomer nantenine, and the dicentrinone (3.2- R₁-H, R₂/R₃-OCH₂O, R₄-OCH₃, R₅-OCH₃, R₆-H) exhibited antineoplastic activity. Therefore, this class of compounds arouse a great interest in the researches of pharmacological studies (QUAVE; PH; QU, 2013; SALLEH; AHMAD, 2017; ZANIN; LORDELLO, 2007).

Figure 6 - (1) benzyloquinoline, (2.1) aporphine, (2.2) dihydroaporphine (2.3) didehydroaporphine (2.4) C5-*O*-aporphine (2.5) C4-*O*-aporphine (3.1) oxo-aporphine (3.2) didehydroxo-aporphine, (4) pro-aporphine and (5) phenanthrene alkaloids from *Ocotea* spp

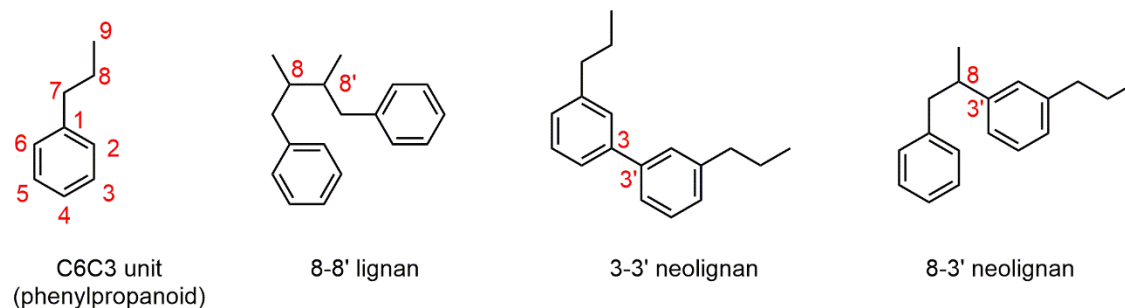


Source: From the author.

The chemical composition of *Ocotea* genus also includes other secondary metabolites, such as lignans and neolignans, sesquiterpenes, flavonoids, butenolide, benzopyrans, steroids, alkylphenols and saponins. The complete list of metabolites already isolated from *Ocotea* genus and the respective structures are at the supplemental material section (SALLEH; AHMAD, 2017). Phenolic compounds, such as lignans and neolignans are the second most common class of secondary metabolites in the *Ocotea* genus, and it is biosynthesized by the shikimate pathway and the *p*-coumaric acid is the precursor (DEWICK, 2009; SALLEH; AHMAD, 2017). Lignans and neolignans are phenylpropanoid dimers that are divided into 3 main classes: lignans, neolignans, and oxyneolignans. The differentiation is based on the character of the C–C bond and oxygen bridge joining the two characteristic phenyl propane units that make up their general structures (LI et al., 2018). Lignans occur only when the two phenylpropane units are coupled at the central carbon of the side-chain, and thus only when

the two C6C3 units are linked by a bond between positions 8 and 8' the compound is referred as lignan (Figure 7) (LI et al., 2018).

Figure 7 - C6C3 units of a phenylpropanoid and the difference between lignans and neolignans



Source: From the author.

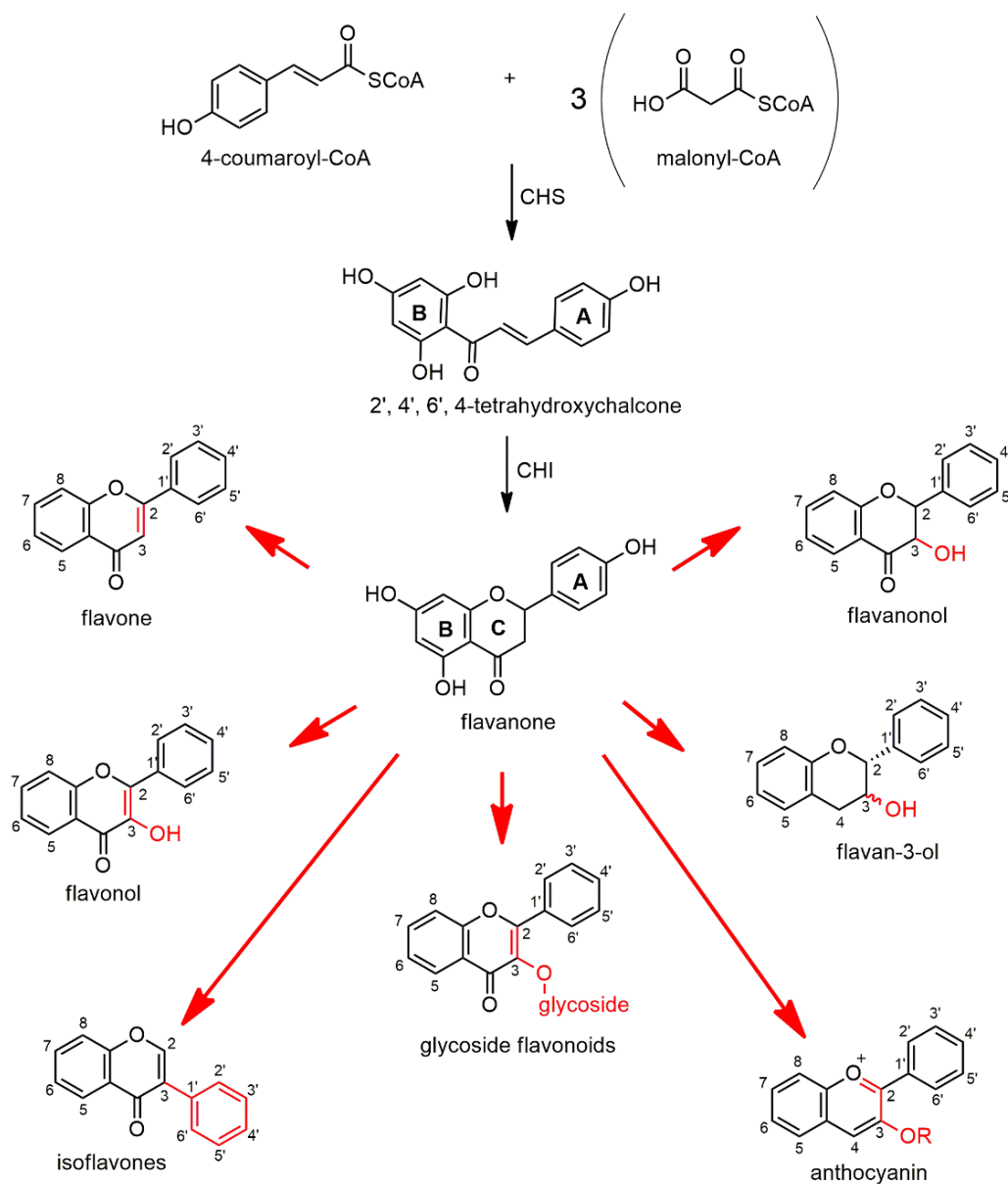
Flavonoids are together with the lignans, oxy and neolignans the second most common class of metabolites encountered in *Ocotea sp.* These secondary metabolites are very common in the Lauraceae family (LI et al., 2018; SALLEH; AHMAD, 2017). Chemically, the flavonoids are characterised by a general structure of a 15-carbon skeleton, that consists of two phenyl rings (A and B) and a heterocyclic ring (C). This carbon structure can be abbreviated C6-C3-C6 unit. The flavonoids can be subdivided into several subclasses, such as flavone, flavonol (3-hydroxy flavone), flavanone, flavanonol (3-hydroxy flavanone), flavan-3-ol, glycoside flavonoids, isoflavonoids, neoflavonoids and anthocyanidins, as showed in Figure 8 (CROZIER; JAGANATH; CLIFFORD, 2007; SANTOS et al., 2017).

A lot of effort has been made by the scientific community in elucidating the biosynthetic pathways of the several polyphenolics metabolites, such as the flavonoids, which is biosynthesized by the shikimate pathway (aromatic amino acids and phenylpropanoids) and can be united with the mevalonate pathway to yield the different existing subclasses of flavonoids. These compounds can possess chirality, and thus bioactivity or enzyme stereospecificity is intimately associated with the research of these secondary metabolites (DEWICK, 2009).

The first step in the biosynthesis of most flavonoids is the conversion of the amino acid phenylalanine in one p-coumaroyl-CoA precursor, followed by the condensation with three molecules of malonyl-CoA. Thus, the B ring is derived from the shikimate, and the A ring is a polyketide origin. The reaction is catalysed by the enzyme chalcone synthase (CHS) gives rise to the chalcone (2', 4', 6', 4-tetrahydroxychalcone). Further, the chalcone is subsequently isomerized by the enzyme chalcone flavanone isomerase (CHI) to originate the

flavanone subclass. Moreover, from these central intermediates, a wide range of branches occur, each yielding a different flavonoids class (Figure 8) (DEWICK, 2009; SANTOS et al., 2017).

Figure 8 - The summarized biosynthesis of flavonoids and the structural variation of the class



Source: From the author.

3.1.5 Mechanism of action described for *Ocotea* metabolites and aporphine alkaloids

The alkaloids classes of benzylisoquinoline and aporphine are well present in *Ocotea* genus and are described in the literature with a wide range of different bioactivities and

mechanisms of action. The aporphine alkaloids are recognised to have affinities by the dopaminergic, adrenergic and serotonergic receptors system, with potent agonist action (KAPADIA; HARDING, 2016). However, due to the purpose of this research, the focus kept only in the anti-inflammatory and cytotoxic properties.

The essential oil of *O. quixos* (*trans*-caryophyllene, methyl cinnamate, beta-selinene, alpha-humulene and delta-cadienene) showed a significant suppression effect on LPS-induced nitric oxide (NO) release from macrophages at non-toxic concentrations, and also inhibited LPS-induced PGE2 production in a significant manner. The western blotting analysis demonstrated that the *O. quixos* could suppress LPS-mediated iNOS and COX-2 elevation, and at higher concentrations revealed even better inhibition results. Also, the study showed that the inhibition ability of *O. quixos* was found to be comparable to that of curcumin, a well known anti-inflammatory natural product (AMILIA DESTRYANA et al., 2014). Diastereomeric lignans of *O. macrophylla* were revealed to be a potent dual COX-2/5-LOX inhibitor as well as platelet-activating factor (PAF) antagonist in a screening of Lauraceae lignans (COY; CUCA; SEFKOW, 2009).

Aporphine alkaloids from *Dactylicapnos scandens* (Papaveraceae) and semi-synthetic alkaloids based on these type of alkaloids demonstrated potent *in vivo* anti-inflammatory activity, and the bioassay results suggested that the mechanism involved possibly caused peripherally anti-inflammatory effects by inhibition of the expression of cytokines TNF- α , IL-1 β , and PGE2 (WANG et al., 2020).

The aporphine derivatives found in *Ocotea* genus, dicentrine and glaucine showed *in vitro* cytotoxic activity. The possible mechanisms investigated revealed that these compounds can bind to DNA and act as intercalating agents. Also part of these metabolites, such as dicentrine and dicentrinone can interfere with the catalyst activity of topoisomerases, which are enzymes that participate in the overwinding of DNA and are important for keeping the proper topology of the double-helical structure (HOET et al., 2004; SALLEH; AHMAD, 2017; ZHOU et al., 2000).

Furthermore, it is becoming clear that aporphines represent an interesting and potentially useful group of anticancer agents, and recently anti-inflammatory, however, their practical application is still limited by a lack of solid knowledge of their mechanisms of action, despite the motivating screening *in vitro* and *in vivo* results in the literature.

3.1.6 Computational chemical studies: a way forward in metabolomics analyses

Under metabolomics studies, the chemical composition of an organism, a specific metabolite or metabolic via can be detected using one or a set of hyphenated analytical techniques, such as LC-MS and Nuclear Magnetic Resonance (NMR). Metabolomics can act as a relevant tool for the identification of the majority, if not all of the plant metabolites under a given condition, qualitatively and quantitatively. As the samples, usually contain complex composition with several different molecules, metabolomic studies typically are followed by computational chemical studies with deep data mining, multivariate statistical analyses (MSA) and visual interpretation of the dataset (CHAGAS-PAULA et al., 2015a; KATAJAMAA; OREŠIČ, 2007; SHAO; LE, 2019; VINAYAVEKHIN; SAGHATELIAN, 2010).

Metabolomics analyses generate an extensive amount of raw data. This is unavoidable, and for that, we rely on software such as MZmine, Target Analyses, Masslyn, UNIFI, Weka, SIMCA and others, which perform the data treatment and still facilitate the process of spectrometric dereplication of peaks among the different samples. In general, this software allows the use of free and commercial databases as well as *in-house* ones, which facilitates targeting new substances to isolate or to evidence those with pharmacological interest. To achieve that result, the analysis of all this previously treated data is performed through statistical models, which are suitable for the study of the correlation between variables using MSA methods such as PCA (Principal Component Analysis), HCA (Hierarchical Cluster Analysis), PLS (Partial Least Squares Regression) and OPLS (Orthogonal Partial Least Squares™). The main objective of these statistical analyses is to clean the data, to facilitate the visualisation of most important differences in the chemical composition of the species. For example, by these strategies minority compounds common to plants with anti-inflammatory or any other property, that are absent in plants without this property can be statistically evidenced (JAE-WON; HEON, 2015; KATAJAMAA; OREŠIČ, 2007; YULIANA et al., 2011).

The metabolomics approaches can help to find new drug candidates more quickly by discovering active plant compounds for an increased amount of samples. The approaches include creating standards for grouping chemical components into a crude extract, as well as targeting substances that can be correlated to a particular biological activity before beginning any lengthy isolation procedure. There are two main approaches: targeted and untargeted. The targeted consist of sample analyses that are already known, and thus the extraction is more selective for quantitative monitoring of the analytes. In general, these technics require the use of chemical patterns to uncover a potential mechanism of a disease or a primary study

regarding genetic and epigenetic changes. While the untargeted is looking at unknown components in a sample, and thus a more comprehensive extraction is necessary to look for any type of biomarkers of activity. Moreover, biomarkers of activity can be defined as a substance that indicates a normal biological process, pathological process or a pharmacological response (CHAGAS-PAULA; OLIVEIRA; FALEIRO, 2015; DE VOS et al., 2007; VINAYAVEKHIN; SAGHATELIAN, 2010).

At present, the metabolic profile can be subdivided into metabolic fingerprinting and metabolic footprinting. In the untargeted approach, it is common to obtain the metabolic fingerprints, which consist of obtaining a semi-quantitative chemical profile of a sample in a given biological condition that is reliable to the set of all metabolites produced by that organism. The footprinting comes from metabolic engineering that refers to the production of metabolites by a cell under controlled and determined conditions that is used to increase the variability of metabolites or to increase the production of specific metabolites and a biosynthetic pathway (SUMNER et al., 2007; VAN DER KOOY et al., 2009). However, above all, employing metabolomics studies significant breakthroughs in biomarker discovery have been achieved together with faster identification of novel metabolites. In addition to new biological activities for the known as well as an in-depth investigation of biological pathways and mechanisms of action in many different organisms (KOSMIDES et al., 2013; VAN DER KOOY et al., 2009; YI et al., 2016). Also, a series of essential applications are already available tools on the market, such as for the obtainment of consistent quality control of the herbal material through the comparative metabolic profile (metabolic fingerprints and footprinting) (KOSMIDES et al., 2013; VAN DER KOOY et al., 2009; YI et al., 2016).

Currently, in the field of drug discovery, metabolomics is being used to analyse several plant products, for tracing the profile of the metabolites present and statistically correlate with pharmacological bioactivity or even to key metabolic routes for drug targeting. Thus, these novel chemical approaches represent a viable modern tool for the drug discovery process and to the screening of complex mixtures of numerous chemical components in crude extracts (CHAGAS-PAULA et al., 2015a; ROUX et al., 2011; VINAYAVEKHIN; SAGHATELIAN, 2010; WOLFENDER; MARTI; QUEIROZ, 2010; YULIANA et al., 2011).

Thus, in this work, we have applied the Ultra-Performance Liquid Chromatography (UPLC) with Electrospray Ionisation (ESI) coupled to a quadrupole time-of-flight mass spectrometer (UPLC-ESI-QTOF/MS) to analyse metabolites produced by the *Ocotea* genus and correlate them with LPS-induced PGE2 inhibition pathway throughout metabolomics means.

3.2 Material and methods

3.2.1 Plant material (*Ocotea* spp.)

A total of 60 vouchers containing 60 different *Ocotea* spp. were donated for this research from CESJ herbarium – Federal University of Juiz de Fora (UFJF) and OUPR herbarium from Federal University of Ouro Preto (UFOP) in Brazil (Tables S1 and S2). It was provided 1 to 3 leaves by specie according to the leaf size and availability of more than one voucher for the same species. Most of the evaluated species are endemic to Brazilian biomes. The study had the access registered on the National System for Governance of Genetic Heritage and Associated Traditional Knowledge (SisGen # A5A8F67).

The *Ocotea* samples investigated in this work received an identification code (ID) according to the herbarium of obtainment (I-UFOP-OUPR and II- UFJF-CESJ). The voucher specimens is also described: *O. aciphylla* (AY II – CESJ 62125), *O. acutifolia* (AU II – CESJ 70433), *O. amazonica* (AM II – CESJ 37028), *O. brachybotrya* (BA II – CESJ 45562), *O. bragai* (BR II - CESJ 43604), *O. bicolor* (BI II – CESJ 50826), *O. caesia* (CA I – OUPR 20972), *O. calliscypha* (CL I – OUPR 18196), *O. catharinensis* (CT II – CESJ 43309), *O. cernua* (CE II - CESJ 32533), *O. complicata* (CM II – CESJ 42369), *O. corymbosa* (CO II - CESJ 43310), *O. cujumarum* (CJ II – CESJ 38725), *O. diospyrifolia* (DO II – CESJ 62011), *O. dispersa* (DI I – OUPR 27830), *O. divaricata* (DV II – CESJ 41125), *O. elegans* (EL II – CESJ 44370), *O. felix* (FE I - OUPR 8331), *O. glauca* (GL I – OUPR 5467), *O. glaucina* (GU II – CESJ 50402), *O. glaziovii* (GZ II – CESJ 50895), *O. guianensis* (GA II – CESJ 52484), *O. hypoglauca* (HY I – OUPR 1430-A), *O. indecora* (IN II – CESJ 31537), *O. kuhlmannii* (KU I - OUPR 62356), *O. lanata* (LA II - CESJ 30009), *O. lanceolata* (LN II - CESJ 59481), *O. lancifolia* (LC II – CESJ 45567), *O. langsdorffii* (LG II – CESJ 16362), *O. laxa* (LX I - OUPR 6827), *O. lobbii* (LO II – CESJ 42370), *O. longifolia* (LF II - CESJ 32218), *O. minarum* (MI II – CESJ 47503), *O. nitidula* (NT I – OUPR 18161), *O. nectandrifolia* (NE II – CESJ 59418), *O. nitida* (NI II – CESJ 44602), *O. notata* (NO II – CESJ 62057), *O. nummularia* (MU I - OUPR 20426), *O. nutans* (NU I - OUPR 24804), *O. odorifera* (OD II - CESJ 31144), *O. paranaensis* (PA II – CESJ 63922), *O. percoriacea* (PE I – CESJ 7649), *O. pomaderroides* (PO I – OUPR 44369), *O. porosa* (PR II - CESJ 38347), *O. pretiosa* (PT II - CESJ 27831), *O. puberula* (PU I – OUPR 21697), *O. pulchra* (PL II - CESJ 47987), *O. pulchella* (PC II 1 – CESJ 49900), *O. pulchra* (PH II - CESJ 59429), *O. spectabilis* (SP I – OUPR 33301), *O. spixiana* (SX I - OUPR 1390), *O. tabacifolia* (TA I – OUPR 45565), *O. teleiandra* (TL II 2 -

CESJ 34581), *O. tenuiflora* (TE II 1 – CESJ 33596), *O. tristis* (TR I – OUPR 6504), *O. vaccinioides* (VA I – OUPR 18269), *O. variabilis* (VR I – OUPR 19806), *O. velloziana* (VZ II 2 – CESJ 20721), *velutina* (VL II - CESJ 61392) and *O. villosa* (VI II - CESJ 50002).

3.2.2 Drugs and reactants

Dexamethasone (Eurofarma), Indomethacin (UNIFAL pharmacy), Cloranfenicol (UNIFAL pharmacy), PGE2 standard (Sigma Aldrich), *E. coli* Lipopolysaccharides (Sigma Aldrich), and Liquid Nitrogen (Linde). All solvents used were HPLC grade, Hexane (Synth and Tedia), Methanol (Synth and Tedia), Ethanol (Synth and Tedia), Acetonitrile (Synth and Tedia), deuterated H₂O (miliQ) and Formic acid (Chemco-Brazil).

3.2.3 Metabolomics extracts preparation

The 60 samples containing the different species were separately weighed (20 mg) and then crushed using pistil and liquid nitrogen until pulverized. To the powdered material, 1.7 mL of the ethanol grade HPLC: water MiliQ, 7:3 ratio, was added to extract the most of the polar and semi-polar compounds. For extraction, all samples were placed in a warm ultrasound bath (35°C) for 15 minutes (170 W, 50 kHz, L100 Schuster), and then centrifuged at 22°C and 10.000 rpm. The supernatant was collected, partitioned with HPLC hexane grade (2 x 200 µL), to ensure removal of fatty substances, and then filtered through the polytetrafluoroethylene (PTFE) filters with 22 µm diameter of the pore. All extracts were dried using Speed Vacuum equipment for 3 h at 40°C (Figure 2). The dried samples were kept at freezer -20°C until the moment of the analyses (DE VOS et al., 2007; RUDAZ, 2015).

3.2.4 Analytical UPLC-ESI-QTOF-MS metabolomics experiments

For metabolomic MS Fragment ion spectra (MS^E) analyses were performed using a MasslynxsTM MS Software (Waters Corp., Milford, USA) and UPLC-QTOF-MS (Xevo-QTOF/MS, Waters Corp., Milford, USA). All extracts previously partitioned with hexane and filtered on a PTFE filter, as mentioned above, were subjected to UPLC-QTOF-MS at 1 mg/mL. For the development of the chromatographic method, an analytical Quality Control (QC) sample was prepared by gathering together 10 µL of each *Ocotea* sp. extract involved

in the experiment, for the obtainment of 600 μL in a total volume for the QC sample, and it was injected an aliquot of 5 μL .

The initial chromatographic separations were applied only the QC sample, performed on an ultra-analytical C18 reverse phase column ACQUITY UPLC®HSS T3 (1.8 μm , 100 x 2.1 mm) to develop the method of analysis. The column oven was maintained at 40°C, and the mobile phases consisted of solvent A, water MiliQ acidified (1% formic acid v/v), and solvent B, acetonitrile (ACN). The gradient elution method of 10 min with 0.5 mL/min of flow rate. The chromatographic run started with 1% ACN and 99% H₂O, in 0.1 min 85% H₂O and 15% ACN, in 7.5 min 20% H₂O and 80% ACN, in 8.5 min 1% H₂O and 99% ACN, in 8.6 min 99% H₂O 1% ACN and until 10 min with 99% H₂O 1% ACN. The injection volume was defined as 5 μL .

The ESI was operated in the positive and negative ionisation mode. The mass spectrometers parameters were executed with alternative high and low energy scans, which are recognised as the MS^E acquisition mode. The operating equipment parameters were as follows: cone voltage, 40V; capillary voltage, 3.0 kV; cone gas flow, 30 L/h; desolvation temperature, 300°; source temperature, 120°; and desolvation gas flow, 600 L/h. The mass scan range was set to 100 and 1000 m/z . The MS data were collected in continuous mode, using the lock spray for calibration of the MS equipment, and therefore to guarantee accuracy and reproducibility of the analyses. A concentration of 200 pg/mL leucine enkephalin was used as lock mass, identified by the m/z 554.2622 (ESI-) and m/z 556.2768 (ESI+). The lock spray frequency was established of 10 s.

Samples were analysed randomly, with one replicate, one blank and the QC sample at the beginning, middle and end of the chromatographic batch. Data treatment and MS^E dereplication step were performed for all samples using the UNIFI Scientific Information System software 1.8.1 (Waters Corp., Milford, USA). It was used UNIFI software platform to combine high-performance LC and MS data (both quadrupole and TOF) into a single solution that encompasses data acquisition, processing, visualisation, reporting, and compliance of the raw data (ROSNACK et al., 2016; YI et al., 2016), as detailed at section 3.2.6.1

3.2.5 *Ex vivo* anti-inflammatory evaluation

An *ex-vivo* anti-inflammatory screening was performed using human blood (Research Ethics Committee of Federal University of Alfenas 89325818.1.0000.5142) for quantitative evaluation of inflammation chemical mediators in plasma by quadrupole LC-MS/MS. The

dried plant extracts samples were resuspended at a ratio of 8:2 (Ultrapure water: HPLC ethanol) to reach the initial concentration of 1 mg/mL. The sample preparation followed the same method used for metabolic analysis. The pure substances were tested at a concentration of 1 µg/mL, while extracts at 10 µg/mL, for dilution PBS 1x was prepared and added. The Lipopolysaccharides (LPS, *E. coli* O26: B6) was used as blood inflammation inducer. The LPS solution was prepared at a concentration of 100 µg/mL. Initially, the samples were incubated with blood and diluted LPS in sterile 96-well plates. The sample sequence plating was 25 µL of the sample at 10 µg/mL, 200 µL of blood in all wells and 25 µL of LPS solution, with a total volume of 250 µL in each well (blood + samples + LPS), and thus extracts reach the concentration of 1 µg/mL inside the wells.

For the positive control, the anti-inflammatory references, SAID and NSAID, dexamethasone and indomethacin were used respectively. Thus, for the positive control, 25 µL of DEX and IND at 10 µg/mL + 200 µL blood + 25 µL LPS at 100 µg/mL, the same plating order was followed. Thus, the final concentration in the plate reaches 1 µg/mL for controls and 100 µg/mL for the LPS. For the negative control, 25 µL of Phosphate buffered saline 1x (PBS - pH 7.2; 0.15 M chloride; 0.01 M phosphate) + 200 µL blood + 25 µL LPS at 100 µg/mL. Plates were placed for 24 hours in an incubator with 5% CO₂ atmosphere at 37 °C. After incubation time, the plates were centrifuged for 5 min at 1000 rpm and 4 °C and 100 µL of plasma was removed from the blood of each well and frozen for posterior analyses. This methodology can be used for determining several important chemical mediators, such as PGE₂, TNF-α and different interleukins. Through LC-MS/MS we performed the PGE₂ quantification.

3.2.5.1 Prostaglandin E₂ (PGE₂) quantification by UPLC-MS/MS

The plasma aliquot obtained from the previous step was carefully manipulated in the absence of direct light once PGE₂ is photo sensible. For sample preparation, 100 µL of each plasma sample was spiked with 500 µL of the precipitating agent, ACN:MeOH (1:1, v/v) and centrifuged (6000 rpm, 4°C) for 10 min. The supernatant was transferred to a polypropylene tube (15 mL) containing 4.5 mL of ultrapure water.

The plasma samples were carefully manipulated for avoiding direct contact with light. The samples were loaded on a Supelco (LC-18 SPE 500mg, #57012) cartridge after conditioning with 2 mL of MeOH, followed by 2 mL of acidified ultrapure water (0.1 %) with acetic acid. The cartridges were washed with 2 mL of aqueous acetic acid solution (0.1%),

and the analyte was eluted into pre-labelled eppendorf tubes using a 1.8 mL solution of 0.1% methanolic acetic acid solution. The eluate was evaporated to dryness in a Speed Vacuum system and for the LC-MS analyses reconstituted with 100 μ L of ACN (HPLC grade). Chloramphenicol (CAP) at the concentration of 25 $\text{ng}\cdot\text{mL}^{-1}$ was used as an Internal Standard (IS).

The UPLC-MS/MS analyses were carried out using an ultra-performance liquid chromatography system model 8030 (Shimadzu®, Kyoto, Japan) equipped with a triple-quadrupole mass analyser operating in the negative mode. Positive control samples (20 μ L), QC or calibration points were injected in the chromatographic system containing a Kinetex® C18 (1,7 μm , 2,1 x 100 mm) column maintained at 30°C. The mobile phase consisted of (A) ultrapure water (with formic acid 0.1%) and (B) acetonitrile at a constant flow rate of 300 $\mu\text{L}\cdot\text{min}^{-1}$. The gradient elution increased gradually from 40% B to 100% B (0-3 min), which remained in this configuration up to 4 min. After, the method returned to 40% B in 0.5 min, followed by 4 min of re-equilibration.

The overall analysis time was 8.5 min. The source and MS parameters were as follow: nebulizing gas nitrogen at flow 2 L/min, drying gas nitrogen at flow 15 $\text{L}\cdot\text{min}^{-1}$, interface voltage 3.5 kV, DL temperature 250 °C, oven temperature 35 °C, detector voltage 2.44 kV and Collision gas argon at 230 kPa. Treatment and data acquisition were performed using LabSolutions® software. Table 1 shows the SRM transitions for the PGE2 and the IS. Analytical validation was performed previously (SANTOS et al., 2019) and based on the ANVISA resolution RDC N° 27, 17/05/2012. Linearity, precision, accuracy, limit of quantification (LOQ), selectivity, matrix and carry-over effect were evaluated and determined. The calibration curve for PGE2 was linear from the lower quantification limit (LQL – 6.25 ng/mL) to the higher quantification limit (HQL – 400 ng/mL).

Table 1 - The SRM parameters for PGE2 and CAP. Q1 – Precursor ion SRM transition, CE- collision energy (eV), Q3- Fragment ion SRM transition – CAP/PGE2 negative mode

Compound	Transition (m/z)	Q1	CE	Q3
CAP	320,90>152,10	16	20	29
PGE2	351,10>271,30	13	18	28

Source: From the author.

3.2.6 Metabolomic studies

3.2.6.1 Data treatment and dereplication strategies

For the metabolomics study, 17 voucher replicates were included to check the chemical composition similarity of few *Ocotea* species of this study. The replicates of each specie were collected from different locations in Brazil. These replicates were also donated from UFOP and UFJF, as these vouchers were present in high quantity in the respective herbariums. The replicates vouchers included were *O. dispersa* (DI II – CESJ 51299), *O. glauca* (GL II – CESJ x), *O. lancifolia* (LC III – CESJ 44598A), *O. langsdorfii* (LG I – OUPR 44370), *O. laxa* (LX II – CESJ 46058), *O. nutans* (NU II – CESJ 59363), *O. percoriaceae* (PE II – CESJ x), *O. pomaderroides* (PO II – CESJ x), *O. puberula* (PU II – CESJ 68881), *O. pulchella* (PC II - CESJ 60060), *O. spectabilis* (SP II – CESJ x), *O. spixiana* (SX II – CESJ x), *O. ternuiflora* (TE II – CESJ 38743), *O. tristis* (TR II – CESJ 61089), *O. tristis* (TR III – CESJ 49707), *O. vaccinoides* (VA II – CESJ 50822), *O. velloziana* (VZ II 1 – CESJ 50423).

All MS^E data collected from the MasslynxsTM MS Software was processed within UNIFI software for ESI MS+ and ESI MS-. The chromatographic data at UNIFI goes through automatic 2 phases pre-treatment data: 1) Peak detection and alignment processing algorithms for chromatographic peak corrections. 2) Deconvolution, deisotope, peak alignment and baseline correction stages. Subsequently, the parameters used for the data treatment were peak intensity threshold of 250 counts for high-energy prior to fragment detection and 500.0 counts for low energy to detect precursor ions. The noise was established as 10.000 peaks per channel and the error 10 ppm (mass tolerance). For adduct search, it included in the positive mode Na⁺ and K⁺ and +Cl⁻, +HCO₂⁻ for the negative mode. RT tolerance was defined as 0.3 min. The area of each ion was normalised regarding the total ion count, to generate a data matrix with the *m/z* value, RT and the normalized peak area.

An *in-house* database was constructed using 292 monoisotopic mass and structures in .mol extension of the already identified substances in the literature for the *Ocotea* genus. The database was built by the use of DNP© (Dictionary of Natural Products), SciFinder Scholar®, HMDB® (The Human Metabolome Database), Pubchem® (MoNA – Massbank of North America), Chemspider®, J-Global® and KNApSAcK (A Comprehensive Species Metabolites Relationship Database). For literature research, the key-words “*Ocotea*”, “chemistry of *Ocotea*”, “bioactivity of *Ocotea*”, “pharmacological activity of *Ocotea*” and “medicinal property of *Ocotea*” were used to search in the google scholar platform. It was

considerate published articles from the years 1980-2019. The database included chemical and usual name, molecular formula, monoisotopic mass, class of secondary metabolites, *Ocotea* species found, related activity and literature source. The structures were manipulated using the software ChemSketch 2.0 2019.2 (ACDLabs, Toronto, Canada) and ChemDraw ultra 12.0 (Perkin Elmer Informatics, Cambridge, England). The metabolites were dereplicated also using the UNIFI standard database. Through MS^E we proceeded the dereplication of most the compounds and few of them by MS/MS experiments. The confidence level of the identification performed was stated as level two according to the current metabolomics identification standards (CREEK et al., 2014; SPICER; SALEK; STEINBECK, 2017; SUMNER et al., 2007).

3.2.6.2 Multivariate Statistical Analyses (MSA)

The UPLC three-dimensional raw data including peak area and RT-*m/z* pair was exported from UNIFI software in .xlsx (excel reading format) and imported through EZinfo 3.0.3 (UMETRICS, Umeå, Sweden) for MSA. The analysis of the pharmacological activity was analysed *in-silico* together the metabolic profile. The dataset was initially analysed by unsupervised statistical analyses, the PCA (Principal Component Analyses) followed by supervised PLS-DA (Partial Least Squares Regression - Discriminant Analysis). The data were mean-centered or Pareto scaled before PCA and PLS-DA analysis (CHAGAS-PAULA et al., 2015b; CRAGG; PEZZUTO, 2016; ROUX et al., 2011; XI et al., 2015; YULIANA et al., 2011).

3.3 Results and discussion

3.3.1 *Ocotea* extracts and *in-house* database

The dried extract was separately weighted; each respective extract yield was calculated and shown in the attachment section (Table S3). The *in-house* database has previously indicated that the most frequently occurring class of alkaloids in the *Ocotea* genus is the aporphine alkaloids, which are derived from benzyloisoquinoline core when the C2' is attached to the C8 position at backbone structure through an oxidative coupling mechanism. From this chemical pattern, several other derivatives are possible, such as different substituted

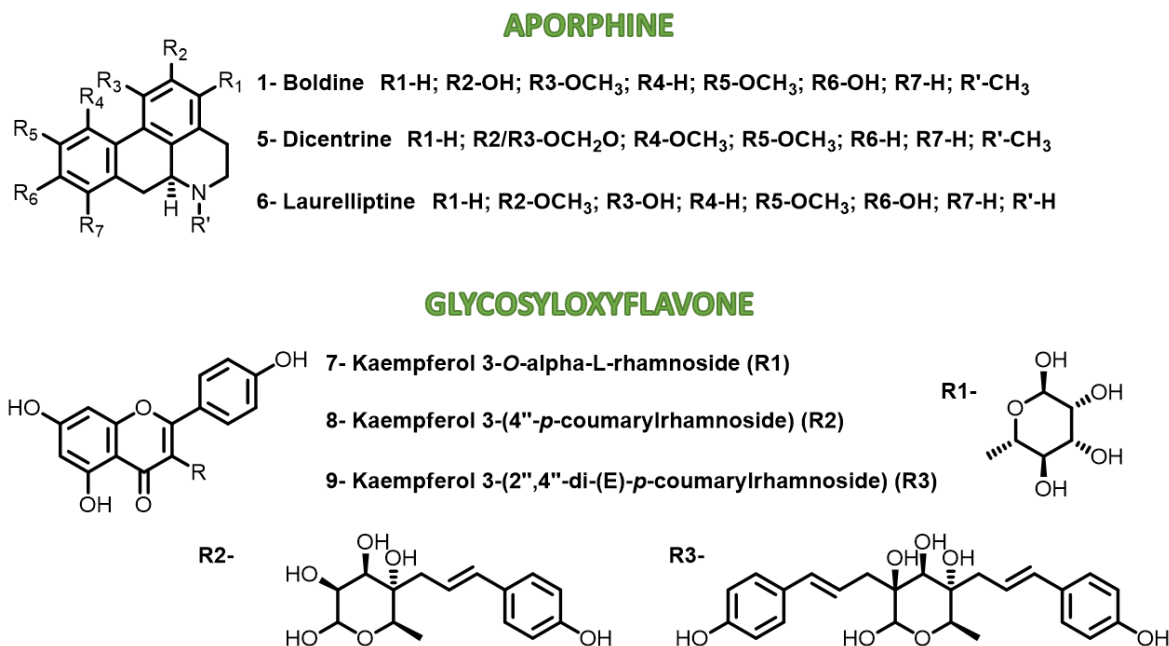
aporphines and also oxo-aporphine, pro-aporphine, and phenanthrene alkaloids (CARNEVALE NETO et al., 2019; DEWICK, 2009; ZANIN; LORDELLO, 2007).

The aporphine alkaloids are common not only in the Lauraceae family but also in the Magnoliaceae, Menispermaceae, Papaveraceae, Ranunculaceae, Hernandiaceae, Annonaceae and others (COSTA et al., 2013; DEWICK, 2009; WANG et al., 2019). This class of alkaloids is one of the largest groups of the isoquinoline alkaloids, with more than 500 representatives known in the literature. The isoquinoline derivatives alkaloid classes come from the mixture of the shikimate and pentose-erythrose-phosphate pathways, which the main precursors are the aromatic amino acids tyrosine (L-Tyr), L-phenylalanine and L-tryptophan. The biosynthetic pathway in plants of the aporphines and other with the tetrahydro-benzylisoquinoline core is derived from L-Tyr, and a result of the condensation of dopamine and 4-hydroxyphenylacetaldehyde (DEWICK, 2009).

Also as revealed by the *in-house* database the aporphine alkaloids of the evaluated *Ocotea* species have the tetrahydro-benzylisoquinoline core with multiple methoxys, methylenedioxy and hydroxy substituents attached to the aromatic cycles. These different substituents in different positions confer to the class an appreciable structural diversity and a broad variety of pharmacological activities (CARNEVALE NETO et al., 2019; SALLEH; AHMAD, 2017).

A wide range of aporphinic structures was putatively identified in the *Ocotea* extracts using the comprehensive *in-house* database built. In figure 9 is shown the summary of the highest peak areas found in the QC sample for both positive and negative ionization modes.

Figure 9 - Molecular structure of metabolites annotated with high peak intensity levels identified within the QC ESI MS+ and MS- sample



Source: From the author.

For example, the aporphine isomers of (1) boldine, (5) dicentrine and (6) laurelliptine were dereplicated and found with high-intensity levels in QC ESI MS⁺ extract. Moreover, the most detected class of compounds in the QC ESI MS⁻ were glycosides flavonoids, such as (7) afzelin, (8) kaempferol 3-(4''-p-coumarylrhamnoside) and (9) kaempferol 3-(2'',4''-di-(E)-p-coumarylrhamnoside). However, the presence of a considerable amount of hydroxyl groups in the alkaloid backbone radicals of some aporphine alkaloids guaranteed their annotation in the QC ESI MS⁻ as well, such as the aporphine alkaloids (1) and (6) due to deprotonations of hydroxyl groups in the chemical core.

3.3.2 Data treatment and QC metabolic fingerprint

Electrospray ionization (ESI) was chosen for this work to provide an analysis of non-volatile metabolites from low to high molecular weight compounds in the samples. The ESI spectrum is best explored when associated with MS Fragment ion spectra (MS^E) and tandem mass spectrometry (MS/MS) which can increase the identification level of the profiling compounds. The ESI technic displays a low degree of fragmentation and fewer product ions in chromatograms when the obtained precursor ions are associated to a high energy

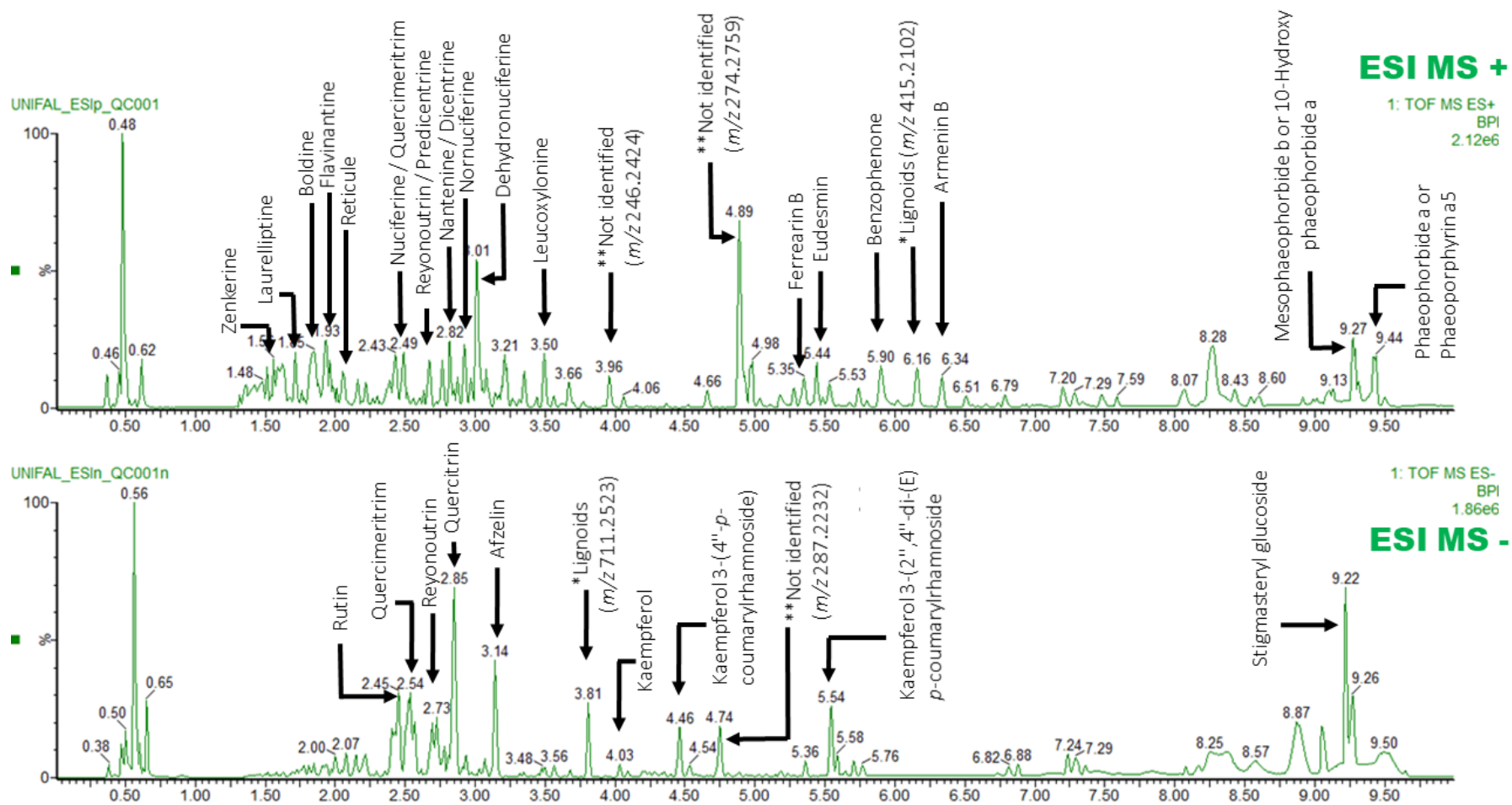
fragmentation strategies, a more complete MS data can be achieved (CARNEVALE NETO et al., 2019; STÉVIGNY et al., 2004).

A rapid and consistent method of analyses was employed using UPLC-ESI-QTOF-MS supported by MS^E data acquisition for chemical structure identification of the *Ocotea* compounds. This technique possesses high MS sensitivity and allows getting the exact mass and fragmenting ion spectra of every detectable component in the sample. Thus, more comprehensive chemical profiling was accomplished.

For the metabolomics approaches, the QC sample, which is the sample that gathers most of the metabolites in the study, was used to determine the most satisfactory chromatographic method for separation of the compounds. Thus, as appropriate distribution of the peaks was observed in the QC chromatograms, the method was applied to the different species investigated, what has indicated that the developed method was well fitted for the metabolomic purpose.

By the MS^E acquisition, more than 10.000 peaks were detected accounting for both ESI MS⁺ and ESI MS⁻. By the developed QC MS method, we explored the chemical profile of the extracts and created a reliable MS metabolic fingerprint for each *Ocotea* species involved in the study. The metabolic fingerprint of samples is at the attachment section (Fig S1-S26). Most of the *Ocotea* extracts ionised preferably in the positive mode, as the QC ESI MS⁺, which showed an increased number of peaks when comparing the same RT shift of the QC ESI MS⁻ metabolic fingerprint. The highest intensity peaks were assigned in Figure 10.

Figure 10 - ESI MS metabolic fingerprint of the positive (above) and the negative (below) mode of the QC sample. TICs chromatograms are displayed as Based Peak Ion (BPI)



Source: From the author.

The raw data treatment was done through UNIFI software combining LC and MS data (peak area, m/z and RT), which was exported for compounds identification, metabolic fingerprint obtainment and to the visual data interpretation by MSA models. The reproducibility of the analytical chromatographic runs performed in this study consisted of injections of the QC replicate and a randomly selected sample (extract VI II). These samples were injected in the beginning, the middle and at the end of the UPLC-ESI-QTOF-MS 78 sample sequence, and reproducibility was double-checked by matching data (peak area, m/z and RT) of different chromatograms and by PCA analyses.

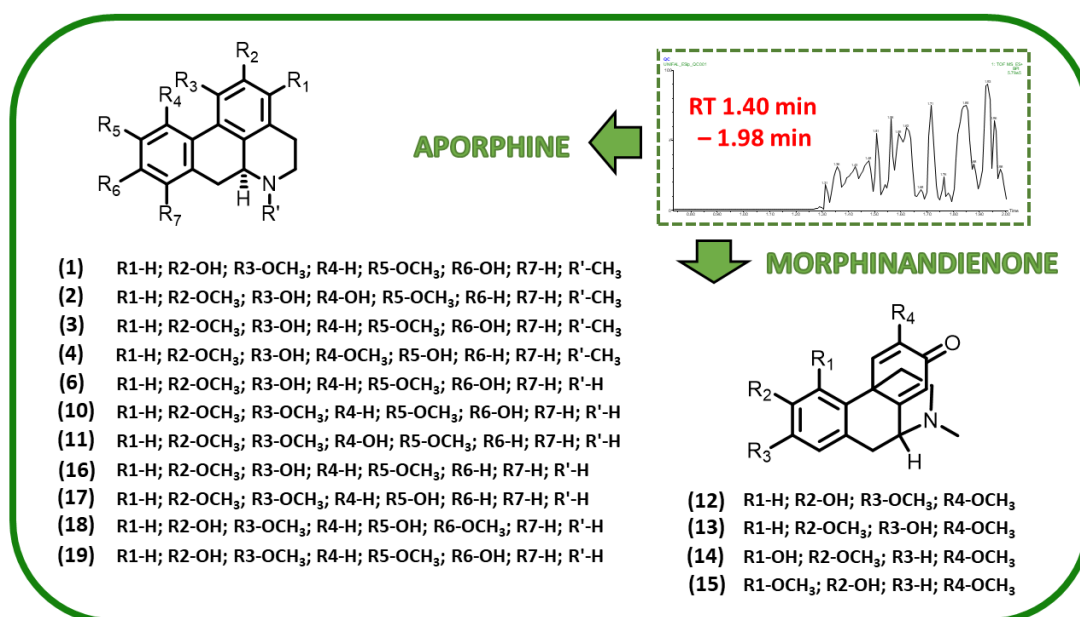
At this stage, different classes of metabolites were identified, such as phenolic and fatty acids, flavonoids, sesquiterpenes, lignans, neolignans, butenolide and alkaloids (mainly the aporphine class). In general, the aporphinic alkaloids display characteristic MS fragmentation patterns, which are strategic to get a faster identification. Although, unequivocal characterization can be challenging only by one analytical technique, due to the widespread isomerism of the class, associated with potential peripheral oxidation reactions on the isoquinoline core. These facts lead to structurally similar metabolites and the same elemental composition (CARNEVALE NETO et al., 2019; STÉVIGNY et al., 2004). The proper identity of an isomer can only be discriminated in MS by co-elution with chemical standard and MS/MS experiments. However, isomers as epimers sometimes still can not distinguishable. The stereochemistry of compounds with a high degree of structural similarity need other additional analytical characterization strategies to confirm the chemical differentiation, as the case of the aporphines: (1), (2) corytuberine, (3) isoboldine and (4) isocorytuberine, which display the same parent ion and almost the same product ions (Figure 11/12; Table 2). Nevertheless, the ratio and proportion of fragments might help to elucidate epimers, and also biosynthesis studies can provide substantial support for identification, for example, there is the stereochemistry of some secondary metabolites which are characteristic of a specific plants family.

Through the *in-house* database and the UNIFI spectral database metabolites were assigned by monoisotopic match (MS^1). Subsequently, by the MS^E high-energy channel spectrum analyses the MS^E ion fragments were matched with fragments described in scientific publications, and from the MoNA and HMDB spectral library. For example, in the QC ESI MS^+ nine alkaloids eluted at very close RTs 1.83 – 1.96 min and displayed the same elemental composition of $C_{19}H_{21}NO_4$ and observed parent ion at $m/z = 328.154$. Throughout of MS^E fragment analyses, compounds were putatively annotated as (1), (2),

(3), (4), (10) laurotetanine and (11) norisocorydine and the other four alkaloids dereplicated as (12) flavinantine, (13) pallidine, (14) sinoacutine and (15) isosinoacutine (Figure 11; Table 2). The compounds (1), (2), (3), (4), (10) and (11) are representatives of aporphine alkaloids, while the (12), (13), (14) and (15) belongs to the morphinandienone alkaloids class, which are also derived from benzyltetrahydroisoquinoline intermediates, however, the classical B/C rings are fused cycles. The stereochemistry of the fused rings is crucial for proper binding in the receptors and thus for the expression of biological activity (FUJII et al., 1970).

Also, at the beginning of the QC ESI MS+ chromatographic run, two alkaloids were dereplicated at RT 1.55-1.58 min with elemental composition $C_{18}H_{19}NO_3$ and parent ion at m/z 298.143 as the aporphines (16) zenkerine and (17) tuduranine. Additionally, four other alkaloids were dereplicated at close RT 1.60-1.76 min with elemental composition $C_{18}H_{19}NO_4$ and parent ion at m/z 314.139, as the aporphines (6), (18) laetanine and (19) laurolitsine (Figure 11; Table 2). More specifically, these alkaloids isomers alternate the radical positions of the hydroxyl and methoxy groups attached to the aromatic rings, however, they only differ from boldine isomers due to the N-substituted radical be hydrogen ($R'-H$) instead of a methyl group ($R'-CH_3$), and thus their molecular formula display 14 daltons fewer mass units ($[M-CH_2]^+$).

Figure 11 - Structure of the aporphine alkaloids isomers with elemental composition $C_{19}H_{21}NO_4$, (1-boldine, 2-corytuberine, 3-isoboldine, 4- isocorytuberine, 10-laurotetanine, 11-norisocorydine 12-flavinantine, 13-pallidine, 14-sinoacutine and 15-isosinoacutine), the isomers with elemental composition $C_{18}H_{19}NO_3$ (16-zenkerine and 17- tuduranine) and the isomers with elemental composition $C_{18}H_{19}NO_4$ (6-laurelliptine, 18- laetanine and 19- laurolitsine)

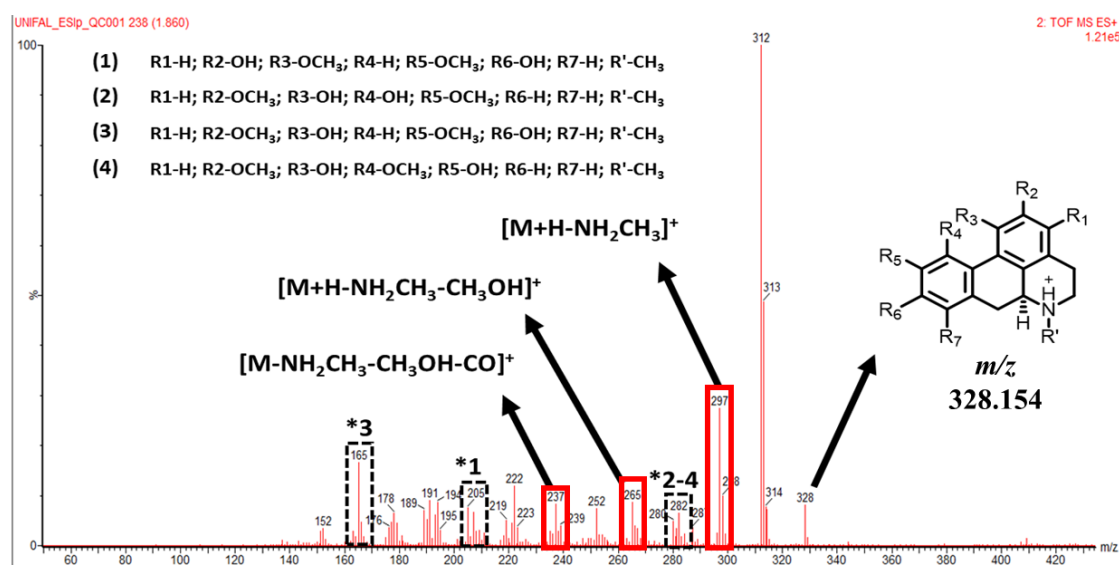


Source: From the author.

For the MS^E fragments analyses, the data were obtained from the high-energy channel chromatograms. For the isomers (1), (2), (3) and (4) the appearance of the fragment ion at m/z 297.1028 (C₁₈H₁₇O₄⁺) in the high-energy chromatogram was attributed to the elimination of CH₃NH₂. Successively, the presence of the fragment ion at m/z 265.0842 (C₁₇H₁₃O₃⁺) attributed to the loss of CH₃OH. The neutral loss of the CH₃OH might occur from vicinal hydroxyl and methoxy groups in the aromatic aporphine rings (WANG et al., 2019). The presence of the fragment ion at m/z 237.0919 (C₁₆H₁₃O₂⁺) has resulted from the neutral loss of CO from fragment ion at m/z 265.0859. Furthermore, the neutral loss of CH₃OH followed by CO in vicinal hydroxyl and methoxy groups is a consequence of the electron-withdraw inductive effect, which plays a significant role in the fragmentation pathway of aporphine alkaloids (WANG et al., 2019).

The differentiation of the isomers is only possible throughout the presence of low-intensity fragment ions in the MS^E spectrum, according to spectral databases in the literature. The fragment ion 205.0641 is exclusively derived from the boldine structure, while the fragment ion 165.0711 is derived from isoboldine. In addition, the fragment ion 282.0982 might be found in both corytuberine and isocorytuberine fragmentation patterns (Figure 12; Table 2).

Figure 12 - QC ESI MS⁺ high-energy channel evidencing the parent ion at m/z 328.154 and the MS^E fragment ions of the isomers (1) – boldine, (2) – corytuberine, (3) – isoboldine, (4) isocorytuberine



Source: From the author.

Table 2 - The putative identification of aporphine isomers at m/z 298, m/z 314 and m/z 328 by ESI-MS^E in the positive ionisation mode

Observed m/z	RT (min)	MF	ESI-MS ^E data	Error (mDa)	ID
298.14361	1.55-1.58	C ₁₈ H ₁₉ NO ₃	281.1499; 235.0756; 207.0779	0.70	16 / 17
314.13857	1.60-1.76	C ₁₈ H ₁₉ NO ₄	297.1133; 282.0902; 237.0898; 219.0806	0.14	6
314.13912	1.60-1.76	C ₁₈ H ₁₉ NO ₄	297.1133; 265.0875; 209.0929; 165.0684	0.38	18 / 19
328.15466	1.83-1.96	C ₁₉ H ₂₁ NO ₄	297.1028; 265.0842; 237.0899; 205.0641	0.25	1
328.15465	1.83-1.96	C ₁₉ H ₂₁ NO ₄	297.1028; 282.0982; 265.0842; 237.0899; 219.0806	0.25	2 / 4
328.15468	1.83-1.96	C ₁₉ H ₂₁ NO ₄	297.1028; 265.0842; 237.0899; 165.0689	0.26	3
328.15470	1.83-1.96	C ₁₉ H ₂₁ NO ₄	312.1250; 297. 1028; 296.0919; 282.0902; 280.0981; 265.0875; 252.1015; 237.0898; 222.0662; 205.0641	0.38	10 / 11
328.15420	1.88-1.96	C ₁₉ H ₂₁ NO ₄	178.0851; 163.0619	0.36	12 / 13
328.15424	1.88-1.96	C ₁₉ H ₂₁ NO ₄	297.1028; 265.0842; 239.0683	0.37	14 / 15

Source: From the author.

High-intensity levels were found for these aporphines, morphinandienones alkaloids isomers in the several *Ocotea* species studied, such as the VI II, VL II, and VZ II 1 extracts. In general, aporphines alkaloids are also reported in other genera of Lauraceae family, for example in the *Litsea* species. The aporphine alkaloids are also common in other family plants such as the Menispermaceae and Annonaceae. Another study isolated (10) and (12) with other aporphine and noraporphine alkaloids from the stem of the *Xylopi* *laevigata* (Annonaceae), a plant widely used in folk medicine in Northeastern Brazil to treat painful disorders, heart diseases and inflammatory conditions (MENEZES et al., 2016).

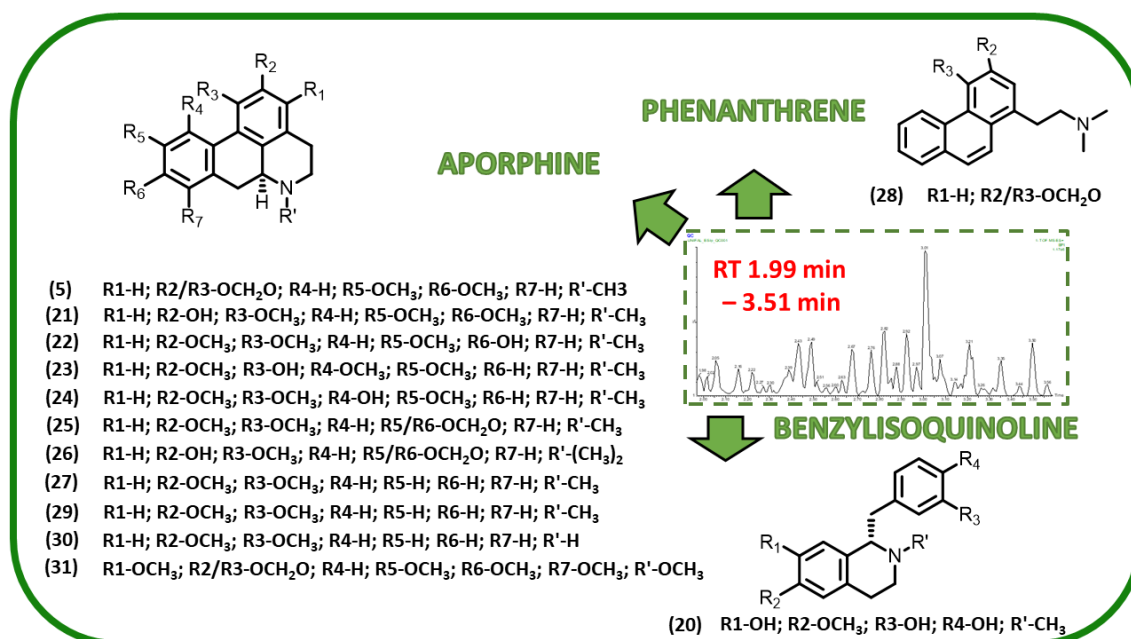
Furthermore, at RT 2.05 min with elemental composition $C_{19}H_{23}NO_4$, parent ion at m/z 330.16983 and MS^E at m/z 192.1000, m/z 175.0741, m/z 143.0489 and m/z 137.0576 the substance was dereplicated as the alkaloid (20) reticuline. This benzyloisoquinoline core is a branch-point intermediate in the biosynthesis of important natural products in pharmaceutical usage such as codeine and morphine (DEWICK, 2009). At RT 2.34-2.59 min, elemental composition $C_{20}H_{23}NO_4$ and parent ion at m/z 342.169 more other four aporphine alkaloids were dereplicated as (21) predicentrine, (22) lauroscholtzine and (23) corydine and (24) isocorydine, which were differentiated by MS^E ions shown in table 3. In addition, five other aporphine alkaloids detected at RT 2.80 – 2.82 min with high-intensity levels in the QC ESI MS+ metabolic fingerprint and were dereplicated with elemental composition $C_{20}H_{21}NO_4$ and observed parent ion at m/z = 340.154. Through the MS^E ion fragments obtained, the alkaloids were annotated as the isomers of the alkaloid (5) (25- nantenine; 26- N-Methyl isodomeesticine).

Subsequently, at the RT 3.01-3.10 min two alkaloids with elemental composition $C_{19}H_{19}NO_2$ and observed m/z = 294.148 were dereplicated as containing an aporphinic and phenanthrenic nuclei, the (27) dehydronuciferine (28) stephenanthrine alkaloids isomers respectively, which were differentiated by fragment ions that matched to the literature (Figure 13; Table 3). These compounds were found in 38 out of the 60 analysed *Ocotea* samples, and according to a recent scientific publication, it acts as a moderated acetylcholinesterase (AChE) inhibitor, with applicability to neurological illnesses (YANG et al., 2014). The aporphine alkaloid (27) is well presented in *Ocotea* extracts, and possibly widespread in the *Ocotea* genus and Lauraceae family. However, it reported in other plants, such as those from the Nymphaeaceae family, encountered in the “sacred lotus”, the *Nelumbo nucifera* and also in the American *N. lutea* species. A scientific NP research on the *N. nucifera* allowed the authors isolated the aporphine (27) together with other aporphines (29) nuciferine and (30) nornuciferine that are also common compounds in the *Ocotea* genus. Thus, we have also dereplicated (29) and (30) in the QC ESI MS+ metabolic fingerprint ($C_{19}H_{21}NO_2$; $[M+H] = 296.164348$; RT 2.43 and $C_{18}H_{19}NO_2$; $[M+H] = 282.1482038$; RT 3.12), which have different precursor ions although the same product ion (Figure 13; Table 3).

The last high-intensity aporphines found in the QC ESI MS+ metabolic fingerprint are the dereplicated (31) leucoxylophine with elemental composition $C_{22}H_{25}NO_6$, precursor ion at m/z 400.175, detected at RT 3.48-3.51 min. The MS^E fragments identified were m/z 386.1942, m/z 369.1334, m/z 333.1600 and m/z 326.1017. This alkaloid is

reported in the literature as produced by species of the *Ocotea* genus, such as *O. leucoxyton* and *O. minarum* (VECCHIETTI et al., 1979; ZHOU et al., 2000). However, in this study the aporphine (31) was successfully dereplicated with high-intensity values in VZ II 1, VA I and PU I extracts (Figure 13; Table 3).

Figure 13 - Structure of the aporphine alkaloids isomers with elemental composition $C_{19}H_{23}NO_4$ (20- reticuline). $C_{20}H_{23}NO_4$ (21- predicentrine, 22- lauroschoztzine, 23- corydine and 24- isocorydine). $C_{20}H_{21}NO_4$ (5-dicentrine, 25- nantenine, 26- N-methyl isodomeesticine). $C_{19}H_{19}NO_2$ (27- dehydronuciferine, 28- stephenanthrine). $C_{19}H_{21}NO$ (29- nuciferine). $C_{18}H_{19}NO_2$ (30- nornuciferine). $C_{22}H_{25}NO_6$ (31- leucoxytonine)



Source: From the author.

Table 3 - The putative identification of aporphine isomers at m/z 282, m/z 294, m/z 296, m/z 340, m/z 342 and m/z 400 by ESI-MS^E in the positive ionization mode

Observed m/z	RT (min)	MF	ESI-MS ^E data	Error (mDa)	ID
282.14826	3.12	C ₁₈ H ₁₉ NO ₂	265.1241; 250.0987; 235.0756; 219.0806 207.0809	0.65	30
296.16431	2.43	C ₁₉ H ₂₁ NO ₂	265.1241; 250.0987; 235.0786; 219.0806 207.0809	0.38	29
294.14837	3.01-3.10	C ₁₉ H ₁₉ NO ₂	249.0907; 219.0806; 191.0837	0.52	28
294.14835	3.01-3.11	C ₁₉ H ₁₉ NO ₂	263.1027; 249.0907 235.0786; 207.0809	0.52	27
330.16983	2.05	C ₁₉ H ₂₃ NO ₄	192.1000; 175.0741; 143.0489; 137.0576	0.15	20
340.15449	2.80-2.82	C ₂₀ H ₂₁ NO ₄	309.1108; 279.1030; 264.0762 ; 251.1056;	0.16	5
340.15443	2.80-2.82	C ₂₀ H ₂₁ NO ₄	309.1154; 279.1030; 251.1056; 193.0649	0.15	25
340.15403	2.80-2.82	C ₂₀ H ₂₁ NO ₄	295.0969; 263.0702; 235.0756; 205.0641;	0.33	26
342.16989	2.34-2.59	C ₂₀ H ₂₃ NO ₄	311.1286; 279.1030; 251.1056; 236.0832; 205.0641	0.06	21
342.16992	2.34-2.59	C ₂₀ H ₂₃ NO ₄	296.1019; 282.0906; 265.0873; 237.0892; 205.0641	0.05	22
342.16990	2.34-2.59	C ₂₀ H ₂₃ NO ₄	311.1286; 279.1030; 264.0795; 236.0832	0.05	23 / 24
400.17527	3.48-3.51	C ₂₂ H ₂₅ NO ₆	386.1942; 369.1334 333.1600; 326.1017	0.19	31

Source: From the author.

Moreover, two neolignans were dereplicated in higher intensity levels in the QC ESI MS⁺ metabolic fingerprint, at RT 5.35 min with elemental composition C₂₀H₂₂O₆ and precursor ion at *m/z* 359.185 the benzofuran 8, 1' neolignan type (32) ferrearin-B or (33) ferrearin-G were dereplicated. In addition, at RT 6.34 min also the 8, 1' neolignan type armenin-B (34) with elemental composition C₂₁H₂₄O₆ and observed parent ion at *m/z* 373.165. Additionally, at RT 5.44 with elemental composition C₂₂H₂₆O₆ and precursor ion at *m/z* 387.179 the non-phenolic furofuran lignan (35) eudesmin was tentatively assigned. These compounds were annotated by MS^E dereplication through UNIFI database with no alternative assignments possibilities (metabolites) for the detected ionised monoisotopic mass and theoretical fragments (Table 4). The neolignan (34) showed was putatively identified in the popularly known “Canela preta” (*O. catharinensis*, CT II). The dereplication result is corroborated by recent research, where the armenin B was isolated from the wood of *O. catharinensis* together with other neolignans analogues (LI et al., 2018).

Lastly, at RT 5.90 the peak with the elemental composition C₁₃H₁₀O, precursor ion at *m/z* 183.081 and MS fragments 105.0334 and 77.0381 was dereplicated as the (36) benzophenone. And at RT 6.16 min, the peak with elemental composition C₂₄H₃₀O₆ at *m/z* 415.2102 was dereplicated as lignoids compounds. Additionally, at RT 9.28 the peak with precursor ion at *m/z* 609.271 and main fragment ion *m/z* 581.2441, with the elemental composition C₃₅H₃₇N₄O₆ was dereplicated as the compounds (37) Mesophaeophorbide b or (38) 10-Hydroxy- phaeophorbide a. And at RT 9.44, the precursor ion at *m/z* 593.277 and main fragment ion at *m/z* 533.2537 obtained elemental composition C₃₅H₃₇N₄O₅ and was dereplicated as (39) Phaeophorbide a or (40) Phaeoporphyrin a5. The complete dereplication result list of ESI MS⁺ metabolic fingerprint is attached to the supplemental material (table S7).

Table 4 - The putative identification of the compounds at m/z 183, m/z 246, m/z 274, m/z 359, m/z 373, m/z 387, m/z 415, m/z 593 and m/z 609 by ESI-MS^E in the positive mode.

Observed m/z	RT (min)	MF	ESI-MS ^E data	Error (mDa)	ID
183.08132	5.90	C ₁₃ H ₁₀ O	105.0334; 77.0381	0.31	36
246.24242	3.96	C ₁₄ H ₃₂ NO ₂	-	0.92	*NI
274.27598	4.89	C ₁₆ H ₃₆ NO ₂	256.2651; 230.2468	1.30	*NI
359.18517	5.35	C ₂₀ H ₂₂ O ₆	123.0433	0.12	32/33
373.16463	6.34	C ₂₁ H ₂₄ O ₆	343.1899; 341.1395	0.01	34
387.17962	5.44	C ₂₂ H ₂₆ O ₆	189.0903; 174.0662; 151.0741	0.59	35
415.21023	6.16	C ₂₄ H ₃₀ O ₆	-	1.93	*C
593.27703	9.44	C ₃₅ H ₃₇ N ₄ O ₅	533.2537	0.61	39/40
609.27371	9.28	C ₃₅ H ₃₇ N ₄ O ₆	581.2441	2.40	37/38

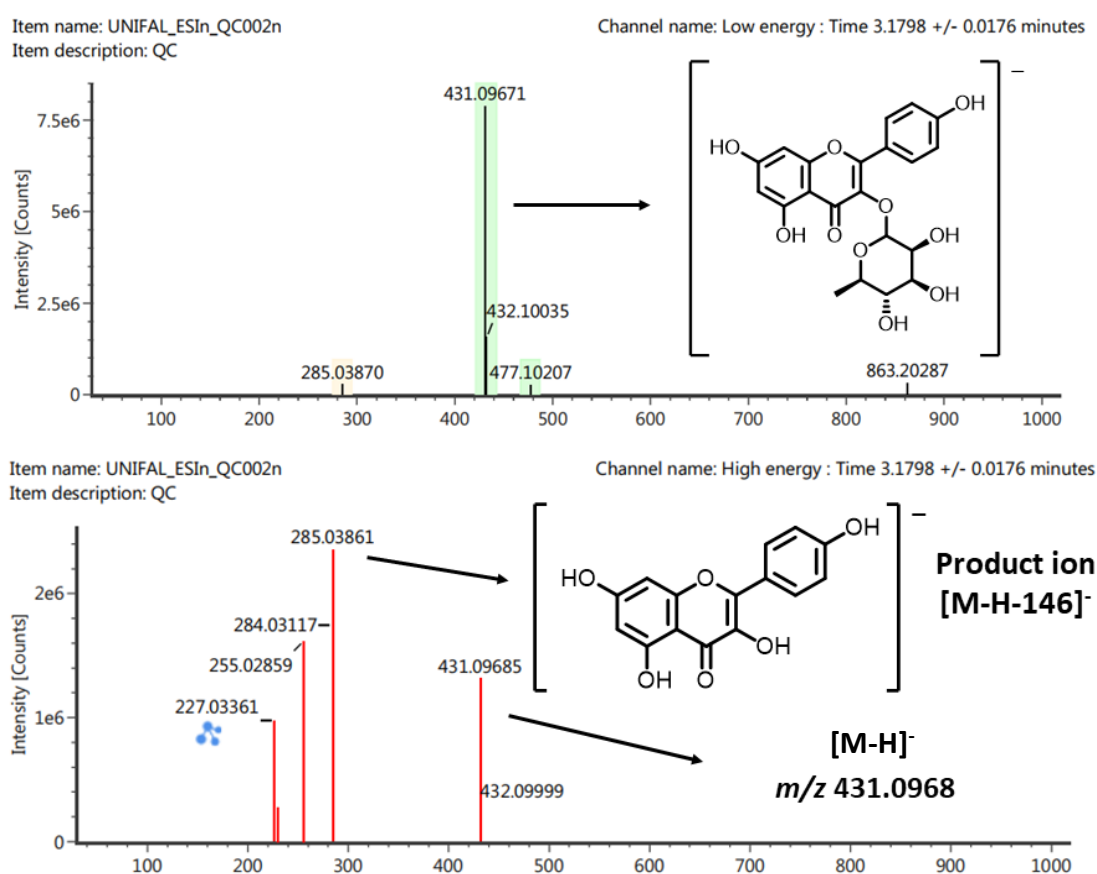
Source: From the author.

Note: *NI - not identified; *C - only the compound class assigned.

On the other hand, the majority of the high-intensity ionized metabolites in the QC ESI MS- metabolic fingerprint were assigned as glycosylated flavonoids. These compounds were detected in all *Ocotea* extracts evaluated. For example, the compound (7) with elemental composition C₂₁H₂₀O₁₀ and observed parent ion at m/z 431.096 at 3.14 min it is a glycosyl flavone, which the kaempferol aglycone is joined to alpha-L-rhamnosyl residue by a 3-*O*-glycosidic bond. Additionally, the compounds (8) and (9) were also annotated. The (8) with elemental composition C₃₀H₂₆O₁₂ is also a glycosyl flavone, which has eluted at RT 4.43 min with parent fragment ion at m/z 577.135. The (9) is a glycosyl flavone as well, with elemental composition C₃₉H₃₂O₁₄, which was eluted at 5.70 min with a parent fragment ion at m/z 723.173. While the glycosyl flavone (8) possess only one radical of a coumarylrhamnoside, the (9) has one additional coumaryl radical in its chemical structure.

From the ESI low and high-energy channel spectra, it was possible to investigate the main precursor and product ions of the dereplicated compounds. The parent ion at m/z 431.0968 related to the glycosyl flavone (7) gave the deprotonated aglycone at m/z 285.03870 ($C_{15}H_9O_6^-$), which refers to the loss of a rhamnose sugar (m/z 146.05791), and it was detected at a low-intensity value by the low energy channel (Figure 14). Furthermore, the aglycone was further confirmed by the MS^E characteristic product ions at m/z 255.0286 ($C_{15}H_{11}O_4^-$) and at m/z 227.0336 ($C_{14}H_{11}O_3^-$), which matches the literature and confirms the aglycone is a kaempferol derivative (LI et al., 2016b).

Figure 14 - The low energy and high-energy ESI MS- spectra of the glycosyl flavone (7) and the corresponding $[M-146]^-$ ion derived from the neutral loss of rhamnose residue ($C_6H_{10}O_4$)

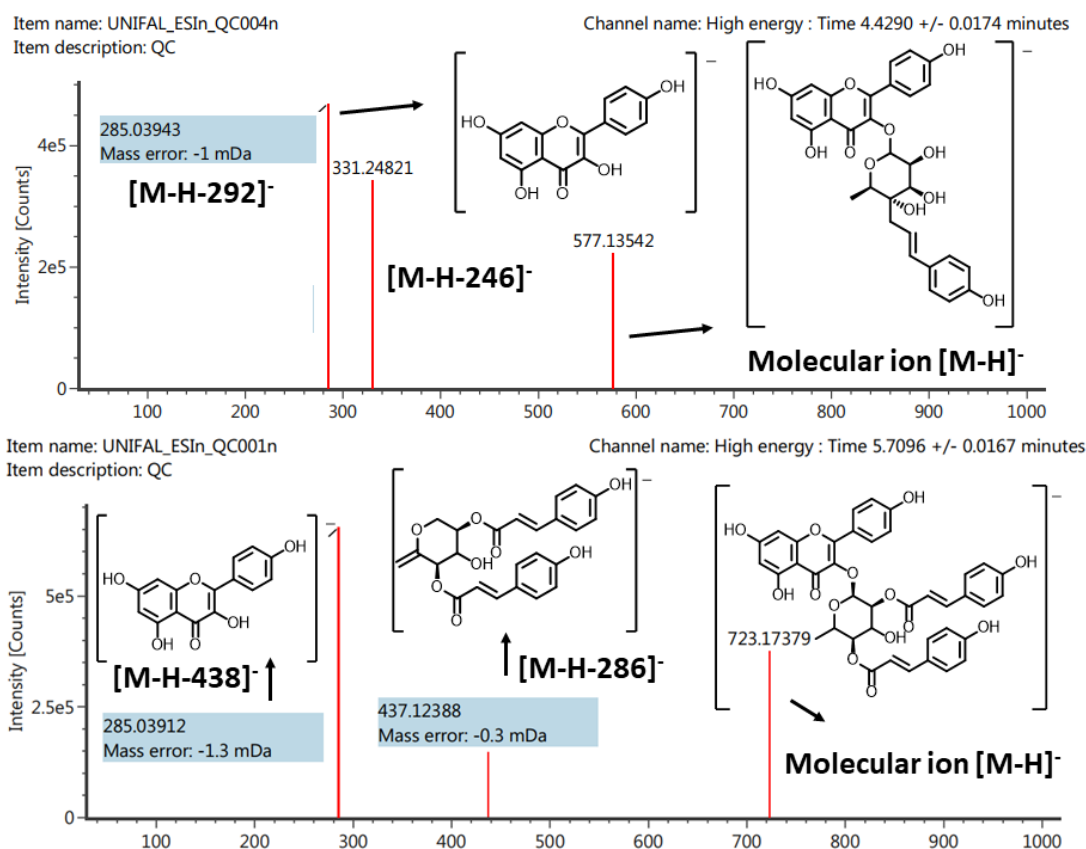


Source: From the author.

Figure 15 shows the compounds 8 (m/z 577.1342) and 9 (m/z 723.1737) and the deprotonated aglycone fragment at m/z 285.0390 in the high and low energy ESI MS-channel spectra, suggesting kaempferol derivatives. Confirmation of the compounds was made MS/MS fragments match. Initially by confirming fragments of glycosyl groups,

such as the loss of a coumaryl rhamnose (m/z 292.0961) and dicoumaryl rhamnose (m/z 437.1238) respectively. Secondly by identifying the characteristic product ions at m/z 255.0286 and m/z 227.0336 (LI et al., 2016b). The complete dereplication result list of ESI MS- metabolic fingerprint is attached to the supplemental material (table S8).

Figure 15 - The high-energy QC ESI MS- spectra of the glycosyl flavone (8) kaempferol 3-(4''-*p*-coumarylrhamnoside and the (9) kaempferol 3-(2'',4''-di-(*E*)-*p*-coumarylrhamnoside and the corresponding product ions derived from the loss of coumaryl/dicoumaryl rhamnose respectively.



Source: From the author.

Moreover, a tetrahydroxy flavone with elemental composition $C_{21}H_{20}O_{12}$, parent fragment ion at m/z 463.08766 and RT 2.53 min were dereplicated as the (41) quercimeritrin, which is a quercetin *O*-glucoside due to the β -D-glucosyl residue attached at position 7 of quercetin structure. A high-intensity peak at 2.85 min, with elemental composition $C_{21}H_{20}O_{11}$ and observed parent ion at m/z 447.09273 was dereplicated as the (42) quercitrin, which is also tetrahydroxyflavone *O*-glycosyl, where the quercetin is substituted by α -L-rhamnosyl moiety at position 3 via a glycosidic linkage. The compound dereplicated as (43) reynoutrin is quercetin-3-*O*-xylopyranoside ($C_{20}H_{18}O_{11}$)

which was detected at m/z 433.0772 at 2.75 min. The MS^E fragments of these compounds are shown in Table 5, and each product ion was compared to the literature. The most common fragments are [M-162]⁻, which is referred the loss of a glucose residue and the [M-142]⁻ correspondent to the loss of a pentose residue (ABDULLA et al., 2017; LI et al., 2016a; OUYANG et al., 2016; SCHIEBER et al., 2002).

A tetrahydroxy flavone with elemental composition C₂₁H₂₀O₁₂ and parent ion at m/z 609.1470 was detected at 2.45 min and dereplicated as (44) rutin. This flavonoid is quercetin 3-rutinoside, which the hydroxy group at position C-3 of the quercetin substituted with two sugar groups, the glucose and rhamnose, and thus the compound was tentatively identified by the presence of the aglycone fragment at m/z 300.0241 resulted from the disaccharide neutral loss of 309.1187 (C₁₂H₂₀O₉) mass units. At the end of the chromatography run (9.26-9.22 min) a metabolite belonging to the stigmastanes class with elemental composition C₃₅H₅₈O₆ and parent ion at m/z 609.3904 was identified with chlorine adduct and dereplicated as a (45) stigmasteryl glucoside (Table 5). However, the peak at 3.81 min only the compound class was dereplicated as a neolignan/furofuran lignans with parent ion at m/z 711.252 and elemental composition C₃₃H₄₄O₁₇.

Table 5 - The putative identification of the compounds at m/z 287, m/z 431, m/z 433, m/z 447, m/z 463 and m/z 609 by ESI-MS^E in the negative ionization mode.

(Continue)

Observed m/z	RT (min)	MF	ESI-MS ^E data	Error (mDa)	ID
287.2232	4.76	C ₁₆ H ₃₂ O ₄	-	1.02	*NI
431.09757	3.14	C ₂₁ H ₂₀ O ₁₀	285.0387; 255.0286; 227.0336	0.79	7
433.07721	2.75	C ₂₀ H ₁₈ O ₁₁	300.0241; 271.0251; 255.0290; 243.0272; 227.0312	0.48	43
447.09270	2.85	C ₂₁ H ₂₀ O ₁₁	300.0241; 271.0251; 255.0290; 243.0272; 178.9972; 151.0009	0.60	42
463.08760	2.53	C ₂₁ H ₂₀ O ₁₂	300.0241; 271.0251; 255.0290; 243.0272; 178.9972; 151.0009	0.50	41
577.13541	4.43	C ₃₀ H ₂₆ O ₁₂	331.2482; 285.0394; 255.0290	0.61	8
609.14701	2.45	C ₂₇ H ₃₀ O ₁₆	300.0241; 271.0251; 255.0290; 243.0272; 227.0343 178.9972	1.43	44

Table 5 - The putative identification of the compounds at m/z 287, m/z 431, m/z 433, m/z 447, m/z 463 and m/z 609 by ESI-MS^E in the negative ionization mode.

Observed m/z	RT (min)	MF	ESI-MS ^E data	(Conclusion)	
				Error (mDa)	ID
609.39041	9.06-9.22	C ₃₅ H ₅₈ O ₆	-	2.25	45
711.25236	3.81	C ₃₃ H ₄₄ O ₁₇	665.2491; 519.1857; 205.0699; 163.0596	2.31	*C
723.17379	5.70	C ₃₉ H ₃₂ O ₁₄	437.1238; 285.0391; 255.0290	1.73	9

Source: From the author.

Note: *NI- not identified; *C- only the compound class assigned.

3.3.3 Anti-inflammatory *ex vivo* evaluation (PGE2)

The lipopolysaccharide (LPS) obtained from Gram-negative pathogens was used to activate the immune system blood cells and cause inflammation induction. Thus, LPS was chosen to activate COX 2 expression (DICKSON; LEHMANN, 2019). In this assay, the inhibition production of PGE2 from the LPS-induced signalling pathway by 60 different *Ocotea* spp. extracts were evaluated by measuring the plasmatic concentration of the inflammatory PGE2 in the developed SPE-UPLC-MS/MS method. The method was linear from the lower limit of quantification (LLOQ) (6.25 ng.mL⁻¹) to the upper limit of quantification (ULOQ) (400 ng.mL⁻¹). The linear equation of the calibration curve was $y = 0.0351x + 0.5637$, where y is the relative area of PGE2/IS and x is the concentration of PGE2 measured in ng.mL⁻¹. The [PGE2] and % of inhibition for each evaluated *Ocotea* sample is shown in Table 6.

Table 6 - Percentage of PGE2 inhibition of the anti-inflammatory assay evaluated by SPE-UPLC-MS/MS PGE2 quantification method.

Code	[PGE2 ng.mL ⁻¹] ^a	% PGE2 Inhibition ^b	Code	[PGE2 ng.mL ⁻¹] ^a	% PGE2 Inhibition ^b	Code	[PGE2 ng.mL ⁻¹] ^a	% PGE2 Inhibition ^b	Code	[PGE2 ng.mL ⁻¹] ^a	% PGE2 Inhibition ^b
AY II	79.47	76.22	FE I	62.00	81.45	NE II	177.95	46.75	TA I	29.43	91.20
AU II	169.22	49.37	GL I	160.67	51.93	NI I	12.71	96.19	TL II 2	42.15	87.39
AM II	158.58	52.56	GU II	218.60	34.59	NO II	100.74	69.85	TE II 1	30.19	90.97
BA II	217.27	34.99	GZ II	207.68	37.86	MU I	56.01	83.24	TR I	27.43	91.79
BR II	204.45	38.83	GA II	124.24	61.93	NU I	9.86	97.04	VA I	18.51	94.46
BI II	73.30	78.06	HY I	124.01	62.89	OD II	9.29	97.21	VR I	41.39	87.62
CA I	51.93	84.46	IN II	122.40	63.38	PA II	56.11	83.21	VZ II 2	7.87	97.64
CL I	138.26	58.63	KU I	134.08	59.88	PE I	33.99	89.83	VL II	13.01	96.11
CT II	128.00	61.70	LA II	119.65	64.20	PO I	77.86	76.71	VI II	1.60	99.52
CE II	108.72	67.47	LN II	140.49	57.96	PR II	52.60	84.26	DEX	0	100
CM II	90.49	72.93	LC II	152.22	54.45	PT II	44.53	86.68	IND	0	100
CO II	154.31	53.83	LG I	171.78	48.60	PU II	57.20	82.90	NEG	334.24	0
CJ II	156.44	53.19	LX I	287.26	14.05	PL II	75.11	77.53			
DO II	48.42	85.51	LO II	99.51	70.22	PC II 1	58.29	82.55			
DI I	43.77	86.90	LF II	69.31	79.26	PH II	21.83	94.78			
DV II	51.55	84.57	MI II	132.08	60.48	SP I	36.74	89.01			
EL II	49.46	85.20	NT I	210.81	36.92	SX I	22.11	93.38			

a- The concentration in ng/mL represents the final media concentration of the extract (n=3).

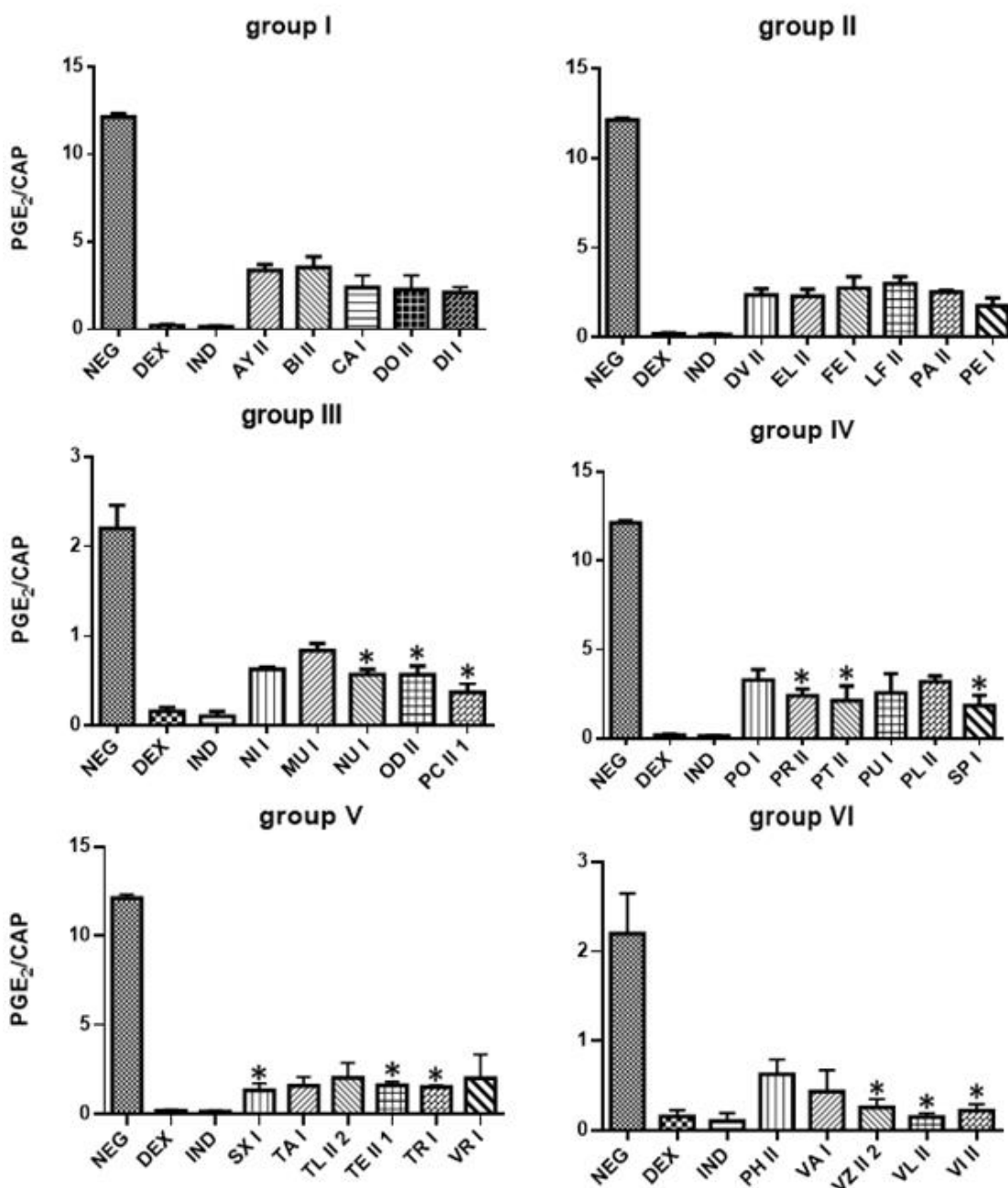
b- Anti-inflammatory activity calculated by the mean percent reduction in LPS-induced PGE2 levels as compared to the NEG control (PBS + blood + LPS).

3.3.4 Statistical analyses of the active anti-inflammatory samples

According to the ANOVA one-way and the Dunnett's multiple comparisons test, 33 of the 60 *Ocotea* extracts evaluated were statistically different from negative control (334.254 ng.mL⁻¹ of PGE2) and PGE2 inhibition was superior to 75%. The second statistical analyses performed included only the controls and active samples (>75% inhibition), and thus the 33 active samples were subdivided into six groups, classified by alphabetic order into groups of 5 and 6 members to express the results (I, II, III, IV, V and VI). 12 out of the 33 samples revealed to be statistically similar to the positive controls DEX and IND. Therefore, these 12 *Ocotea* spp. were considered the most promissory species of the anti-inflammatory prospection realized (NU I, OD II, PC II 1; PR II, PT II, SP I, SX I, TE II 1, TR I, VZ II 2, VL II and VI II).

The statistical graphs of the active samples (Figure 16) were plotted using the PGE2/CAP peak area ratio obtained from the SPE-UPLC-MS/MS chromatograms. The *Ocotea* spp. that were statistically similar to the positive controls are represented with *. The positive controls DEX and IND were considered statistically similar to each other and different from negative control (NEG). This result was necessary for the confidence of the results from the screening activity.

Figure 16 - Evaluation of 33 out the 60 *Ocotea* spp. with anti-inflammatory activity, 12 statistically similar to positive controls DEX/IND with high PGE₂ inhibition ratio.



Source: From the author.

Note: The results were analysed by *one-way* ANOVA, followed by the Dunnett multiple comparison test.

* Indicates statistical similarity when compared to the positive control DEX and IND, where $p \leq 0.05$.

There are no scientific publications in the literature regarding the chemical composition and biological activity of the majority of the active *Ocotea* species evaluated in this prospective screening, for instance, those endemic from the Atlantic Brazilian

Forest the SP I, TE II 1, TRI, VL II and VI II. In addition, some of the species are related to other biological activities and not only anti-inflammatory. For example, the VZ II2, which is found mainly in the Brazilian Pantanal, there is a report of larvicidal alkaloid compounds, such as the aporphine alkaloid dicentrine that has shown high larvicidal potential activity against *Aedes aegypti* larvae (GARCEZ et al., 2009). The SX I is found mainly in the Brazilian Cerrado biome, and there is no scientific publication reporting chemical or biological activity of this *Ocotea* species in the literature. On the other hand, the PR II is not endemic of Brazil, however, it is found in the Brazilian Atlantic Forest phytogeographic domain. There are few research investigations on the essential oil of this plant leaves, which are related as a weak antibacterial effect against the Gram-positive bacterium *S. aureus* and modest cytotoxic against murine melanoma (B16F10) and human breast adenocarcinoma (MCF7) (BRITO, 2009; BRUSTULIM, 2019).

Furthermore, the PC II 1 and NU I are found in both Cerrado and Atlantic Forest biome in the Brazilian territory. The NU I leaf essential oil recently showed moderate inhibition for *Enterococcus faecalis* (MIC=500 $\mu\text{g}\cdot\text{mL}^{-1}$) and remarkable larvicidal activity potential (LC50= 250 $\mu\text{g}/\text{mL}$) activity against *Aedes aegypti* larvae (BETIM et al., 2019). The PC II 1 root extract also showed larvicidal activity against the *Aedes aegypti* larvae in 24 hours, in addition to herbicide effects and antiviral activity against animal herpesviruses (SuHV-1 strain) (CANDIDO, 2016; PADILLA et al., 2018). Moreover, the PT II is a heterotypic of OD II, which is an endemic tree also native of both Cerrado and Atlantic Brazilian Forest biome. This *Ocotea* specie is the only sample from the 12 most active extracts with already previous ethnopharmacological reports of anti-inflammatory activity, which was already confirmed in another work by our research group as a dual inhibitor of COX and LOX pathways (ALCÂNTARA, 2018). Herein, the results obtained of anti-inflammatory potential of these crude extracts (PT II and OD II) through LPS-induced PGE2 experiment assay corroborated the previous bioactivity works. Also, there are other scientific studies in literature evidencing also antifungal properties of Ellagitannin isolated from the leaves of OD II (YAMAGUCHI et al., 2011).

Additionally, as there are no reports regarding anti-inflammatory activities of the others evaluated species, thus we report that NU I, SPI, SX I, PC II 1, TE II 1, TRI, VL II, VZ II 2 and VI II might be considered as a new promising source for anti-inflammatory agents that act via PGE2 pathway inhibition. The PGE2 is a specific eicosanoid which is a PG that has a main role in a wide range of inflammatory diseases that rely on COX-2 enzyme activation pathway, and it is also important for the development of different types

of cancer. More than one COX-2 inhibitor exhibited adjuvant potential in the cancer therapy, increasing the therapeutic index and effectiveness of the radiotherapy and chemotherapy (MAJUMDER et al., 2014; ROZIC; CHAKRABORTY; LALA, 2001; SALEHIFAR; HOSSEINIMEHR, 2016). The PGE2 plays an essential role in cancer disease and makes it a therapeutic target to reduce the pathological response of some types of epithelial cancers. The current clinical data shows that some NSAIDs increase the survival of cancer patients by reducing metastases and tumor growth. Recent research has uncovered the anticancer mechanisms of anti-inflammatory agents indicating inhibition of COX 2 enzymes and VEGF signalling pathway. Thus, the PGE2 degradation restart and thus a less EP4 receptor activation occurs on lymphatic vessels what directly avoids tumor cell to metastasise through lymphangiogenesis (MAJUMDER et al., 2014; NANDI et al., 2017). Thus, the 12 active extracts can be promissory to development of new treatments with anti-inflammatory and anti-tumoral properties.

There are studies in the literature evidencing the *Ocotea* genus with a promising anti-inflammatory potential. For example, the essential oil of *O. quixos* is reported as LPS-induced NO release inhibitor and the diastereomeric lignans of the *O. macrophylla* demonstrated potent COX/LOX pathway inhibition. The meso and threo-isomers of the hexamethoxy lignan from *O. macrophylla* were found to be the most active COX-2/5-LOX dual inhibitors at non-toxic concentrations. Furthermore, the lignan 2'-epi-Guianin is described as a potent inhibitor of PAF-induced aggregation (AMILIA DESTRYANA et al., 2014; COY; CUCA; SEFKOW, 2009; SALLEH; AHMAD, 2017). However, this work is the first scientific research regarding the chemical and biological activity of 12 never investigated *Ocotea* species by an *ex-vivo* anti-inflammatory screening through LC-MS/MS, despite the great interest in the pharmacological activities of the *Ocotea* genus.

The aporphine derivatives found in *Ocotea* genus, dicentrine and glaucine are cytotoxic agents. The possible mechanisms investigated revealed that these compounds can bind to DNA and act as intercalating agents. Others derivatives, such as dicentrine and dicentrinone can interfere with the catalyst activity of topoisomerases, which are enzymes that participate in the overwinding of DNA and are important for keeping the proper topology of the double-helical structure (HOET et al., 2004; SALLEH; AHMAD, 2017). Furthermore, it is becoming clear that aporphines represent an interesting and potentially useful group of anticancer agents, and recently anti-inflammatory. However, their practical application is still limited by a lack of solid knowledge of their mechanisms

of action and clinical studies, in spite of the few motivating *in vitro* and *in vivo* screening results in the literature.

3.3.5 MS^E dereplication of the highest intensity peaks of active *Ocotea* species

We have putatively annotated 773 substances in the QC ESI MS+ and 120 in the QC ESI MS- according to the UNIFI database. Moreover, 82 compounds for the positive mode and 21 for the negative mode matched with the *in-house* database, whereas 40 compounds from positive and 9 from negative mode were already described in section 3.3.2. By the use of MS^E spectral data acquisition and MS/MS mode, most of the compounds presented in samples were putative annotated. The major compounds of the best anti-inflammatory extracts profile are showed and summarized in Table 7, with TOF elemental composition for molecular formula prediction, class of biomarker secondary metabolism, sample code, observed *m/z* and MS^E data (obtained by ESI-QTOF/MS), adduct detected, retention time (min) and error (mDa).

Table 7 - Summary of the ESI-MS^E dereplication of active anti-inflammatory *Ocotea* spp. evidencing the highest peak areas of samples.

(Continue)

Compound name	MF	Class	Sample	Observed <i>m/z</i>	Fragment ions (<i>m/z</i>)	Adduct	RT (min)	Error (mDa)
Reynoutrin	C ₂₀ H ₁₈ O ₁₁	Flavonoids	NU I	435.0917	303.0508; 287.0546; 219.0525	+H	2.64	0.47
Quercitrin	C ₂₁ H ₂₀ O ₁₁	Flavonoids	NU I	447.0927	300.0241; 271.0251; 255.0290; 243.0272; 178.9972; 151.0009	-H	2.87	0.55
Reticuline	C ₁₉ H ₂₃ NO ₄	Alkaloids	OD II	330.1688	192.1000; 175.0741; 143.0489; 137.0576	+H	2.09	1.21
Afzelin	C ₂₁ H ₂₀ O ₁₀	Flavonoids	OD II	431.0978	285.03870; 255.0286; 227.0336	-H	3.14	0.56
Reynoutrin	C ₂₀ H ₁₈ O ₁₁	Flavonoids	PC II 1	435.0915	303.0508; 287.0546; 229.0525	+H	2.63	0.65
Boldine	C ₁₉ H ₂₁ NO ₄	Alkaloids	PC II 1	328.1546	297.1028; 265.0842; 237.0899; 205.0641	+H	1.85	0.25
Reynoutrin	C ₂₀ H ₁₈ O ₁₁	Flavonoids	PC II 1	433.0772	300.0241; 271.0251; 255.0290; 243.0272; 227.0312	-H	2.74	0.45
Armenin-B	C ₁₂ H ₂₄ O ₆	Neolignans	PR II	373.1632	343.1899; 341.1395; 386.1942; 369.1334	+H	6.36	1.3
Kaempferol 3-(2",4"- di-(E)- <i>p</i> - coumarylrhamnoside)	C ₃₉ H ₃₂ O ₁₄	Flavonoids	PR II	723.1734	437.1238; 285.0391; 255.0286; 227.0338	-H	5.66	1.50
Flavinantine	C ₁₉ H ₂₁ NO ₄	Alkaloids	PT II	328.1534	178.0851; 163.0619	+H	1.89	0.97
Laurelliptine	C ₁₈ H ₁₉ NO ₄	Alkaloids	SP I	314.1382	298.1082; 283.0838; 255.0879	+H	1.74	0.47
3- <i>O</i> -Feruloylquinic acid	C ₁₇ H ₂₀ O ₉	Phenolic acids	SP I	367.1037	193.0489; 191.0543; 173.0432; 149.0249	-H	1.91	0.67
Lauroschoztine	C ₂₀ H ₂₃ NO ₄	Alkaloids	SX I	342.1697	311.1286; 296.1025; 281.0813; 280.1084; 265.0842; 237.0898	+H	2.52	0.02

Table 7 - Summary of the ESI-MSE dereplication of active anti-inflammatory *Ocotea* spp. evidencing the highest peak areas of samples.

								(Conclusion)
Compound name	MF	Class	Sample	Observed m/z	Fragment ions (m/z)	Adduct	RT (min)	Error (mDa)
Quercitrin	C ₂₁ H ₂₀ O ₁₁	Flavonoids	SX I	447.0930	300.0241; 271.0251; 255.0290; 243.0272; 178.9972; 151.0009	-H	2.87	0.26
Licarin B	C ₂₀ H ₂₀ O ₄	Neolignans	TE II 1	325.1426	203.1056; 163.0772; 135.0798; 107.0486	+H	6.61	0.93
Farnesyl acetate	C ₁₇ H ₂₈ O ₂	Sesquiterpenoids	TE II 1	309.2063	221.1930; 187.0961	+HCOO	5.65	0.77
Quercimeritrin	C ₂₁ H ₂₀ O ₁₂	Flavonoids	TR I	465.1033	303.0508; 287.0546; 257.0416; 153.0159	+H	2.49	0.55
Quercimeritrin	C ₂₁ H ₂₀ O ₁₂	Flavonoids	TR I	463.0876	300.0241; 271.0251; 255.0290; 243.0272; 178.9972; 151.0009	-H	2.53	0.65
Dicentrine	C ₁₉ H ₁₉ NO ₄	Alkaloids	VZ II 1	340.1540	309.1108; 279.1030; 264.0762 ; 251.1056; 236.0832	+H	2.82	0.32
Dicentrinone	C ₁₉ H ₁₃ NO ₅	Alkaloids	VZ II 1	336.0862	320.0548; 292.0588; 275.0588; 263.0569	+H	3.56	0.43
Kaempferol 3-(4''- <i>p</i> -coumarylrhamnoside)	C ₃₀ H ₂₆ O ₁₂	Flavonoids	VZ II 1	577.1349	331.2408; 285.0391; 255.0286; 227.0338	-H	4.43	0.20
Flavinantine	C ₁₉ H ₂₁ NO ₄	Alkaloids	VL II	328.1539	178.0851; 163.0619	+H	1.91	0.44
Ocokryptine	C ₁₈ H ₂₁ NO ₃	Alkaloids	VL II	356.1494	293.0893; 265.0878; 250.0632;	+H	2.95	0.18
Laudanine	C ₂₀ H ₂₅ NO ₄	Alkaloids	VI II	344.1848	298.1082; 206.0815; 137.0596	+H	1.85	0.80
Laurelliptine	C ₁₈ H ₁₉ NO ₄	Alkaloids	VI II	314.1381	298.1082; 283.0838; 255;0879	+H	1.76	0.56
Laurelliptine	C ₁₈ H ₁₉ NO ₄	Alkaloids	VI II	312.1238	296.0936; 282.0764; 254.0817	-H	1.72	0.31

Source: From the author.

3.3.6 Metabolomics studies and biomarkers determination by MSA

Only the ESI MS- data was evaluated by MSA.

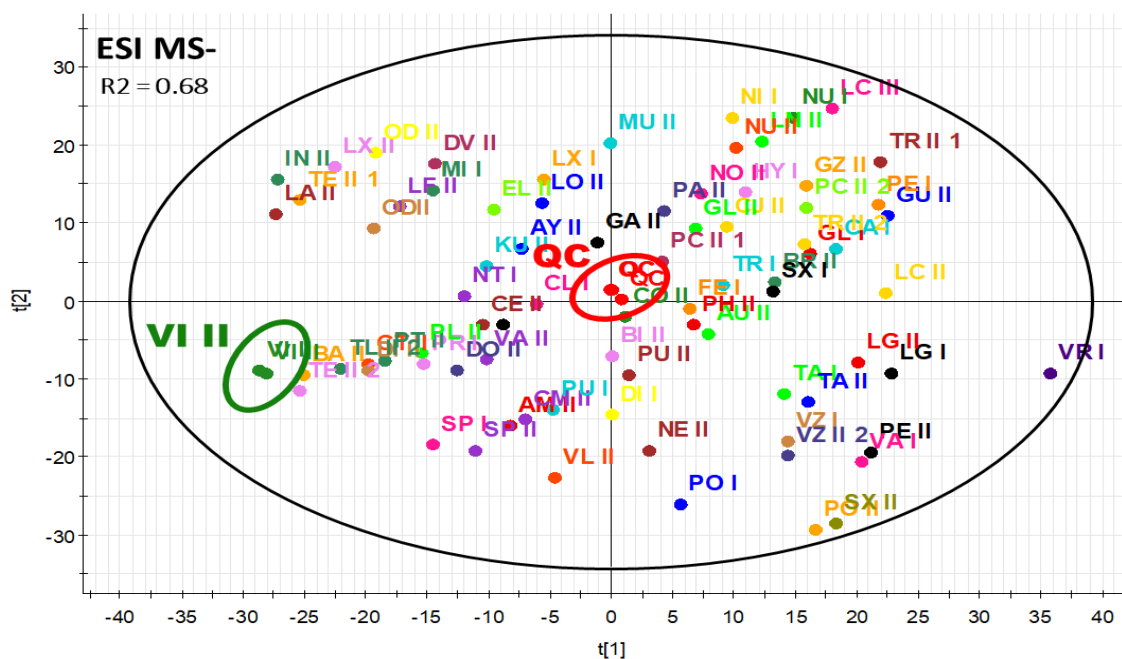
3.3.6.1 *Principal Component Analyses (PCA)*

The unsupervised PCA multivariate analyses assist in reducing the dimensionalities of complex datasets and provide an overview of all observations, by evidencing groupings and outliers of the model. It was initially applied to visualise the general clustering trends and verify the metabolic characteristics of the extracts, independently of their class or group (XI et al., 2015). The analytical replicates (QC controls and VI II – *Ocotea villosa*) were clustered together in the negative mode PCA plot, and the QC clustered in the plot center, corroborating the fitness of the developed model. These samples were used to indicate if the analyses were reproductive and if the data treatment was accurate. The scores $t[1]$ and $t[2]$ are the two most important in summarizing the dataset.

The PCA was mean centered scaled with 4 components obtained $R^2 = 0.68$, indicating that the MSA model was well fitted since R^2 was > 0.5 (CHAGAS-PAULA et al., 2015; YULIANA et al., 2011). In this type of unsupervised MSA, the observations near each other in the score plot are chemically similar, while observations far away from each other are dissimilar (CHAGAS-PAULA et al., 2015b; XI et al., 2015; YULIANA et al., 2011). Therefore, the samples with similar metabolite contents are clustered together, whereas those having different metabolites are dispersed inside the Hotelling T2 Ellipse.

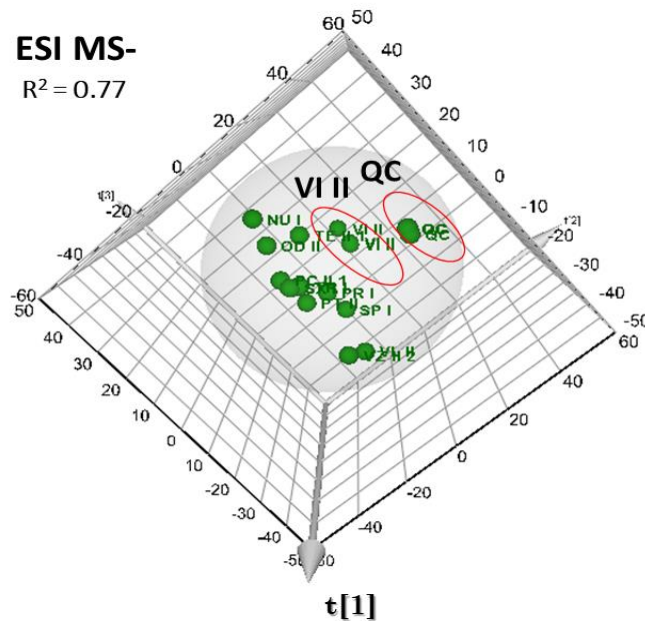
The score plots in figure 17 show the presence of a few atypical observations. By the developed model, the VR I (purple dot coloured), SX II (brownish-green dot coloured), and PO II (orange dot coloured), localized at the right bottom were not considered an outlier, although it reaches the 95% ratio limit of the Hotelling T2 Ellipse. Thus, it indicates that these *Ocotea* species have the most different metabolite composition when compared to the others of the dataset. Moreover, the PCA 3D for the active samples with 3 components and center scaling obtained $R^2 = 0.72$. Again we could confirm that data treatment was accurate and the model was well fitted (Figure 18).

Figure 17 - Score plot of Principal Component Analyses (PCA) of all samples, hotelling ellipse= 95%, for UPLC-ESI MS-, 4 components and $R^2 = 0.68$. QC – Quality control; VI II - *Ocotea villosa*



Source: From the author.

Figure 18 - Score plot 3D of Principal Component Analysis (PCA) of active anti-inflammatory samples, hotelling ellipse= 95%, 3 components and $R^2 = 0.77$. QC – Quality control; VI II- *Ocotea villosa*



Source: From the author.

3.3.6.2 Partial Least Square – Discriminant Analyses (PLS-DA)

The supervised MSA was used to visualise the chemical difference of samples, and to find potential biomarkers (variables important to projection - VIPs) by classification of the samples into distinct groups, the active and inactive. The PLS-DA is considered robust dual matrix (X and Y) classification model and it is used to find the fundamental relations between X and Y matrices (CHAGAS-PAULA et al., 2015a; XI et al., 2015). The PLS-DA analysis was efficiently applied for UPLC-ESI MS- and it was normalised by unit variance (UVar) and supervised by the anti-inflammatory profile. The PLS developed model was well fitted with 4 components, obtaining an excellent value of the goodness of fit $R^2=0.98$, and also fair predictability of model $Q^2=0.62$, where values higher than 0.5 are considered robust models (CHAGAS-PAULA et al., 2015; YULIANA et al., 2011). The model was also normalized by Pareto, and the obtained VIPs and positively correlated metabolites with PGE2 inhibition pathway showed accordance of biomarkers. However, UVar accomplished better R^2 and Q^2 values.

Firstly, from PLS-DA statistical analysis, it was possible to discriminate the samples according to the presence of the anti-inflammatory activity and determine the VIPs. Those VIP values > 1 are estimated the most important variables to differentiate the samples according to their respective class (active and inactive) (CHAGAS-PAULA et al., 2015). Subsequently, the loading plots (covariance p [1] x correlation p (corr) [1] between variables) analysis, positive correlation coefficients with the anti-inflammatory group and VIP > 1.5 indicated the metabolites most correlated with the anti-inflammatory activity (Figure 19).

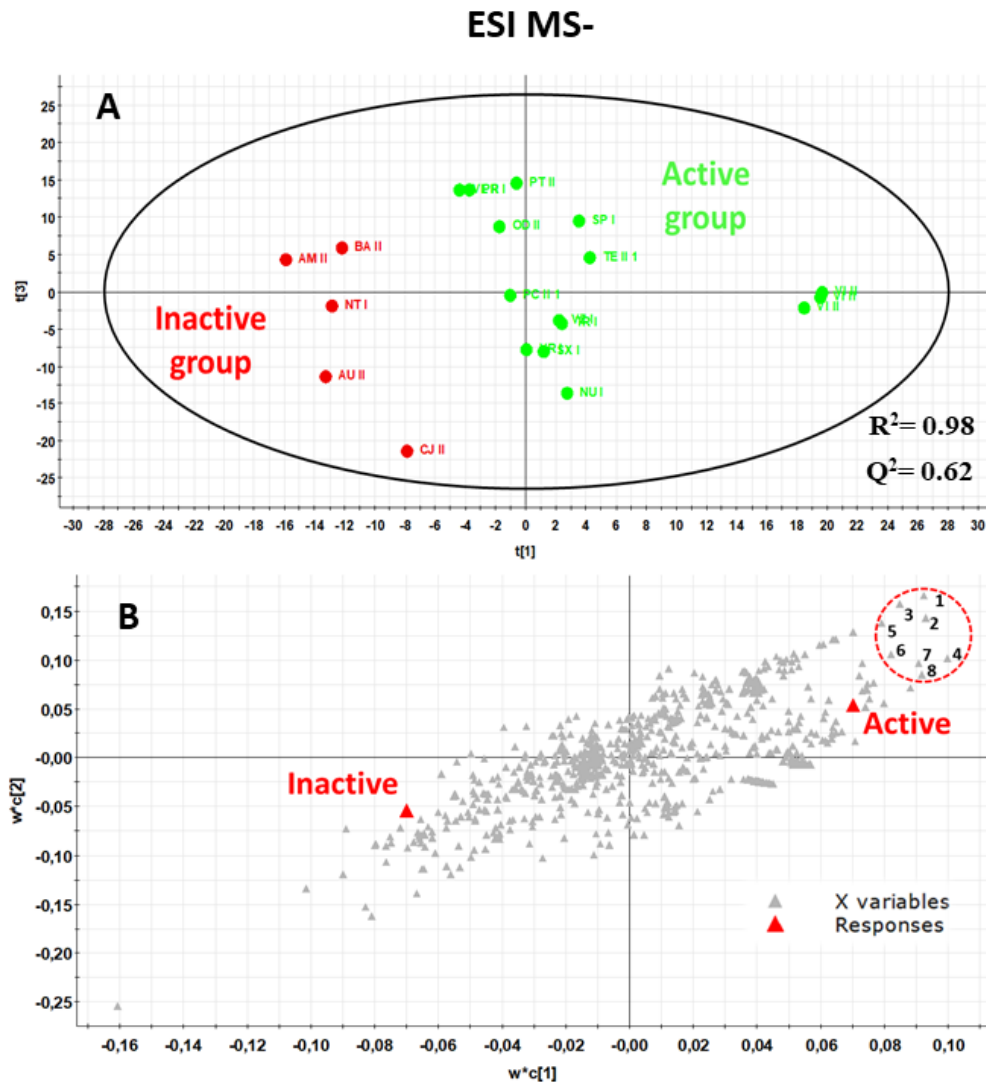
To develop the PLS model, initially, 5 inactive *Ocotea* sp. (AM II, AU I, BA II, CJ II and NT I) in the anti-inflammatory screening were randomly added to the model. The loading plots represent the variables m/z -RT pairs of molecules in a grey triangle shape. Those most correlated with the active samples are shown in the upper right quadrant of the plot (Active group response) and those metabolites more correlated with the Inactive group response are displaced to the plot bottom left. Those variables not well explained by the model are close to 0 (Figure 20). When the dot occurs farther along the x-axis and y-axis, the assigned metabolite has a more significant contribution and higher reliability to the variance between two groups (JAE-WON; HEON, 2015). By only the analyses of the loading plots, we have assigned 10 potential biomarkers candidates. For the Correlation coefficient within the Active group, the statistical model corroborated all

the biomarkers previously indicated by the loading plots, plus the addition of more 2 biomarkers (m/z 249.1125/ RT 5.14; m/z 312.1234/ RT 1.76). The dereplication of all biomarkers is described in Table 8 and 9.

The strategies used for molecular formula determination of the compounds of the extracts were based on the scientific i-FIT Norm, which is a core methodology for the analyses of small molecular weight metabolites obtained through TOF instrumentation (KATCHBORIAN-NETO et al., 2020). Based on Waters elemental composition calculator, the list of proposed elemental compositions was according to the highest agreement of theoretical isotopic pattern and lower error of mass in mDa. The low i-FIT Norm score is the better result (IGLESIAS, 2013). The M+2 isotope proportion in the spectra was analysed to verify the presence or absence of adducts, such as the ions Cl⁻ and Br⁻.

The structure identification of the biomarkers as proceeded was supported by MS^E independent data acquisition. This technique encompasses exact mass and fragment ion spectra of the candidate component in the sample, thus it increases the identification confidence level of the chemical analyses (ROSNACK et al., 2016). By using the non-targeted, data-independent approach to data acquisition all fragments from all detectable metabolites in samples were obtained and product ions of the assigned biomarkers compared with a spectral library in the literature.

Figure 19 - Score plot and loading plot of PLS-DA model indicating the discrimination of the active and inactive sample groups, normalized by UVar, 4 components, and the 8 variables (metabolites) and the responses (active and inactive), normalized by Pareto. *m/z* / RT - 1- 521.20213_2.65; 2- 539.21349_2.98; 3- 551.21317_3.03; 4-555.223362_2.88; 5- 395.15510_2.31; 6- 326.13901_2.00; 7- 591.26175_9.48; 8-879.4965_7.76



Source: From the author.

Table 8 - The list of potential biomarkers with the anti-inflammatory activity via PGE2 inhibition pathway. The sample column refers to the sample with the highest detector counts acquired for the biomarker. The detector counts (DC) is the intensity of the peak.

Sample [#]	Observed <i>m/z</i>	RT	DC	VIP	MF	Error (mDa)	Adduct	I- FIT	Hits (DNP)	Compound name or class	Observed product ions (<i>m/z</i>)
NUI	249.1125	5.14	1.1x10 ³	2.72	C ₁₄ H ₁₈ O ₄	0.2	-H	0.6	104	Pterosins* (sesquiterpenoids)	-
NUI	555.2230	2.88	2.9x10 ³	1.79	C ₃₀ H ₃₆ O ₁₀	1.3	-H	1.6	30	Neoligans and sesquilignans	-
TRI	395.1551	2.31	9.4x10 ³	1.79	C ₁₆ H ₂₈ O ₁₁	0.2	-H	0.8	3	Fatty acid-glycosides*	-
VZ II 2	326.1390	2.00	1.5x10 ⁴	1.73	C ₁₉ H ₂₁ NO ₄	0.2	-H	0.6	145	Boldine*	311.1147; 296.0900; 281.0698; 280.0581
TE II 1	591.2617	9.48	1.6x10 ³	1.69	C ₃₅ H ₃₆ N ₄ O ₅	0.8	-H	0.7	4	Pheophorbide*	-
VI II	312.1234	1.76	6.3x10 ⁴	1.59	C ₁₈ H ₁₉ NO ₄	0.6	-H	0.3	81	Laurelliptine*	296.0936; 282.0764; 254.0817

Source: From the author.

Note: # The table displays only the sample which the biomarker was found with the highest peak area. Other samples also have these biomarkers.
 * Pterosins Q, S and T
 * Fatty acid-glycosides – 1) 1-(3-Methylbutanoyl)-6-apiosylglucose; 2) 6'-*O*-(β-D-Xylopyranosyl)-1'-*O*-[(2ξ)-2-methylbutanoyl]-β-D-glucopyranose (Nonoside); 6'-*O*-(α-L- Arabinopyranosyl)-1'-*O*-[(*S*)-2-methylbutanoyl]-β-D-glucopyranose
 * Boldine has two isomers with same major product ions in ESI MS- at *m/z* [326→ 311→ 296] – isoboldine and corytuberine
 * Pheophorbide has 2 isomers with *m/z* 592.2686, the epimer –pheophorbide and the phaeoporphyrin
 * Laurelliptine is also known as norboldine and it has two isomers with major product ions in ESI MS- at *m/z* [314→ 296→ 282] – norisoboldine and laetanine

The metabolites with VIP value > 1.5 that acquired zero hits on chemical databases are detailed in Table 8. The dereplication shows that they are unknown biomarkers and therefore potential novel metabolites.

Table 9 - The list of unknown biomarkers with the anti-inflammatory activity via PGE2 inhibition pathway.

Sample#	Observed <i>m/z</i>	RT	DC	VIP	MF	Error (mDa)	Adduct	I-FIT	Hits (DNP)	Compound name or class
TE II 1	879.4965	7.76	1.1 x10 ³	1.63	C ₅₇ H ₆₄ N ₆ O ₃	0.2	-H	0.9	0	Unknown
TR I	521.2021	2.65	6.4 x10 ³	2.26	C ₂₂ H ₃₀ N ₆ O ₉	0.0	-H	0.6	0	Unknown
VZ II 2	539.2126	2.98	3.6 x10 ³	1.97	C ₂₆ H ₃₆ O ₁₂	0.3	-H	1.1	0	Unknown
TR I	551.2131	3.03	1.1x10 ⁴	1.54	C ₂₈ H ₃₂ N ₄ O ₈	0.3	-H	0.3	0	Unknown

Source: From the author.

Note: # The table displays only the sample which the biomarker was found with the highest peak area. Other samples also have these biomarkers.

The supervised MSA of UPLC-ESI MS- data revealed the presence of the sesquiterpenoids with elemental composition $C_{14}H_{18}O_4$, and parent ion at m/z 249.1125, tentatively identified as pterosins T, S and Q. This class of organic compounds are known as indanones, which is a vast class of secondary metabolites from plants. The indanones are compounds containing an indane ring bearing a ketone group to form the structural pattern of this class, which is becoming recently investigated in NP research (LU et al., 2019). Pterosins are divided into categories according to the number of skeletal carbon, which varies from 13 to 15 carbon chain giving rise to different derivatives, which could be also glycosyl derivatives (CHEN et al., 2013; LU et al., 2019). Our results are corroborated by an increasing number of publications that indicate that pterosins hold several pharmacological activities, such as anticancer, anti-inflammatory and antitubercular properties (CHEN et al., 2013; LU et al., 2019).

The classical aporphine alkaloids isomers of boldine and laurelliptine were also assigned at m/z 326.1390 and m/z 312.1234 in the ESI MS- with the respective main product ion at m/z 311.1147 and m/z 296.0936. These metabolites were indicated by MSA as potentially correlated with the anti-inflammatory activity. The literature is already filled with significant *in-vitro* and *in-vivo* studies of boldine anti-inflammatory and antipyretic effects and other benzyloquinoline and aporphine alkaloids. Our findings are in line with a recent study involving the boldine, reticuline, and boldine + reticuline alkaloids combination treatments, where they significantly decreased paw edema induced by carrageenan and PGE2 in a time and dose-dependent manner (BACKHOUSE et al., 1994; PENG et al., 2019; YANG et al., 2018). The authors also evidenced that the alkaloids association enhanced the inhibitory effect when compared to single boldine or reticuline group, suggesting a possible potentiation and synergism when compounds are administered together. The boldine is also related as a potential agent in the inflammatory bowel disease with beneficial effects in alleviating colonic inflammation throughout suppression of the NF- κ B, MAPK and IL-6/STAT3 signalling pathways (PENG et al., 2019).

Moreover, the metabolite pheophorbide A indicated by MSA as correlated with the anti-inflammatory activity is a product of the chlorophyll breakdown, and it was first isolated from Chinese medicinal herbs (CHAN et al., 2006). However, it was already identified in other plant species in worldwide, and the anti-proliferative effects and more recently the anti-inflammatory potential were described in the literature (CHAN et al., 2006; ISLAM et al., 2013), what

somehow together with the PGE2 inhibition capacity of the aporphine and benzyloquinolines alkaloids endorse the MSA obtained results. The biomarkers with MF $C_{30}H_{36}O_{10}$ and $C_{16}H_{28}O_{11}$ only the secondary class of the metabolites were putatively assigned. Also, four metabolites were assigned as unknown, since no HIT on databases was found for their elemental composition, as described in table 9.

The metabolomics studies commonly generate a substantial amount of complex data, which after acquisition through hyphenated analytical technics, processing through analytical software require MSA techniques to properly evaluate the high number of metabolites and interpret the correlation of the biological response (CHAGAS-PAULA et al., 2015b; KOSMIDES et al., 2013). Thus, throughout MSA from metabolic data, we could indicate the most relevant metabolites for the studied bioactivity by cross-analysis using an *in-house* / UNIFI databases and spectral library available in the literature. These strategies were crucial in benefit to speed-up the time analyses and rapidly identify the dissimilarities of metabolites produced by the *Ocotea* genus and determine the biomarkers responsible for the pronounced anti-inflammatory activity (CHAGAS-PAULA et al., 2015b; CHAGAS-PAULA; OLIVEIRA; FALEIRO, 2015; CRAGG; PEZZUTO, 2016; DEMAIN; VAISHNAV, 2011; ROUX et al., 2011). Therefore, the metabolomics approach based on UPLC-QTOF/MS took less amount of time and costs to produce suitable differences visualizations in the chemical composition of extracts, what was crucial to investigate the biomarkers correlated with the investigated pharmacological activity (CHAGAS-PAULA et al., 2015).

In summary, our results indicated five *Ocotea* extracts with % inhibition higher than 95%: the *O. nutans*, *O. odorifera*, *O. velloziana*, *O. velutina* and *O. villosa*. However, only the *O. odorifera* has an anti-inflammatory report previously described in the literature. While *O. nutans* has only reported antioxidant activity and *O. velloziana* antiviral. The *O. velutina* and *O. villosa* have no report of the biological activity described, and thus the anti-inflammatory potential was revealed for the first time by this research. The aporphine alkaloids isomers of boldine and laurelliptine were dereplicated via level 2 and were highly statistically indicated as biomarkers of anti-inflammatory activity via PGE2 inhibition mechanism.

3.4 Conclusion

As the *Ocotea* genus is known as high oily plants, the several volatile compounds of the genus are already well described in the literature. Thus, herein we fill this gap with a wide range of non-volatile compounds possibly widespread in the genus. The *in-house* database built facilitated a rapid characterization of the metabolites and confirmed *Ocotea* species as alkaloids producers, mainly the aporphine alkaloids class, besides higher levels of glycoside flavonoids. Despite the substantial importance of the *Ocotea* genus in Lauraceae family, with several recent important biological activity discoveries, the genus is still insufficiently known on academic literature, and the majority of selected the species have never been evaluated in bioactivity assays before. Some of them lack even a chemical investigation. In this manner, the present research is also filling this gap, by a comprehensive metabolomic screening for a variety of different metabolites produced by species of the *Ocotea* genus.

From our research, 55% of the evaluated *Ocotea* extracts were statistically different from negative controls, and 20% were statistically similar to the positive controls, DEX and IND. Moreover, it is essential to mention that the anti-inflammatory activity of *Ocotea* species could be attributed to more than one specific biomarker, which suggests that several metabolites can act synergistically, or not, in plant extracts for a pronounced anti-inflammatory pharmacological activity. This work is the first report on the chemical composition of several endemic *Ocotea* of Brazil, and our results indicated the UPLC-QTOF-MS-based metabolomics approach seem promising in reducing time analyses of chemical investigation in the drug discovery process, with advantages of less plant material and chemical reactants consumption.

The efficient analytical UPLC-QTOF-MS model developed in a single run of 10 min was able to qualitative and semi-quantitative dereplicate more than 100 different metabolites in the metabolic fingerprint of the *Ocotea* species, by using very low vegetal material. Thus evidencing that this method as a powerful tool in NP research. Moreover, by suitable MSA and metabolomics untargeted approach, this study revealed LPS-induced PGE2 inhibitors from complex plant extract samples. The work also detected compounds with no molecular formula found in the comprehensive databases, thus, they are likely to be unreported substances. Additionally, these findings might also be employed in future to guide a faster development of pharmaceutical candidates endowed with anti-inflammatory activity to act on the decrease of the PGE2 inflammatory mediator release. The main applicability comprehends cancer adjuvant therapy and acute inflammation inhibition for a broad spectrum of inflammatory pathologies. The mechanisms underlying the pharmacological activity should be investigated in the future.

4 CHAPTER TWO - NEUROPROTECTIVE POTENTIAL OF AYAHUASCA AND UNTARGETED METABOLOMICS ANALYSES: APPLICABILITY TO PARKINSON'S DISEASE

This part of the study was recently published (Journal: JEP, IF: 3.6),

<https://doi.org/10.1016/j.jep.2020.112743>, and the paper header and the graphical abstract is below.

Journal of Ethnopharmacology 255 (2020) 112743



Neuroprotective potential of Ayahuasca and untargeted metabolomics analyses: applicability to Parkinson's disease



Albert Katchborian-Neto^a, Wanderleya T. Santos^b, Karen J. Nicácio^a, José O.A. Corrêa^b, Michael Murgu^c, Thaís M.M. Martins^d, Dawidson A. Gomes^d, Alfredo M. Goes^d, Marisi G. Soares^a, Danielle F. Dias^a, Daniela A. Chagas-Paula^{a,*}, Ana C.C. Paula^{b,**}

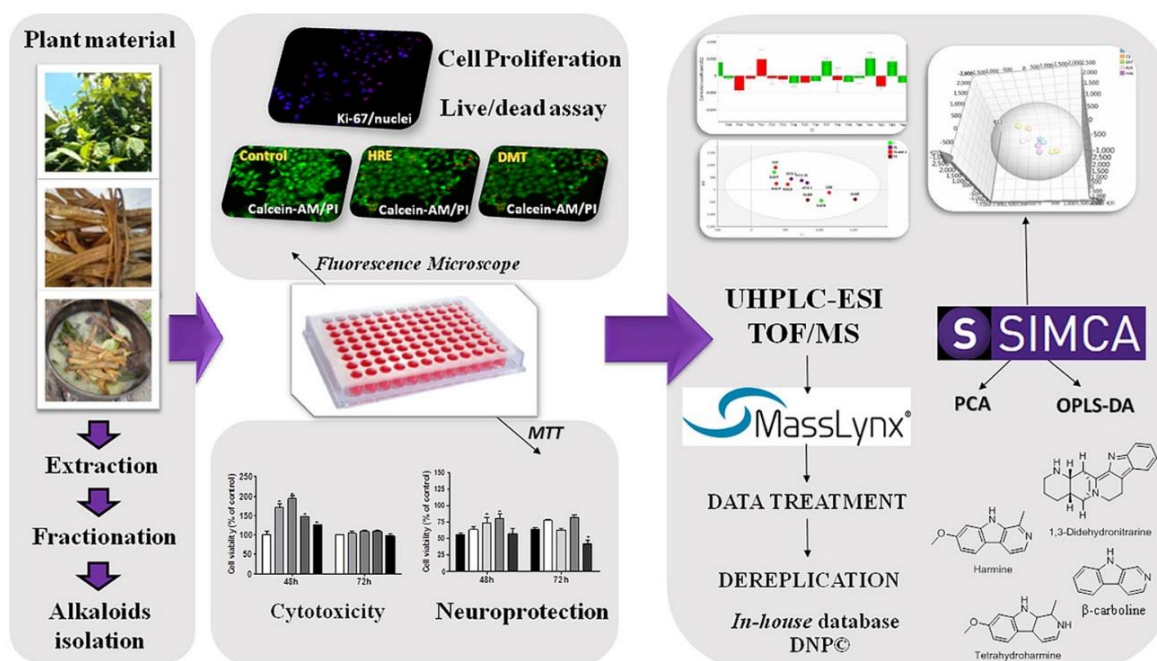
^a Chemistry Institute, Federal University of Alfenas, 37130-001, Alfenas, Minas Gerais, Brazil

^b School of Pharmacy, Federal University of Juiz de Fora, 36036-900, Juiz de Fora, Minas Gerais, Brazil

^c Waters Corporation, Alameda Tocantins 125, 27th Floor, Alphaville, 06455-020, São Paulo, São Paulo, Brazil

^d Biological Sciences Institute, Federal University of Minas Gerais, 31270-901, Belo Horizonte, Minas Gerais, Brazil

Keywords: Metabolomics. Ayahuasca. Traditional medicine. Neuroprotection. Neurodegenerative disease. Parkinson's disease.



5 FINAL CONSIDERATIONS

In chapter I, the chemical profiles of 60 different *Ocotea* species were evaluated by an untargeted metabolomics approach by the use of a hyphenated sensitive high-resolution analytical techniques and a comprehensive analytical method. The exploratory analysis in this work included dereplication, which has smoothed the path for unambiguously level 1 identification, supported by the use of chromatographic mining, spectrometric data and correlation of the dataset with the pharmacological activity. This work evaluated several *Ocotea* spp. of the Brazilian flora territory that has never been studied before and revealed important biomarkers of anti-inflammatory effect through LPS-induced PGE2 inhibition.

Furthermore, in chapter II this study showed for the first time that Ayahuasca and crude extracts of its matrix plant are capable to elicit outstanding neuroprotective effects by using an *in vitro* PD model. In fact, the alcoholic extracts of *B. caapi* and *P. viridis*, together with the Ayahuasca decoction could be considered promising for the treatment of PD and other neurodegenerative disorders as our study evidenced significant neuroprotective activity and neuronal cell proliferation. We have observed that the lowest evaluated doses displayed the most efficacious neuroprotective effect and throughout untargeted metabolomics and MSA results, several compounds were correlated with the neuroprotective profile, such as β -carbolines and monoterpene indole alkaloids (MIAs). Therefore, as the development of candidate neuroprotective therapies remains at a primary goal for PD management, a complete dose-response study *in vivo* and PD volunteers is already needed for Ayahuasca and its matrices plants. This undertaking will hopefully develop a disease-modifying intervention therapy able to reduce the progression of the disease and to provide positive benefits for PD patients

Lastly, this research revealed important biomarkers of pharmacological activity, confirming that metabolomics approaches might have a valuable potential in the drug discovery field. Also, the metabolomics data when interpreted together with genomic and proteomic data, an in-depth understanding of systems could be achieved, including mechanisms, pathways, and the different physiological dynamic interactions of the compounds in organisms. Particularly, this knowledge is well appreciated in diverse areas of study, such as the NP, drug development and disease diagnostics (FIEHN, 2001; KOSMIDES et al., 2013; ROUX et al., 2011; YULIANA et al., 2011). Therefore, metabolomics strategies can be treated as a modern tool in a wide range of research fields.

REFERENCES

- ABDULLA, R. *et al.* Qualitative analysis of polyphenols in Macroporous resin pretreated pomegranate husk extract by HPLC-QTOF-MS. **Phytochemical Analysis**, v. 28, n. 5, p. 465–473, 2017.
- ALCÂNTARA, B. G. V. **Metabolômica e fitoquímica de espécies de Lauraceae e avaliação da inibição das principais vias inflamatórias por seus extratos e substâncias purificadas**. 2019. 72f. Dissertação (Mestrado em Química) - Universidade Federal de Alfenas, Alfenas, 2019.
- AMILIA DESTRYANA, R. *et al.* Antioxidant and anti-inflammation activities of *Ocotea*, copaiba and blue cypress essential oils *in vitro* and *in vivo*. **Journal of the American Oil Chemists' Society**, v. 91, n. 9, p. 1531–1542, 2014.
- BACKHOUSE, N. *et al.* Anti-inflammatory and antipyretic effects of boldine. **Agents and Actions**, v. 42, n. 3–4, p. 114–117, 1994.
- BATISTA, A. N. L. *et al.* Aromatic compounds from three Brazilian Lauraceae species. **Química Nova**, v. 33, n. 2, p. 321–323, 2010.
- BENTLEY, K. W. The morphine alkaloids. **Alkaloids: Chemistry and Physiology**, v. 13, n. C, p. 1–163, 1971.
- BETIM, F. C. M. *et al.* *Ocotea nutans* (Nees) mez (Lauraceae): Chemical composition, antioxidant capacity and biological properties of essential oil. **Brazilian Journal of Pharmaceutical Sciences**, v. 55, n. 18284, p. 1–10, 2019.
- BREITBACH, U. B. *et al.* Amazonian Brazilian medicinal plants described by C.F.P. von Martius in the 19th century. **Journal of Ethnopharmacology**, v. 147, n. 1, p. 180–189, 2013.
- BRITO, A. F. R. **Análise de variação sazonal e das atividades antifúngica e antimicrobiana em óleos essenciais de *Ocotea porosa* (Nees) Barroso e *Nectandra megapotamica* (Spreng.)**. 2009. 123f. Dissertação (Mestrado em Química) - Universidade de São Paulo, São Paulo, 2009.
- BROTTO, M. L.; CERVI, A. C.; DOS SANTOS, É. P. O gênero *Ocotea* (Lauraceae) no estado do Paraná, Brasil. **Rodriguesia**, v. 64, n. 3, p. 495–525, 2013.
- BRUCHER, B. L. *et al.* Imagine a world without cancer. **BioMed Central**, v. 14, n. March 2018, p. 2–8, 2014.
- BRUSTULIM, L. J. S. **Anatomia foliar e caulinar, caracterização química e atividades biológicas do óleo essencial *Ocotea porosa* (Nees & Mart.) Barroso: Uma abordagem disciplinar**. 2019. 67f. Dissertação (Mestrado em Ciências da Saúde) – Universidade Estadual de Ponta Grossa, Ponta Grossa, 2019.
- CAI, Y. *et al.* Antioxidant activity and phenolic compounds of 112 traditional Chinese medicinal plants associated with anticancer. **Life Sciences**, v. 74, n. 17, p. 2157–2184, 2004.
- CAMARGO, M. J. DE *et al.* Sesquiterpenos de *Ocotea lancifolia* (Lauraceae). **Quim. Nova**,

v. 36, n. 7, p. 1008–1013, 2013.

CANDIDO, L. P. **Busca de extratos e compostos ativos com potencial herbicida e inseticida nas espécies *Davilla elliptica* busca de extratos e compostos ativos com potencial herbicida e inseticida nas espécies *Davilla elliptica* St . Hill e *Ocotea pulchella* Nees & Mart.** 2016. 179f. Tese (Doutorado em Ciências) - Universidade Federal de São Carlos, São Carlos, 2016.

CARNEVALE NETO, F. *et al.* Characterization of aporphine alkaloids by electrospray ionization tandem mass spectrometry and density functional theory calculations. **Rapid Communications in Mass Spectrometry**, p. 0–2, 2019.

CASTRO, R. D.; LIMA, E. O. Atividade antifúngica dos óleos essenciais de sassafrás (*Ocotea odorifera* Vell.) e alecrim (*Rosmarinus officinalis* L.) sobre o gênero *Candida*. **Revista Brasileira de Plantas Mediciniais**, v. 13, n. 2, p. 203–208, 2011.

CHAGAS-PAULA, D. *et al.* A metabolomic approach to target compounds from the Asteraceae family for dual COX and LOX Inhibition. **Metabolites**, v. 5, n. 3, p. 404–430, 2015a.

CHAGAS-PAULA, D. A. *et al.* Prediction of anti-inflammatory plants and discovery of their biomarkers by machine learning algorithms and metabolomic studies. **Planta Medica**, v. 81, n. 6, p. 450–458, 2015b.

CHAGAS-PAULA, D.; OLIVEIRA, T.; FALEIRO, D. Outstanding anti-inflammatory potential of selected Asteraceae species through the potent dual inhibition of Cyclooxygenase-1 and 5-Lipoxygenase. **Planta Medica**, v. 81, p. 1296–1307, 2015.

CHAN, J. Y. W. *et al.* Pheophorbide a, a major antitumor component purified from *Scutellaria barbata*, induces apoptosis in human hepatocellular carcinoma cells. **Planta Medica**, v. 72, n. 1, p. 28–33, 2006.

CHASE, M. W. *et al.* An update of the angiosperm phylogeny group classification for the orders and families of flowering plants: APG IV. **Botanical Journal of the Linnean Society**, v. 181, n. 1, p. 1–20, 2016.

CHAVERRI, C.; CICCIO, J. F. Essential oil of trees of the genus *Ocotea* (Lauraceae) in Costa Rica. I. *Ocotea brenesii*. **Revista de Biologia Tropical**, v. 53, n. 3–4, p. 431–436, 2005.

CHEN, J. J. *et al.* New pterosin sesquiterpenes and antitubercular constituents from *Pteris ensiformis*. **Chemistry and Biodiversity**, v. 10, n. 10, p. 1903–1908, 2013.

CLAVEL, J. Progress in the epidemiological understanding of gene-environment interactions in major diseases: cancer. **Comptes Rendus - Biologies**, v. 330, n. 4, p. 306–317, 2007.

COSTA, E. V. *et al.* Aporphine alkaloids from the leaves of *Guatteria friesiana* (Annonaceae) and their cytotoxic activities. **journal Braz. Chem. Soc. Braz. Chem. Soc.**, v. 24, n. 5, p. 788–796, 2013.

COUSSENS, L. M.; WERB, Z. Inflammation and cancer. **Nature**, v. 90, n. 1, p. 58–73, 2012.

COY, E. D.; CUCA, L. E.; SEFKOW, M. COX, LOX and platelet aggregation inhibitory properties of Lauraceae neolignans. **Bioorganic and Medicinal Chemistry Letters**, v. 19, n. 24, p. 6922–6925, 2009.

CRAGG, G. M.; NEWMAN, D. J. Plants as a source of anti-cancer agents. **Journal of Ethnopharmacology**, v. 100, n. 1–2, p. 72–79, 2005.

CRAGG, G. M.; PEZZUTO, J. M. Natural products as a vital source for the discovery of cancer chemotherapeutic and chemopreventive agents. **Medical Principles and Practice**, v. 25, n. 2, p. 41–59, 2016.

CREEK, D. J. *et al.* Metabolite identification: are you sure? And how do your peers gauge your confidence? **Metabolomics**, v. 10, n. 3, p. 350–353, 2014.

CROZIER, A.; JAGANATH, I. B.; CLIFFORD, M. N. Phenols, polyphenols and tannins: An overview. **Plant Secondary Metabolites: Occurrence, Structure and Role in the Human Diet**, n. April 2016, p. 1–24, 2007.

CUSTÓDIO, D. L.; VEIGA JUNIOR, V. F.; Lauraceae alkaloids. **RSC Adv.**, v. 4, n. 42, p. 21864–21890, 2014.

DE VOS, R. C. H. *et al.* Untargeted large-scale plant metabolomics using liquid chromatography coupled to mass spectrometry. **Nat. Protoc.**, v. 2, n. 4, p. 778–791, 2007.

DEMAIN, A. L.; VAISHNAV, P. Natural products for cancer chemotherapy. **Microbial Biotechnology**, v. 4, n. 6, p. 687–699, 2011.

DEWICK, P. M. **Medicinal natural: a biosynthetic approach**. 3rd ed. New Jersey: Wiley & Sons, 2009.

DICKSON, K.; LEHMANN, C. Inflammatory response to different toxins in experimental sepsis models. **International Journal of Molecular Sciences**, v. 20, n. 18, 2019.

FIEHN, O. Combining genomics, metabolome analysis, and biochemical modelling to understand metabolic networks. **Comparative and Functional Genomics**, v. 2, n. 3, p. 155–168, 2001.

FLORA do Brasil. Rio de Janeiro: Jardim Botânico, 2020. Disponível em: <http://floradobrasil.jbrj.gov.br/reflora/PrincipalUC/PrincipalUC.do>. Acesso em: 04.set.18 .

FUJII, I. *et al.* The syntheses of 3,4-Dimethoxy-6-morphinanone and isomorphinanone. Spectral inspection of the stereochemistry in cis and trans b/c ring fusion. **Chemical Pharmaceutical Bulletin**, v. 31, n. 11, p. 4670–4673, 1970.

GARCEZ, W. S. *et al.* Larvicidal activity against *Aedes aegypti* of some plants native to the west-central region of Brazil. **Bioresource Technology**, v. 100, n. 24, p. 6647–6650, 2009.

GOTTLIEB, O. R. Chemosystematics of the Lauraceae. **Phytochemistry**, v. 11, n. 5, p. 1537–1570, 1972.

GRAZIANI, V. *et al.* Metabolomic approach for a rapid identification of natural products with cytotoxic activity against human colorectal cancer cells. **Scientific Reports**, v. 8, n. 1, p.

1–11, 2018.

HOET, S. *et al.* Alkaloids from *Cassytha filiformis* and related aporphines: antitrypanosomal activity, cytotoxicity, and interaction with DNA and topoisomerases. **Planta Medica**, v. 70, n. 5, p. 407–413, 2004.

IBAMA. Ministério do Meio Ambiente. **National biodiversity plan. Anais, Brasília**, 2017

IGLESIAS, H. A. Introdução ao acoplamento cromatografia líquida - espectrometria de massas. **Journal of Chemical Information and Modeling**, v. 53, n. 9, p. 1–13, 2013.

ISLAM, M. N. *et al.* Anti-inflammatory activity of edible brown alga *Saccharina japonica* and its constituents pheophorbide a and pheophytin a in LPS-stimulated RAW 264.7 macrophage cells. **Food and Chemical Toxicology**, v. 55, p. 541–548, 2013.

JAE-WON, L.; HEON, J. S. Metabolomics based on UPLC-QTOF/MS applied for the discrimination of *Cynanchum wilfordii* and *Cynanchum auriculatum*. **Journal of Postgenomics Drug & Biomarker Development**, v. 05, n. 04, 2015.

JOHANSSON, M.; PERSSON, J. Cancer therapy: targeting cell cycle regulators. **Anti-Cancer Agents in Medicinal Chemistry**, v. 8, n. 7, p. 723–731, 2012.

KAPADIA, N.; HARDING, W. Aporphine alkaloids as ligands for serotonin receptors. **Medicinal chemistry**, v. 06, n. 04, p. 241–249, 2016.

KARNEZIS, T. *et al.* The connection between lymphangiogenic signalling and prostaglandin biology: a missing link in the metastatic pathway. **Oncotarget**, v. 3, n. 8, p. 890–903, 2012.

KATAJAMAA, M.; OREŠIČ, M. Data processing for mass spectrometry-based metabolomics. **Journal of Chromatography A**, v. 1158, n. 1–2, p. 318–328, 2007.

KOSMIDES, A. K. *et al.* Metabolomic fingerprinting: challenges and opportunities. **Critical Reviews in Biomedical Engineering**, v. 41, n. 3, p. 205–221, 2013.

LANDSKRON, G. *et al.* Chronic inflammation and cytokines in the tumor microenvironment. **Journal of Immunology Research**, v. 2014, 2014.

LI, Y. *et al.* Chemical structures of lignans and neolignans isolated from Lauraceae. **Molecules**, v. 23, n. 12, 2018.

LI, Z. *et al.* Simultaneous quantification of hyperin, reynoutrin and guaijaverin in mice plasma by LC-MS/MS: Application to a pharmacokinetic study. **Biomedical Chromatography**, v. 30, n. 7, p. 1124–1130, 2016a.

LI, Z. H. *et al.* Rapid identification of flavonoid constituents directly from PTP1B inhibitive extract of raspberry (*Rubus idaeus* L.) leaves by HPLC-ESI-QTOF-MS-MS. **Journal of Chromatographic Science**, v. 54, n. 5, p. 805–810, 2016b.

LIU, M.; KALBASI, A.; BEATTY, G. L. Functio Laesa: Cancer inflammation and therapeutic resistance. **Journal of Oncology Practice**, v. 13, n. 3, p. 173–180, 2017.

LU, J. *et al.* Four New Pterosins from *Pteris cretica* and their cytotoxic activities. **Molecules (Basel, Switzerland)**, v. 24, n. 15, p. 1–8, 2019.

- LUDY CRISTINA, P.; LUIS ENRIQUE, C. Aporphine alkaloids from *Ocotea macrophylla* (Lauraceae). **Quimica Nova**, v. 33, n. 4, p. 875–879, 2010.
- LYONS, T. R. *et al.* Cyclooxygenase-2-dependent lymphangiogenesis promotes nodal metastasis of postpartum breast cancer. **Journal of Clinical Investigation**, v. 124, n. 9, p. 3901–3912, 2014.
- MAJUMDER, M. *et al.* Prostaglandin E2 receptor EP4 as the common target on cancer cells and macrophages to abolish angiogenesis, lymphangiogenesis, metastasis, and stem-like cell functions. **Cancer science**, v. 105, n. 9, p. 1142–1151, 2014.
- MANTOVANI, A. The inflammation – cancer connection. **FEBS Journal**, v. 285, n. 4, p. 638–640, 2018.
- MARINUS, M. G.; LØBNER-OLESEN, A. DNA Methylation. **EcoSal Plus**, v. 6, n. 1, p. 1–62, 2014.
- MARQUES, C. A. Importância econômica da família Lauraceae Lindl. **Floresta e Ambiente**, v. 8, n. 1, p. 195–206, 2001.
- MEIRER, K.; STEINHILBER, D.; PROSCHAK, E. Inhibitors of the arachidonic acid cascade: interfering with multiple pathways. **Basic and Clinical Pharmacology and Toxicology**, v. 114, p. 83–91, 2014.
- MENEZES, L. R. A. *et al.* Cytotoxic alkaloids from the stem of *Xylopia laevigata*. **Molecules**, v. 21, n. 7, p. 1–10, 2016.
- MUKHERJEE, P. K. *et al.* The sacred lotus (*Nelumbo nucifera*) - phytochemical and therapeutic profile. **Journal of Pharmacy and Pharmacology**, v. 61, n. 4, p. 407–422, 2009.
- MULTHOFF, G.; MOLLS, M.; RADONS, J. Chronic inflammation in cancer development. **Frontiers in Immunology**, v. 2, n. JAN, p. 1–17, 2012.
- NANDI, P. *et al.* PGE2 promotes breast cancer-associated lymphangiogenesis by activation of EP4 receptor on lymphatic endothelial cells. **BMC Cancer**, v. 17, n. 1, p. 1–17, 2017.
- OUYANG, H. *et al.* Identification and quantification analysis on the chemical constituents from traditional Mongolian medicine Flos Scabiosae using UHPLC-DAD-Q-TOF-MS combined with UHPLC-QqQ-MS. **Journal of Chromatographic Science**, v. 54, n. 6, p. 1028–1036, 2016.
- PADILLA, M. A. P. *et al.* *In vitro* antiviral activity of Brazilian Cerrado plant extracts against animal and human herpesviruses. **Journal of Medicinal Plants Research**, v. 12, n. 10, p. 106–115, 2018.
- PADUCH, R. The role of lymphangiogenesis and angiogenesis in tumor metastasis. **Cellular Oncology**, v. 39, n. 5, p. 397–410, 2016.
- PALOMINO, E. *et al.* Caparratriene, an active sesquiterpene hydrocarbon from *Ocotea caparrapi*. **Journal of Natural Products**, v. 59, n. 1, p. 77–79, 1996.
- PENG, J. *et al.* Plant-derived alkaloids: The promising disease-modifying agents for

inflammatory bowel disease. **Frontiers in Pharmacology**, v. 10, n. APR, p. 1–15, 2019.

QUAVE, C. L. **Medicinal Plant Monographs**. Emori University, p. 1–661, 2013.

RAQUEL, J. *et al.* Sesquiterpenes of *Ocotea lancifolia* (Lauraceae). **Quimica Nova**, v. 33, n. 9, p. 1980–1986, 2010.

RAYAN, A.; RAIYN, J.; FALAH, M. Nature is the best source of anticancer drugs: indexing natural products for their anticancer bioactivity. **PLoS ONE**, v. 12, n. 11, p. 1–12, 2017.

ROSNACK, K. J. *et al.* Screening solution using the software platform UNIFI: An integrated workflow by waters. **ACS Symposium Series**, v. 1242, p. 155–172, 2016.

ROUX, A. *et al.* Applications of liquid chromatography coupled to mass spectrometry-based metabolomics in clinical chemistry and toxicology: a review. **Clinical Biochemistry**, v. 44, n. 1, p. 119–135, 2011.

ROZIC, J. G.; CHAKRABORTY, C.; LALA, P. K. Cyclooxygenase inhibitors retard murine mammary tumor progression by reducing tumor cell migration, invasiveness and angiogenesis. **International Journal of Cancer**, v. 93, n. 4, p. 497–506, 2001.

RUDAZ, S. **Identification and data processing methods in metabolomics**. Future science, University of Geneva, 2015.

SACCHETTI, G. *et al.* Essential oil of wild *Ocotea quixos* (Lam.) Kosterm. (Lauraceae) leaves from Amazonian Ecuador. **Flavour and Fragrance Journal**, v. 21, n. 4, p. 674–676, 2006.

SALEHIFAR, E.; HOSSEINIMEHR, S. J. The use of cyclooxygenase-2 inhibitors for improvement of efficacy of radiotherapy in cancers. **Drug Discovery Today**, v. 21, n. 4, p. 654–662, 2016.

SALLEH, W. M. N. H. W.; AHMAD, F. Phytochemistry and biological activities of the genus *Ocotea* (Lauraceae): A review on recent research results (2000-2016). **Journal of Applied Pharmaceutical Science**, v. 7, n. 5, p. 204–218, 2017.

SANTOS, E. L. *et al.* Flavonoids: Classification, biosynthesis and chemical ecology. **Intech**, p. 13, 2017.

SANTOS, M. F. C. *et al.* New bicyclic [3.2.1] octane neolignans derivatives from *Aniba firmula* with potent *in vivo* anti-inflammatory activity on account of dual inhibition of PGE2 production and cell recruitment. **Phytochemistry Letters**, v. 30, n. January, p. 31–37, 2019.

SCHIEBER, A. *et al.* Detection of isorhamnetin glycosides in extracts of apples (*Malus domestica* cv. “Brettacher”) by HPLC-PDA and HPLC-APCI-MS/MS. **Phytochemical Analysis**, v. 13, n. 2, p. 87–94, 2002.

SEYFRIED, T. N.; HUYSENTRUYT, L. C. On the origin of cancer metastasis. **Cancer**, v. 18, n. 3, p. 43–73, 2013.

SHAO, Y.; LE, W. Recent advances and perspectives of metabolomics-based investigations in Parkinson ’ s disease. v. 2, p. 1–12, 2019.

SILVA, J. A. A. *et al.* **The Brazilian Forest Code and Science: contributions to the dialogue**. 2nd Ed., São Paulo. The Brazilian Society for the Advancement of Science, 2012.

SILVA, A. F. **Estudo metabolômico e anti-inflamatório de *Ocotea diospyrifolia* (Meins.) Mez para identificação de suas substâncias ativas e inéditas**. 2019. 108f. Dissertação (Mestrado em Química) - Universidade Federal de Alfenas, Alfenas, 2019.

SPICER, R. A.; SALEK, R.; STEINBECK, C. Comment: a decade after the metabolomics standards initiative it's time for a revision. **Scientific Data**, v. 4, p. 2–4, 2017.

STÉVIGNY, C. *et al.* Key fragmentation patterns of aporphine alkaloids by electrospray ionization with multistage mass spectrometry. **Rapid Communications in Mass Spectrometry**, v. 18, n. 5, p. 523–528, 2004.

SUBHASHINI, J.; MAHIPAL, S. V. K.; REDDANNA, P. Anti-proliferative and apoptotic effects of celecoxib on human chronic myeloid leukemia *in vitro*. **Cancer Letters**, v. 224, n. 1, p. 31–43, 2005.

SUMNER, L. W. *et al.* Proposed minimum reporting standards for chemical analysis chemical analysis working group (CAWG) Metabolomics Standards Initiative (MSI). **Metabolomics**, v. 3, n. 3, p. 211–221, 2007.

THE POLISTES Corporation. Missouri Botanical Garden, 2020.. Disponível em: <https://www.discoverlife.org/mp/20q>. Acessado em: 20.jan.2019.

ULLAH, M. F.; AATIF, M. The footprints of cancer development: cancer biomarkers. **Cancer Treatment Reviews**, v. 35, n. 3, p. 193–200, 2009.

VAN DER KOOY, F. *et al.* Quality control of herbal material and phytopharmaceuticals with MS and NMR based metabolic fingerprinting. **Planta Medica**, v. 75, n. 7, p. 763–775, 2009.

VECCHIETTI, V. *et al.* New aporphine alkaloids of *Ocotea minarum*. **Farmaco, Edizione Scientifica**, v. 34, n. 10, p. 829–40, 1979.

VINAYAVEKHIN, N.; SAGHATELIAN, A. Untargeted metabolomics. **Current Protocols in Molecular Biology**, v. 30.1.1, p. 1–24, 2010.

WANG, B. *et al.* Exploring aporphine as anti-inflammatory and analgesic lead from *dactylicapnos scandens*. **Organic Letters**, v. 22, n. 1, p. 257–260, 2020.

WANG, K. *et al.* A new aporphine alkaloid from *Illigeria aromatic*. **Records of Natural Products**, v. 13, n. 6, p. 440–445, 2019.

WANG, M. T.; HONN, K. V.; NIE, D. Cyclooxygenases, prostanoids, and tumor progression. **Cancer and Metastasis Reviews**, v. 26, n. 3–4, p. 525–534, 2007.

WOLFENDER, J.; MARTI, G.; QUEIROZ, E. F. Advances in techniques for profiling crude extracts and for the rapid identification of natural products : dereplication, quality control and advances in techniques for profiling crude extracts and for the rapid identification of natural products. **Current Organic Chemistry**, v. 14, n. 16, p. 1808–1832, 2010.

XI, B. *et al.* Statistical analysis and modeling of mass spectrometry-based metabolomics data.

Methods Mol Biol., p. 1–20, 2015.

YAMAGUCHI, U. M. et al. Antifungal effects of ellagitannin isolated from leaves of *Ocotea odorifera* (Lauraceae). **Antonie van Leeuwenhoek Journal of Microbiology**, v. 99, n. 3, p. 507–514, 2011.

YANG, X. et al. Anti-inflammatory effects of boldine and reticuline isolated from *Litsea cubeba* through JAK2/STAT3 and NF- κ B signaling pathways. **Planta Medica**, v. 84, n. 1, p. 20–25, 2018.

YANG, Z. et al. Synthesis and structure-activity relationship of nuciferine derivatives as potential acetylcholinesterase inhibitors. **Medicinal Chemistry Research**, v. 23, n. 6, p. 3178–3186, 2014.

YI, L. et al. Chemometric methods in data processing of mass spectrometry-based metabolomics: a review. **Analytica Chimica Acta**, v. 914, p. 17–34, 2016.

YULIANA, N. D. et al. Metabolomics for bioactivity assessment of natural products. **Phytotherapy Research**, v. 25, n. 2, p. 157–169, 2011.

ZANIN, S. M. W.; LORDELLO, A. L. L. Alcalóides aporfinóides do gênero *Ocotea* (Lauraceae). **Quimica Nova**, v. 30, n. 1, p. 92–98, 2007.

ZHANG, L. et al. Nuciferine inhibits LPS-induced inflammatory response in BV2 cells by activating PPAR- γ . **International Immunopharmacology**, v. 63, n. May, p. 9–13, 2018a.

ZHANG, X. et al. Anti-hyperglycemic and anti-hyperlipidemia effects of the alkaloid-rich extract from barks of *Litsea glutinosa* in ob/ob mice. **Scientific Reports**, v. 8, n. 1, p. 1–10, 2018b.

ZHOU, B. N. et al. Isolation and biochemical characterization of a new topoisomerase I inhibitor from *Ocotea leucoxylon*. **Journal of Natural Products**, v. 63, n. 2, p. 217–221, 2000.

SUPPLEMENTAL MATERIAL

Table S1 - Vouchers from UFJF and UFOP and the *Ocotea* spp. details I

(Continue)

Number	Code	Popular name	Specie Name	Endemic? (42)	Geographical location
1	AY II	canela-amarela	<i>Ocotea aciphylla</i> (Nees & Mart.) Mez	N	13°32'14.0"S 41°54'14.0" W
2	AU II	canela-branca	<i>Ocotea acutifolia</i> (Nees) Mez	N	72°28'18.0"S 58°08'21.0" W
3	AM II	unknown	<i>Ocotea amazonica</i> (Meiss) Mez	N	-
4	BI II	canela-preta	<i>Ocotea bicolor</i> Vattimo-Gil	N	-
5	BA II	louro-verdadeiro	<i>Ocotea brachybotrya</i> (Meisn.) Mez	Y	19°35'28.0"S 42°34'07.0" W
6	BR II	unknown	<i>Ocotea bragai</i> Coe-Teix.	Y	-
7	CL I	unknown	<i>Ocotea calliscypha</i> L.C.S.Assis & Mello-Silva	Y	20°17'15.0"S 43°30'19.1" W
8	CA I	unknown	<i>Ocotea caesia</i> Mez	Y	-
9	CT II	canela-coqueiro	<i>Ocotea catharinensis</i> Mez	N	-
10	CE II	moena negra	<i>Ocotea cernua</i> (Nees) Mez	N	-
11	CM II	unknown	<i>Ocotea complicata</i> (Meisn.) Mez	N	-
12	CO II	canela-fedida	<i>Ocotea corymbosa</i> (Meisn.)Mez	N	-
13	CJ II	cuchumari	<i>Ocotea cujumary</i> Mart.	N	-
14	DO II	canela-louro	<i>Ocotea diospyrifolia</i> (Meisn.) Mez	N	-
15	DI I	canela-sassafrás	<i>Ocotea dispersa</i> (Nees & Mart.) Mez	Y	-
16	DI II	canela-sassafrás	<i>Ocotea dispersa</i> (Nees & Mart.) Mez	Y	20°52'40.5"S 43°49'01.4" W
17	DV II	canela-segueira	<i>Ocotea divaricata</i> (Nees) Mez	Y	-

(Continue)

Number	Code	Popular name	Specie Name	Endemic? (42)	Geographical location
18	EL II	canela-broto	<i>Ocotea elegans</i> Mez/ <i>Ocotea indecora</i> (Schott) Mez	Y	-
19	FE I	unknown	<i>Ocotea felix</i> Coe-Teix.	Y	-
20	GL I	louro	<i>Ocotea glauca</i> (Nees & Mart.) Mez	Y	20°22'40.0"S 43°24'57.9" W
21	GL II	louro	<i>Ocotea glauca</i> (Nees & Mart.) Mez	Y	-
22	GU II	unknown	<i>Ocotea glaucina</i> (Meisn.) Mez	Y	16°35'47.0"S 42°54'05.0" W
23	GZ II	canela-amarela	<i>Ocotea glaziovii</i> Mez	Y	-
24	GA II	canela-seda	<i>Ocotea guianensis</i> Aubl.	N	-
25	HY I	unknown	<i>Ocotea hypoglauca</i> (Nees & Mart.) Mez	Y	-
26	IN II	canela	<i>Ocotea indecora</i> (Schott) Mez	Y	-
27	KU II	canela-burra	<i>Ocotea kuhlmannii</i> Vattimo-Gi/ <i>Ocotea nectandrifolia</i> Mez	Y	-
28	LA II	unknown	<i>Ocotea lanata</i> (Nees & Mart.) Mez	Y	27°37'49.0"S 49°02'58.0" W
29	LN II	canela-pilosa	<i>Ocotea lanceolata</i> (Nees) Nees/ <i>Ocotea lancifolia</i> (Schott)	N	25°32'52.0"S 54°35'17.1" W
30	LC II	canela-sabão	<i>Ocotea lancifolia</i> (Schott) Mez	N	18°06'54.0"S 43°20'28.0" W
31	LG I	unknown	<i>Ocotea langsdorffii</i> (Meisn.) Mez	Y	-
32	LG II	unknown	<i>Ocotea langsdorffii</i> (Meisn.) Mez	Y	19°15'30.0"S 43°33'04.0" W
33	LX I	canela-pimenta	<i>Ocotea laxa</i> (Nees) Mez	Y	20°17'15.0"S 43°30'19.0" W
34	LX II	canela-pimenta	<i>Ocotea laxa</i> (Nees) Mez	Y	-
35	LO II	unknown	<i>Ocotea lobbii</i> (Meisn.) Rohwer	Y	22°05'21.1"S 43°49'40.0" W
36	LF II	louro-ingá	<i>Ocotea longifolia</i> Kunth	N	-
37	MI II	canela-vassoura	<i>Ocotea minarum</i> (Nees & Mart.) Mez	Y	-
38	NT I	unknown	<i>Ocotea nitidula</i> (Nees et Mart. ex Ness)	Y	-

(Continue)

Number	Code	Popular name	Specie Name	Endemic? (42)	Geographical location
39	NE II	canela-burra	<i>Ocotea nectandrifolia</i> Mez	Y	26°54'36.0"S 50°13'13.0" W
40	NI II	louro	<i>Ocotea nitida</i> (Meisn.) Rohwer	Y	19°50'03.0"S 42°33'07.0" W
41	NO II	louro-pipoca	<i>Ocotea notata</i> (Nees & Mart.) Mez / <i>Ocotea glaucina</i>	Y	10°43'58.0"S 41°19'35.0" W
42	MU I	canelinha	<i>Ocotea nummularia</i> / <i>Ocotea tristis</i>	Y	19°52'47.9"S 43°40'10.9" W
43	NU I	unknown	<i>Ocotea nutans</i> (Nees) Mez	Y	-
44	NU II	unknown	<i>Ocotea nutans</i> (Nees) Mez	Y	20°24'73.0"S 43°26'56.0" W
45	OD II	canela-sassafrás	<i>Ocotea odorifera</i> Vell. Rohwer	Y	-
46	PA II	unknown	<i>Ocotea paranaenses</i> Brotto, Baitello, Cervi & E.P.Santos	Y	25°52'58.0"S 48°34'28.9" W
47	PE I	unknown	<i>Ocotea percoriacea</i> Kosterm.	Y	20°17'15.0"S 43°30'19.0" W
48	PE II	unknown	<i>Ocotea percoriacea</i> Kosterm.	Y	-
49	PO II	canela	<i>Ocotea pomaderroides</i> (Meisn.) Mez	Y	-
50	PO I	canela	<i>Ocotea pomaderroides</i> (Meisn.) Mez	Y	-
51	PR II	imbuia	<i>Ocotea porosa</i> (Nees & Mart.) Barroso	N	-
52	PT II	canela-sassafrás	<i>Ocotea pretiosa</i> (Nees) Mez/ <i>Ocotea odorifera</i> (Vell.)	Y	-
53	PU I	canela-babosa	<i>Ocotea puberula</i> (Rich.) Nees	N	20°17'15.0"S 43°30'19.1" W
54	PU II	canela-babosa	<i>Ocotea puberula</i> (Rich.) Nees	N	-
55	PL II	unknown	<i>Ocotea pulchea</i> Vattimo-Gil	Y	-
56	PC II 1	canela-lageana	<i>Ocotea pulchella</i> (Nees & Mart.) Mez	N	21°55'24.9"S 46°23'09.9" W
57	PC II 2	canela-lageana	<i>Ocotea pulchella</i> (Nees & Mart.) Mez	N	-
58	PH II	canela	<i>Ocotea pulchra</i> Vattimo-Gil	Y	27°21'38.0"S 49°08'13.0" W
59	SP I	canela-baraúna	<i>Ocotea spectabilis</i> (Meisn.) Mez	Y	20°22'40.0"S 43°24'57.9" W

(Conclusion)

Number	Code	Popular name	Specie Name	Endemic? (42)	Geographical location
60	SP II	canela-baraúna	<i>Ocotea spectabilis</i> (Meisn.) Mez	Y	-
61	SX II	canelão	<i>Ocotea spixiana</i> (Nees) Mez	Y	-
62	SX I	canelão	<i>Ocotea spixiana</i> (Nees) Mez	Y	20°17'15.0"S 43°30'19.1" W
63	TA I	unknown	<i>Ocotea tabacifolia</i> (Meisn.) Rohwer	Y	-
64	TA II	unknown	<i>Ocotea tabacifolia</i> (Meisn.) Rohwer	Y	20°07'25.1"S 43°28'13.3" W
65	TL II 1	canela-limão	<i>Ocotea teleiandra</i> (Meisn.) Mez	Y	-
66	TL II 2	canela-limão	<i>Ocotea teleiandra</i> (Meisn.) Mez	Y	-
67	TE II 1	unknown	<i>Ocotea tenuiflora</i> (Nees) Mez	Y	-
68	TR I	canelinha	<i>Ocotea tristis</i> (Nees & Mart.) Mez	Y	20°17'15.0"S 43°30'29.1" W
69	TR II 1	canelinha	<i>Ocotea tristis</i> (Nees & Mart.) Mez	Y	-
70	TR II 2	canelinha	<i>Ocotea tristis</i> (Nees & Mart.) Mez	Y	-
71	VA I	unknown	<i>Ocotea vaccinioides</i> (Meisn.) Mez/ <i>Ocotea daphnifolia</i>	Y	-
72	VA II	unknown	<i>Ocotea vaccinioides</i> (Meisn.) Mez/ <i>Ocotea daphnifolia</i>	Y	21°42'00.0"S 43°53'00.0" W
73	VR I	canela-pilosa	<i>Ocotea variabilis</i> Mart./ <i>Ocotea lancifolia</i> (Schott) Mez	N	-
74	VZ I	canela-verde	<i>Ocotea velloziana</i> (Meisn.) Mez	Y	-
75	VZ II 1	canela-verde	<i>Ocotea velloziana</i> (Meisn.) Mez	Y	-
76	VZ II 2	canela-verde	<i>Ocotea velloziana</i> (Meisn.) Mez	Y	-
77	VL II	canelão-amarelo	<i>Ocotea velutina</i> (Nees) Rohwer	Y	-
78	VI II	unknown	<i>Ocotea villosa</i> Kosterm.	Y	-

Source: From the author.

Table S2 - Vouchers from UFJF and UFOP and the *Ocotea* spp. details II

(Continue)

Code	Date	Location	Related activity
AY II	2005	Serra das Almas - Inácio Pinto, Sítio Gaia da Mata, Rio de Contas, Bahia, Brazil	AChE inhibitor
AU II	2013	Santa Rosa, Ruta Ni6acional 118, Km 72, Concepción, Corrientes, Argentina	Cytotoxic
AM II	1935	Fazenda da cachoeira, Tombos, Minas Gerais, Brazil (Jardim Botânico de Belo Horizonte)	No
BI II	2005	Parque Estadual de Ibitipoca, Floresta no acero do parque, Lima Duarte, Minas Gerais, Brazil	Antioxidant
BA II	2004	Paque estadual do vale do rio doce, Timóteo, Minas Gerais, Brazil (ICB-UFMG)	No
BR II	2001	Parque Estadual da Cantareira, Região das águas, Mariporã, São Paulo, Brazil	No
CL I	1974	Serra do Frazão, Ouro Preto, Minas Gerais, Brazil	No
CA I	2007	Serra de Antônio Pereira, Samarco. Alegria 7, Ouro Preto, Minas Gerais, Brazil	PAF antagonistic
CT II	2002	Torre da Embratel, Estação repetidora da serra do Aleixo, Cajati, SP, Brazil	Inhibition of DNA polymerase
CE II	2003	Morro do Imperador, Juiz de Fora, Brazil	Antimycobacterial
CM II	2003	Rodovia BA-001, Una, Bahia, Brazil (Prefeitura de Curitiba)	No
CO II	2002	Eldorado, Mato Grosso do Sul, Brazil	No
CJ II	2003	APA logoa Silvana, Caratinga, Minas Gerais, Brazil	No
DO II	2004	Mata do Baú, Barroso, Minas Gerais, Brazil	Anti-inflammatory
DI I	1993	Serra do Itacolomi, Ouro Preto, Minas Gerais, Brazil	Antileishmanial and cytotoxic
DI II	1993	Mata do Morro do Redentor, Juiz de Fora, Minas Gerais, Brazil	No
DV II	2003	Reserva Biológica da Represa do Grama, Descoberto, Minas Gerais, Brazil	No
EL II	2001	Estrada para São Mateus, Camanducaia, Minas Gerais, Brazil (ICB-UFMG)	Trypanocidal activity
FE I	1999	Parque Estadual do Itacolomi, Ouro Preto, Minas Gerais, Brazil	No

(Continue)

Code	Date	Location	Related activity
GL I	1971	Santa Rita Durão, Mariana, Minas Gerais, Brazil	No
GL II	1972	Marataizes, Espírito Santo, Brazil	No
GU II	2001	Estrada Grão Mongol-Cristália KM 6, Grão Mongol, Minas Gerais, Brazil (USP)	Cytotoxic
GZ II	2006	Mananciais da Serra, Represa do Carvalinho, FOM/FODM, Piraquara, Paraná, Brazil	Anxiolytic and antiviral
GA II	1997	Margem do Rio Xingú, São Jose do Xingú, Mato Grosso, Brazil	No
HY I	1993	Parque Estadual do Itacolomi, Estrada para a Fazenda do Manso, Ouro Preto, Minas Gerais, Brazil	No
IN II	2001	Reserva Biológica da Represa do Grama, Descoberto, Minas Gerais, Brazil	No
KU II	1979	Ilha de Santa Catarina - Lagoa do Peri, Altitude: 300m., Florianópolis, Santa Catarina, Brazil	Antifungal- <i>Candida sp</i>
LA II	2010	Rancho das Tábuas, Angelina, Paraná, Brazil (FURB)	No
LN II	2009	Parque Nacional do Iguaçu, Foz do Iguaçu, Paraná, Brazil (Prefeitura Municipal de Curitiba)	Antiprotozoal
LC II	2003	Parque do São Gonçalo do Rio Preto, São Gonçalo do Rio Preto, Minas Gerais, Brazil (ICB-UFMG)	Antiprotozoal
LG I	1938	Serra do Cipó Minas Gerais, Brazil	No
LG II	1964	Serra do cipó, Minas Gerais, Brazil	No
LX II	2002	Reserva Biológica da Represa do Grama, Descoberto, Minas Gerais, Brazil	No
LX I	1997	Parque Estadual do Itacolomi, Córrego do Belchior, , Ouro Preto, Minas Gerais, Brazil	No
LO II	2003	Canavieiras, Bahia, Brazil (Prefeitura Municipal de Curitiba)	No
LF II	1992	Alto do Galo, Domingos Martins, Espírito Santo, Brazil	Insecticide
MI II	2003	Fazenda Renascença, Bonito, Mato grosso do Sul, Brazil	Anti-inflammatory
NT I	2008	Indisponível	No
NE II	2010	Anta Branca (antigo Alto Rio do Oeste), Rio do Campo, Santa Catarina, Brazil (FURB)	No

(Continue)

Code	Date	Location	Related activity
NI II	2003	Morro do Gavião, Dionísio, Minas Gerais, Brazil	No
NO II	2010	Fazenda Lucuri, Serra do Curral Frio, Umburanas, Bahia, Brazil	Antiherpetic and atioxidant
MU I	2007	Serra da Piedade, Caeté, Minas Gerais, Brazil	No
NU II	1999	Pacas, Tunas do Paraná, Brazil	Antioxidant
NU I	2009	Brazil, Minas Gerais, Mariana, Parque Estadual do Itacolomi	Antioxidant
OD II	2004	Reserva Biológica da Represa do Grama, Descoberto, Minas Gerais, Brazil	Antifungal and anti-inflammatory
PA II	2011	Morro dos Perdidos, Serra da Araçatuba, Guaratuba, Paraná, Brazil	No
PE I	1998	Cachoeira das Androinhas, Estrada à esquerda, Ouro Preto, Minas Gerais, Brazil	AChE inhibitor
PE II	1942	Jardim Botânico de Belo Horizonte, Belo Horizonte, Brazil	AChE inhibitor
PO II	1940	Jardim Botânico de Belo Horizonte, Belo Horizonte, Brazil	No
PO I	1906	Miguel Burneir, Ouro Preto, Minas Gerais, Brazil	No
PR II	1995	Buraco do Padre, Ponta Grossa, Paraná (Prefeitura Municipal de Curitiba)	Antimicrobial
PT II	1994	Mata do Morro Redentor, Juiz de Fora, Minas Gerais, Brazil	Antiplatelet
PU I	2008	Parque Estadual do Itacolomi, Ouro Preto, Minas Gerais,	Antitumoral
PU II	2001	Rodovia La Caldeira KM 18, La Caldeira, Salta, Argentina (USP)	Antitumoral
PL II	2006	Reserva Biológica Municipal Santa Cândida, Juiz de Fora, Minas Gerais, Brazil	No
PC II 1	2008	Pedra Branca, Pocinhos do Rio Verde, Caldas, Minas Gerais, Brazil	Antiviral
PC II 2	1997	Jardim Botânico Municipal de Bauru, São Paulo, Brazil	Antiviral
PH II	2010	Rio Veado, Nova Trento, Santa Catarina, Brazil	No
NE II	2010	Anta Branca (antigo Alto Rio do Oeste), Rio do Campo, Santa Catarina, Brazil (FURB)	No

(Conclusion)

Code	Date	Location	Related activity
SP II	2004	Caieiras, São Paulo, Brazil (Herbario SPF)	No
SX II	1970	Fernão Dias KM-30, Minas Gerais	Anticolinesterassic
SX I	1994	Parque Estadual do Itacolomi, Estrada para a Fazenda do Manso, Ouro Preto, Minas Gerais, Brazil	Anticolinesterassic
TA I	2007	Serra de Antônio Pereira, Samarco. Alegria 7, Ouro Preto, Minas Gerais, Brazil	No
TA II	2003	Parque Natural do Caraça, Caldas Altas, Minas Gerais, Brazil	No
TL II 1	2001	Reserva Biológica da Represa do Grama, Descoberto, Minas Gerais, Brazil	No
TL II 2	2008	Brazil, Bela Vista, Chacarã Mocotó	No
TE II 1	2001	Brazil, Minas Gerais, Descoberto, Reserva Biológica da Represa do grama	No
TR I	1997	Antônio Pereira, Ouro Preto, Minas Gerais, Brazil	No
TR II 1	2001	Reserva do Ibitipoca (Lagoa seca), Lima Duarte, Minas Gerais, Brazil	No
TR II 2	2014	São Lourenço do funil, Rio Preto, Minas Gerais, Brazil	No
VA I	1977	Rancharia, Ouro Preto, Minas Gerais, Brazil	No
VA II	2004	Reserva do Ibitipoca (Mata do Monjolinho), Lima Duarte, Minas Gerais, Brazil	No
VR I	1967	Estrada de Campo Alegre para Araguaí, Campo Alegre, Minas Gerais, Brazil	Antiprotozoal
VZ I	2000	Camarinhas, Ouro Preto, Minas Gerais, Brazil	Larvicide-Dengue
VZ II 1	2009	Mata do Krambeck, Juiz de Fora, Minas Gerais, Brazil	Larvicide-Dengue
VZ II 2	1985	Reserva Biológica Poço D'anta, Juiz de Fora, Minas Gerais, Brazil	Larvicide-Dengue
VL II	1994	Parque Estadual das Lauraceas, Bocaiúva, Paraná, Brazil	No
VI II	2008	Sítio Malícia, Mata do Krambeck, Juiz de Fora, Minas Gerais, Brazil	No

Source: From the author.

Table S3 - The *Ocotea* spp. extracts yield

CODE	YIELD (%)	CODE	YIELD (%)	CODE	YIELD (%)	CODE	YIELD (%)
AY II	20,0	GU II	8,5	NO II	20,5	TA I	21,5
AU II	18,5	GZ II	13,5	NU I	14,5	TA II	19,5
AM II	10,5	GA II	8,5	NU II	13,9	TE II 1	14,2
BA II	10,5	HY I	14,0	OD II	9,5	TE II 2	14,0
BR II	16,0	IN II	10,0	PA II	13,5	TL II 2	8,0
BI II	13,0	KU II	7,5	PE I	16,0	TR I	13,0
CA I	27,0	LA II	9,5	PE II	18,0	TR II 1	13,5
CL I	9,5	LN II	16,0	PO I	16,0	TR II 2	12,5
CT II	13,5	LC II	9,0	PO II	12,0	VA I	13,5
CJ II	12,5	LC III	14,0	PR II	16,5	VA II	14,0
CE II	15,5	LG I	17,5	PT II	10,5	VR I	11,0
CO II	15,0	LG II	21,5	PU I	18,0	VZI	14
CM II	6,0	LX I	23,5	PU II	21,5	VZ II 2	14,5
DI I	14,5	LX II	21,2	PL II	9,5	VL II	9,0
DI II	16,5	LO II	10,0	PC II 1	29,0	VI II	20,5
DO II	15,5	LF II	11,0	PC II 2	24,6		
DV II	13,5	MI II	7,0	PH II	10,5		
EL II	19,0	MU I	23,0	SP I	5,5		
FE I	14,0	NE II	8,0	SP II	8,5		
GL I	11,0	NI II	21,5	SX I	14,0		
GL II	19,5	NT I	7,5	SX II	13,4		

Source: From the author.

Table S4 - The unknown metabolites of the positive ionisation mode detected with the highest intensity counts (32 metabolites). DC represents a peak area in chromatograms

Component name	Identification status	Observed m/z	Observed RT (min)	Detector counts	Response
Candidate Mass 274.2741	None	274,2741	4,88	1294531	1079845
Candidate Mass 634.4544	None	634,4544	8,26	691877	473980
Candidate Mass 389.1596	None	389,1596	6,1	685163	532549
Candidate Mass 590.4280	None	590,428	8,27	679288	468910
Candidate Mass 593.2766	None	593,2766	9,42	671845	454384
Candidate Mass 678.4809	None	678,4809	8,25	569984	385088
Candidate Mass 546.4016	None	546,4016	8,28	566092	402878
Candidate Mass 579.1715	None	579,1715	2,24	552144	391237
Candidate Mass 579.1714	None	579,1714	2,31	527210	372700
Candidate Mass 318.3001	None	318,3001	4,96	456471	369813
Candidate Mass 722.5070	None	722,507	8,24	418141	276928
Candidate Mass 502.3749	None	502,3749	8,28	339194	251700
Candidate Mass 609.2715	None	609,2715	9,27	303928	203831
Candidate Mass 766.5334	None	766,5334	8,24	277003	178706
Candidate Mass 302.3055	None	302,3055	5,74	245663	200755
Candidate Mass 146.0807	None	146,0807	0,49	241217	223018
Candidate Mass 415.2112	None	415,2112	6,16	235280	174871
Candidate Mass 358.3680	None	358,368	7,2	197443	156157
Candidate Mass 810.5596	None	810,5596	8,23	183922	116233
Candidate Mass 330.3368	None	330,3368	6,51	168393	136154
Candidate Mass 387.1802	None	387,1802	5,44	165722	129757
Candidate Mass 343.1539	None	343,1539	5,19	165705	132688
Candidate Mass 439.1386	None	439,1386	5,52	165632	127205
Candidate Mass 288.2897	None	288,2897	9,32	151245	141002
Candidate Mass 230.2477	None	230,2477	4,92	151000	129305
Candidate Mass 458.3479	None	458,3479	8,28	138824	104228
Candidate Mass 362.3264	None	362,3264	5,03	137880	111259
Candidate Mass 218.2111	None	218,2111	2,93	137230	119131
Candidate Mass 246.2426	None	246,2426	3,96	136077	115423
Candidate Mass 496.3398	None	496,3398	7,32	134650	102820
Candidate Mass 346.3317	None	346,3317	5,8	131267	106019

Source: From the author.

Table S5 - The VIP values > 1.5 referred to the putatively identified metabolites of *Ocotea* spp. in the ESI MS-.

Uvar 4 components R2 0.98, Q2 0.62					Pareto 5 components R2 0.99, Q2 0.55				
Primary ID	VIP[4]	M-H - FM	mDa	I-FIT	Primary ID	VIP[4]	M-H - FM	mDa	I-FIT
425.25740_9.177	3,15447				425.25740_9.177	3,61111			
249.11251_5.146	2,72102	C14H17O4	0.2	0.63	521.20213_2.654	2,26401	C22H29N6O9	0.0	0.61
243.12210_3.146	2,45284				409.23692_9.333	2,20363			
221.11719_4.811	2,36056				243.12270_3.146	2,11769			
409.23692_9.333	1,97743				168.97988_0.515	2,08114			
399.09443_0.500	1,90939				539.21269_2.981	1,96564	C26H36O12	0.3	1.11
833.51001_9.288	1,85719				399.09443_0.500	1,87283			
242.17512_4.355	1,81505				555.22336_2.888	1,79725	C30H35O10	1.3	1.64
431.17034_5.527	1,81066				395.15510_2.315	1,79053	C16H27O11	0.2	0.82
833.51103_9.171	1,78304				875.50350_8.882	1,79015			
605.19342_0.634	1,75026				605.19342_0.634	1,76800			
572.43235_9.391	1,74992				326.13901_2.000	1,73160	C19H20NO4	0.2	0.64
793.51429_9.445	1,74666				591.26175_9.482	1,69929	C35H35N4O5	0.8	0.77
722.47385_9.302	1,74441				722.47385_9.302	1,63278			
815.50005_9.285	1,72281				879.49651_7.765	1,62813	C57H63N6O3	0.2	0.98
579.13572_2.788	1,70810				739.16808_4.188	1,62687			
297.15221_7.592	1,70478				431.17034_5.527	1,62393			
555.57019_8.814	1,70315				669.42259_8.933	1,62230			
369.08393_0.502	1,67400				477.10327_2.851	1,61696			
312.12342_1.751	1,66770	C18H18NO4	0.6	0.36	491.19166_2.732	1,59175			
451.10268_3.180	1,61250				312.12342_1.751	1,58770	C18H18NO4	0.6	0.36
329.23248_4.992	1,60809	C20H29N2O2	1.0	0.01	601.13090_0.585	1,57420			
313.23754_6.332	1,60305				833.51001_9.288	1,57316			
265.19245_7.281	1,59464				597.21895_2.609	1,57291			
529.42643_9.200	1,56079				242.17512_4.355	1,56203			
297.15230_7.424	1,54454				265.19245_7.281	1,54788			
326.13901_2.000	1,53990	C19H20NO4	0.2	0.64	369.08393_0.502	1,54317			
555.65174_8.817	1,53878				551.21315_2.605	1,54148	C30H31N2O8	2.0	1.56
879.49651_7.765	1,53704	C57H63N6O3	0.2	0.98	579.13572_2.788	1,53815			
579.28465_8.150	1,52453				733.41782_8.156	1,53429			
539.21269_2.981	1,52156	C26H36O12	0.3	1.11	959.59681_9.025	1,51825			
521.20213_2.654	1,51611	C22H29N6O9	2.5	0.37	683.22561_0.582	1,51606			

Note - * Coloured in green are the variables positively correlated with the PGE2 inhibition and in red the negatively correlated

Source: From the author.

Table S6 - PBS protocol (pH 7.2; 0.15 M chloride; 0.01 M phosphate)

Reactant	Type	1x	10x
Na ₂ HPO ₄	12 H ₂ O	2,9 g	29 g
	7 H ₂ O	2,17 g	21,7 g
	Anidre	1,136 g	11,36 g
KH ₂ PO ₄		0,27 g	2,7 g
NaCl		8,8 g	88 g
H ₂ O		1 L	1 L

Source: From the author.

Table S7 - The metabolites of the QC MS+ detected with the highest intensity counts dereplicated from the *in-house* database (82 annotated metabolites)

(Continue)

Component name	Expected mass (Da)	Observed <i>m/z</i>	Mass error (mDa)	RT (min)	Detector counts	Adducts	Fragments Found	Alternate assignments
(+)-catechin	290,0790382	291,0853621	-0,952	2,0484	4862,7261	+H	2	Yes
(+)-hydroxycalamenene	218,1670653	219,1731092	-1,232	3,5787	2618,5237	+H	0	No
(+)-spathulenol	220,1827154	221,1884506	-1,541	4,8928	1393,7959	+H	0	Yes
1,2,9,10-Tetrahydroxyaporphine	299,115758	300,121451	-1,583	1,5243	24011,5393	+H	3	No
1-Tetradecanal	212,2140155	235,2041249	0,888	4,7347	4445,9009	+Na	0	No
3,5,7,2',5'-Pentahydroxyflavanone	304,0583027	305,0640879	-1,491	2,1096	1608,1919	+H	1	Yes
3'-hydroxy-N-methyl-(S)-coclaurine	315,1470582	354,1088807	-1,335	3,6026	985,3613	+K	7	No
CAS 66408-19-3	371,1368874	372,1428639	-1,299	2,8579	867,8210	+H	2	No
Afzelin	432,1056469	433,1119409	-0,982	3,1446	833,8945	+H	3	No
Apiol	222,0892089	223,095251	-1,234	4,2287	2314,6326	+H	0	No
Armenin-B	372,1572885	373,163177	-1,387	5,6027	75287,1909	+H, +Na, +K	2	No
Artabonatine B	311,115758	312,1222547	-0,779	1,9385	14361,5463	+H	25	Yes

Asaricin	192,0786442	193,0844546	-1,466	7,3498	28304,1543	+H	1	No
Asarone	208,1099444	231,099549	0,383	5,4787	650,3151	+Na	2	No
Burchellin	340,1310737	341,136712	-1,638	6,0382	1045,2802	+H	0	No
Benzophenone	182,0737457	182,080157	1,250	4,75024	5,945849	+H	6	Yes
Caaverine	267,1259288	268,1318023	-1,402	2,7262	1799,6858	+H	2	Yes
Chaetoquadrin G	358,1416384	359,148376	-0,538	6,4237	1060,9712	+H	0	No
Chalconaringenin 4'-glucoside	434,1212969	435,1277974	-0,776	2,9219	1104,1080	+H	13	No
CinerinC.mol	402,1678532	403,1732479	-1,881	5,6690	2560,6816	+H	3	No
Coclaurine	285,1364935	308,1273155	1,601	3,0149	614,6490	+Na	5	Yes
Corymbosin	358,1052529	359,1108399	-1,689	5,2262	4631,6934	+H	1	No
Dicentrine	339,1470582	340,1533966	-0,937	2,5453	8646,0859	+H	0	Yes
Dicentrinone	335,0793725	336,0862133	-0,435	3,4071	24083,7148	+H	6	No
Didymochlaenone B	356,1259884	357,132767	-0,497	6,1726	7532,6426	+H	0	No
Dihydrotricetin	304,0583027	305,0645034	-1,075	2,0436	1266,3069	+H	2	Yes
Diospiriofoline	325,1314081	326,138036	-0,648	3,1288	23638,8510	+H	17	Yes
Eudesmin	386,1729386	387,178708	-1,506	-3,891	1453,61828	+H	2	Yes

Ferrearin D	358,1780239	359,1841354	-1,164	5,4216	85519,0056	+H, +Na, +K	2	No
Flavinantine	327,1470582	328,1541396	-0,194	1,9408	246086,9848	+H	34	Yes
Galgravin	372,193674	373,2004545	-0,495	6,6489	705,4987	+H	0	Yes
Glaucine	355,1783583	356,1849058	-0,728	2,5293	21090,9506	+H	10	No
Glaziovine	297,1364935	298,142667	-1,102	1,9234	18540,3447	+H	13	Yes
Isolinderanolide A	306,2194948	307,2259244	-0,846	6,9851	4087,6985	+H	0	Yes
Isopiline	297,1364935	298,1430561	-0,713	1,5419	85990,5200	+H	2	Yes
Juziphine	299,1521435	300,1584547	-0,965	2,4189	7696,7729	+H	3	Yes
Kaempferol	286,0477381	287,0544248	-0,589	4,0737	3452,4656	+H	0	No
Kaempferol 3-(2",4"-di-(E)-p-coumarylrhamnoside)	724,1792057	725,1873503	0,868	5,8397	1391,2766	+H	0	Yes
Kaempferol 3-(3",4"-di-p-coumarylrhamnoside)	724,1792057	725,1862148	-0,267	5,3544	11920,3589	+H	11	Yes
Kaempferol 3-(4"-p-coumarylrhamnoside)	578,1424263	579,1508477	1,144	1,8874	11071,5869	+H	4	No
Laudanine	343,1783583	344,1851595	-0,475	1,9774	74386,8047	+H	2	No
Laurelliptine	313,1314081	314,1379947	-0,689	1,9535	37796,4711	+H	21	Yes

Lauroschoitzine	341,1627082	342,168788	-1,196	2,3316	6233,0908	+H	3	Yes
Laurotetanine	327,1470582	328,1538779	-0,456	3,3048	4342,0181	+H	3	Yes
Leucoxylophine	399,1681875	400,1752781	-0,185	3,3807	10601,0430	+H	3	No
Licarin B	324,1361591	325,1427509	-0,684	6,6682	6546,4844	+H	16	No
Lirinidine	281,1415789	282,1474389	-1,416	2,5888	1350,4902	+H	3	Yes
Mesophaeophorbide b	609,2737789	608,2640250	2,459	3,985	11681,5410	+H	1	Yes
Methyl eugenol	178,0993797	179,1052517	-1,404	3,0115	1279,7673	+H	0	No
Miquelianin	478,0747407	479,0816116	-0,405	2,5150	38840,2493	+H	9	No
N-methyisopiline	311,1521435	312,1592196	-0,200	3,2185	63813,4492	+H	7	Yes
Nornantenine	325,1314081	326,1375735	-1,111	2,3449	1312,7330	+H	3	Yes
Nornuciferine	281,1415789	282,1475573	-1,298	2,7999	2327,8655	+H	7	Yes
Nuciferoline	311,1521435	312,1582824	-1,137	2,2150	1712,1952	+H	1	Yes
Ookryptine	355,1419728	356,1485008	-0,748	4,8155	1000,8099	+H	0	No
Ocophyllals A	310,0841236	311,0894261	-1,973	2,3243	595,7560	+H	2	No
Ocoteine	369,1576229	370,1643255	-0,573	3,8553	1573,6250	+H	0	No
Ovigerine	309,100108	310,1062942	-1,090	2,7147	9230,2588	+H	1	No

10-Hydroxy phaeophorbide a	609,2737789	608,2640250	2,459	3,985	11681,5410	+H	1	Yes
Predicentrine	341,1627082	342,1688544	-1,130	2,1144	11237,5049	+H	0	Yes
Preocoteine	371,1732729	372,1796019	-0,947	2,5192	9744,1029	+H	9	No
Pulcheotine A	307,0844579	308,0898384	-1,895	5,3591	692,1141	+H	1	No
Pulchine	311,1521435	312,1588506	-0,569	2,0480	779,8701	+H	12	Yes
Purpureine	385,188923	386,1959729	-0,226	3,6001	8119,4839	+H	12	No
Quercetin 3-O-galactoside	464,0954761	465,1026229	-0,129	2,5090	98794,3438	+H	11	Yes
Quercitrin	448,1005615	449,1071355	-0,702	2,9026	7552,0679	+H	0	No
Reynoutrin	434,0849114	435,0916607	-0,527	2,7063	52421,4473	+H	5	No
Salsoline	193,1102787	194,1157964	-1,758	1,3986	1485,8763	+H	0	No
Sibyllenone	370,1416384	371,1480242	-0,890	6,1721	1122,2012	+H	0	Yes
Sinomenine	329,1627082	330,1691871	-0,797	2,1694	90055,4922	+H	8	Yes
Stephanine	309,1364935	310,142573	-1,196	3,0345	1398,9500	+H	10	No
Tetrandrine	622,3042871	623,3128743	1,310	3,4320	2586,8750	+H	4	No
Thalicminine	365,0899372	366,0967195	-0,494	3,2153	4517,2134	+H	3	No
Thalicminine	365,0899372	366,0967245	-0,489	4,1860	1648,9519	+H	1	No

Component name	Expected mass (Da)	Observed <i>m/z</i>	Mass error (mDa)	RT (min)	Detector counts	Adducts	(Conclusion)	
							Fragments Found	Alternate assignments
Thalictuberine	353,1627082	354,1692633	-0,721	3,0095	3816,6398	+H	10	No
Tuduranine	297,1364935	298,1424965	-1,273	2,1475	14431,6146	+H	9	Yes
Virolongin B	402,2042387	425,1927023	-0,757	7,5399	5202,1453	+Na, +H, +K	2	No
Yangambin	446,1940679	469,1865344	3,245	3,7934	621,0673	+Na	1	Yes
Zenkerine	297,1364935	298,1430663	-0,703	1,5465	3715,6255	+H	8	Yes
β-Sitosterol	414,3861662	437,372568	-2,819	7,3276	580,4230	+Na	0	No

Source: From the author.

Table S8 - The metabolites of the QC MS- detected with the highest intensity counts dereplicated from the *in-house* database (21 annotated metabolites)

(Continue)

Component name	Expected mass (Da)	Observed m/z	Mass error (mDa)	Mass error (ppm)	RT	Detector counts	Adducts	Fragments Found	Common Neutral Losses Found
(+)-catechin	290,0790	289,0705	-1,2561	-4,3453	2,0252	10989,5000	-H	0	None Matched
Afzelin	432,1056	431,0978	-0,6202	-1,4386	3,1519	323573,4600	-H, +HCOO	3	146.05791 (Rhamnose [C6H10O4])
Asarone	208,1099	207,1014	-1,3094	-6,3227	4,8912	13793,1836	-H	0	None Matched
Astilbin	450,1162	449,1078	-1,1812	-2,6301	2,6607	7922,1958	-H	0	None Matched
Caaverine	267,1259	312,1236	-0,5141	-1,6472	1,9065	11473,5488	+HCOO	0	None Matched
Chalconaringenin 4'-glucoside	434,1213	433,1132	-0,8022	-1,8521	2,9489	18959,4531	-H	1	None Matched
Farnesyl acetate	264,2089	309,2061	-1,0576	-3,4203	5,0871	8734,5781	+HCOO	0	None Matched
Juziphine	299,1521	298,1438	-1,0679	-3,5818	1,5875	7342,2852	-H	0	None Matched
Kaempferol	286,0477	285,0386	-1,8573	-6,5160	3,1521	6768,2593	-H	2	None Matched
Kaempferol 3-(2",4"-di-(E)- <i>p</i> -coumarylrhamnoside)	724,1792	723,1731	1,2196	1,6865	5,2861	9809,7656	-H	0	None Matched

(Conclusion)

Component name	Expected mass (Da)	Observed m/z	Mass error (mDa)	Mass error (ppm)	RT	Detector counts	Adducts	Fragments Found	Common Neutral Losses Found
Kaempferol 3-(4"-p-coumarylramnoside)	578,1424	577,1352	0,0913	0,1582	4,5731	7628,4653	-H	1	None Matched
Laurelliptine	313,1314	312,1232	-0,9750	-3,1239	1,8201	17386,7559	-H	1	None Matched
Laurotetanine	327,1471	326,1387	-1,0783	-3,3062	1,9744	12501,0986	-H	3	None Matched
Miquelianin	478,0747	477,0665	-0,9778	-2,0495	2,5416	12034,7012	-H	5	None Matched
Quercimeritrin	464,0955	463,0874	-0,7689	-1,6603	2,5356	356696,1250	-H	6	162.05282 (Glucose [C6H10O5])
Quercitrin	448,1006	447,0923	-1,0136	-2,2671	2,2594	6547,6631	-H	0	None Matched
Reynoutrin	434,0849	433,0768	-0,8716	-2,0125	2,7344	155300,6235	-H	3	162.05282 (Glucose [C6H10O5]), 132.04226 (Pentose [C5H8O4])
Rutin	610,1456	609,1470	1,4386	2,3468	2,4668	348611,1598	-H	3	308.11070 (Rutinoside [C12H20O9])
Stigmasteryl glucoside	574,4233	609,3904	-2,2575	-3,7046	9,1928	52263,15967	+Cl	1	162.05282 (Glucose [C6H10O5])

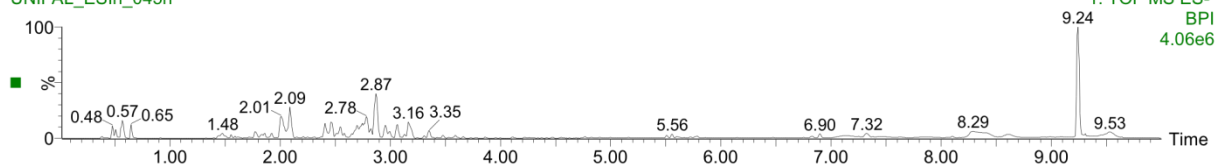
Yangambin	446,1941	491,1914	-0,8857	-1,8032	2,8073	6036,5229	+HCOO	0	132.04226 (Pentose [C5H8O4])
-----------	----------	----------	---------	---------	--------	-----------	-------	---	------------------------------

Source: From the author.

Figure S1 - NU I - *Ocotea nutans* (UFOP), negative mode.

NU I

UNIFAL_ESIn_045n

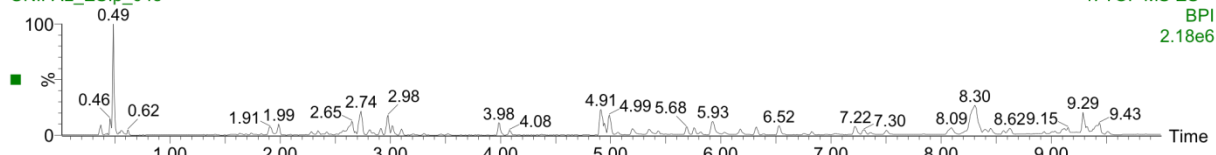


Source: From the author.

Figure S2 - NU I - *Ocotea nutans* (UFOP), positive mode.

NU I

UNIFAL_ESIp_045

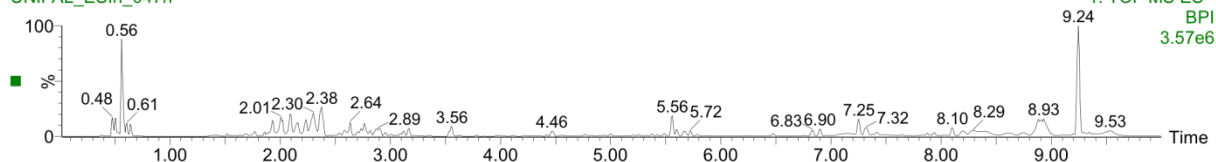


Source: From the author.

Figure S3 - OD II - *Ocotea odorifera* (UFJF), negative mode.

OD II

UNIFAL_ESIn_047n

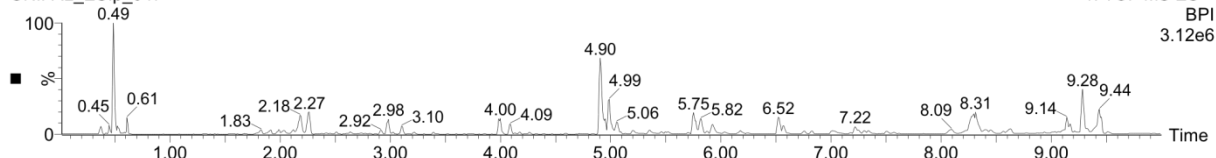


Source: From the author.

Figure S4 - OD II - *Ocotea odorifera* (UFJF), positive mode.

OD II

UNIFAL_ESIp_047

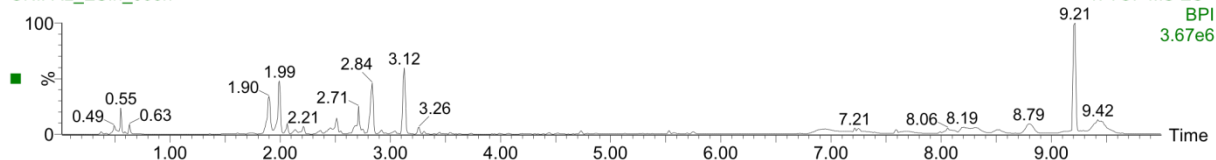


Source: From the author.

Figure S5 - PC II 1- *Ocotea pulchella* (UFJF), negative mode.

PC II 1

UNIFAL_ESIn_058n

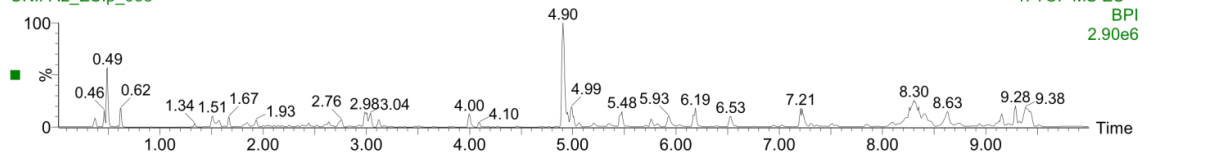


Source: From the author.

Figure S6 - PC II 1- *Ocotea pulchella* (UFJF), positive mode.

PC II 1

UNIFAL_ESIp_058



Source: From the author.

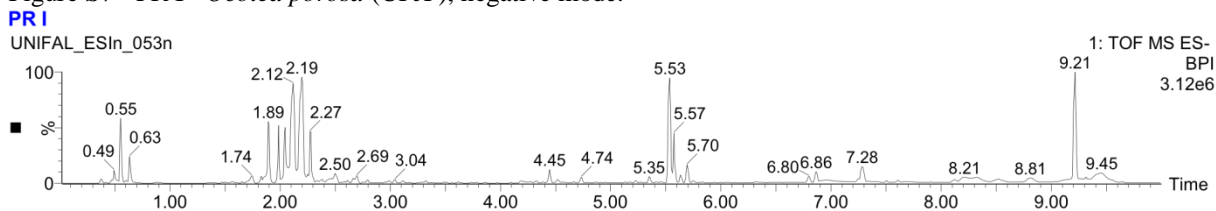
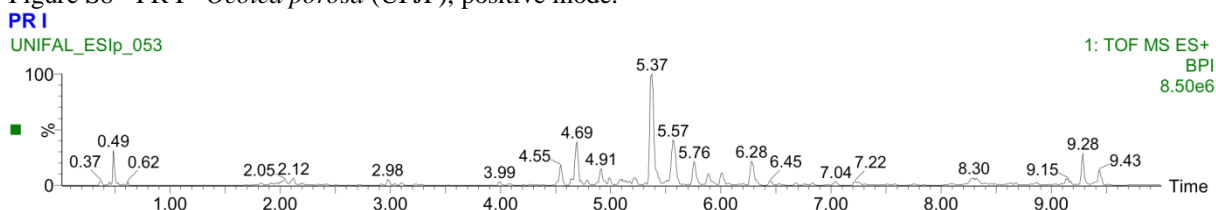
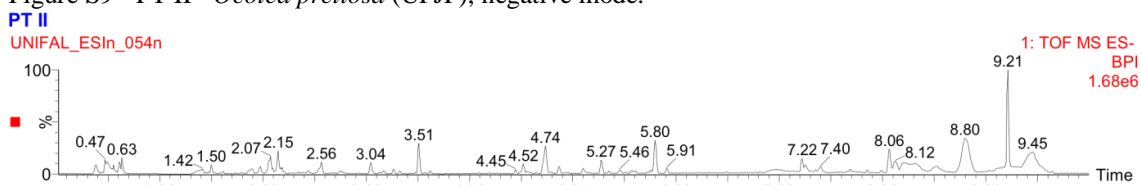
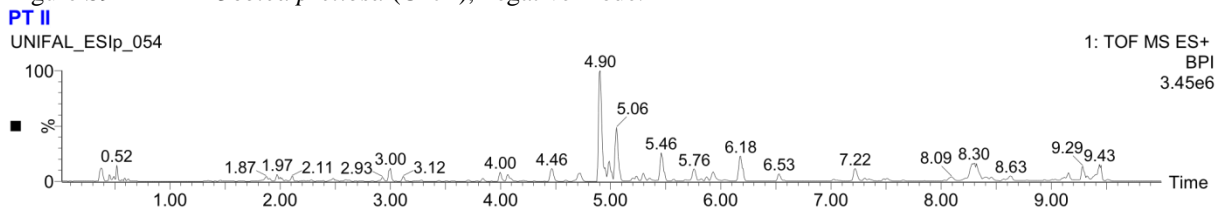
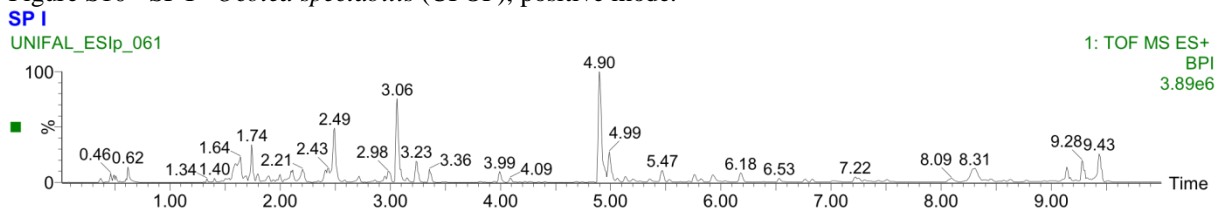
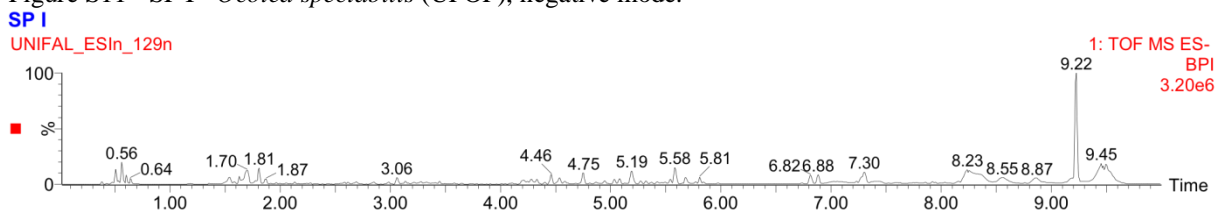
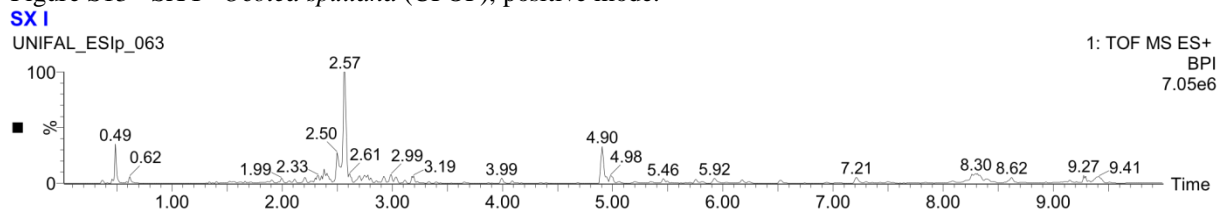
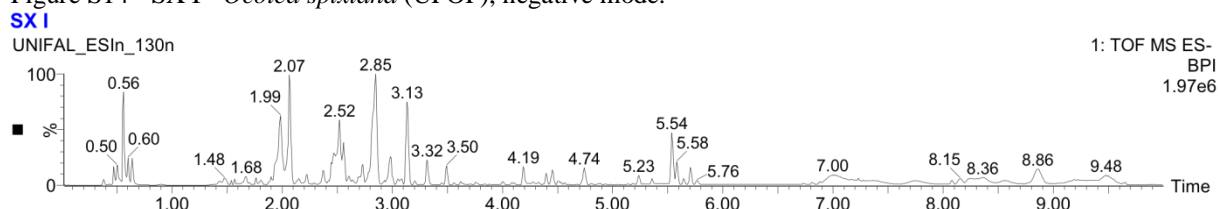
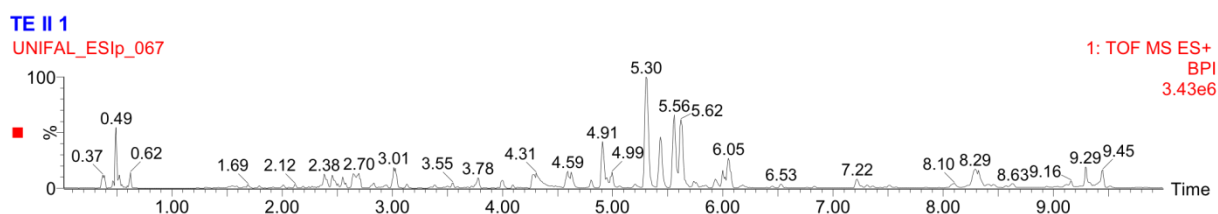
Figure S7 - PR I - *Ocotea porosa* (UFJF), negative mode.Figure S8 - PR I - *Ocotea porosa* (UFJF), positive mode.Figure S9 - PT II - *Ocotea pretiosa* (UFJF), negative mode.Figure S9 - PT II - *Ocotea pretiosa* (UFJF), negative mode.Figure S10 - SP I - *Ocotea spectabilis* (UFOF), positive mode.Figure S11 - SP I - *Ocotea spectabilis* (UFOF), negative mode.

Figure S13 - SX I - *Ocotea spixiana* (UFOP), positive mode.

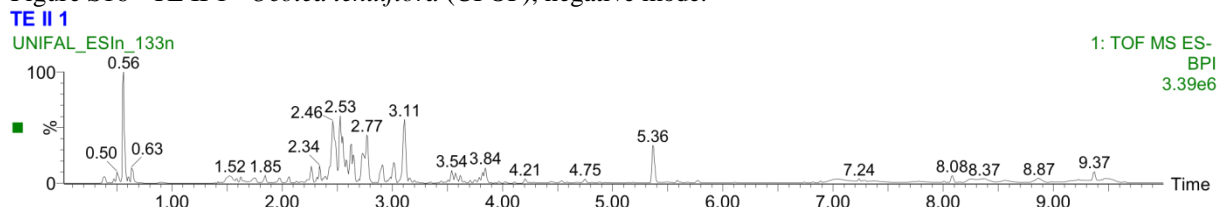
Source: From the author.

Figure S14 - SX I - *Ocotea spixiana* (UFOP), negative mode.

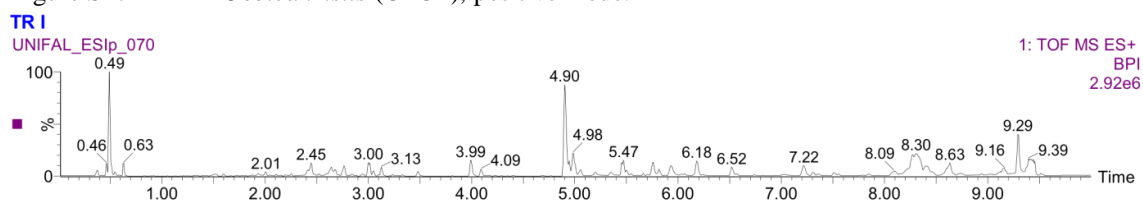
Source: From the author.

Figure S15 - TE II 1 - *Ocotea tenuiflora* (UFOP), positive mode.

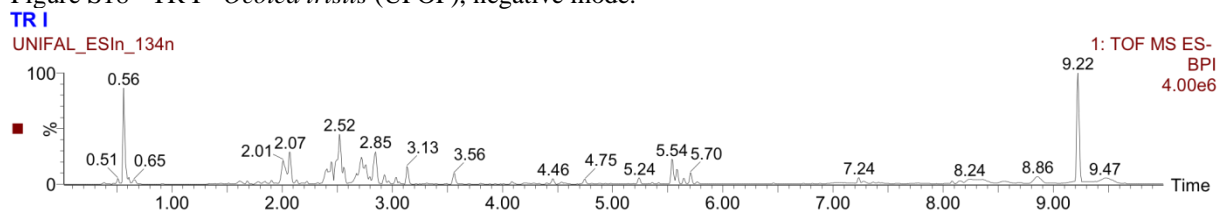
Source: From the author.

Figure S16 - TE II 1 - *Ocotea tenuiflora* (UFOP), negative mode.

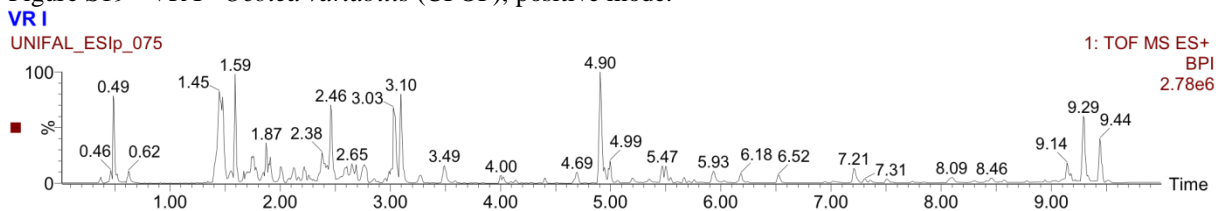
Source: From the author.

Figure S17 - TR I - *Ocotea tristis* (UFOP), positive mode.

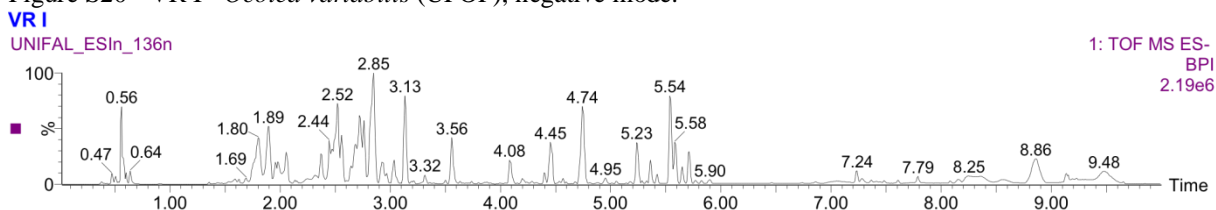
Source: From the author.

Figure S18 - TR I - *Ocotea tristis* (UFOP), negative mode.

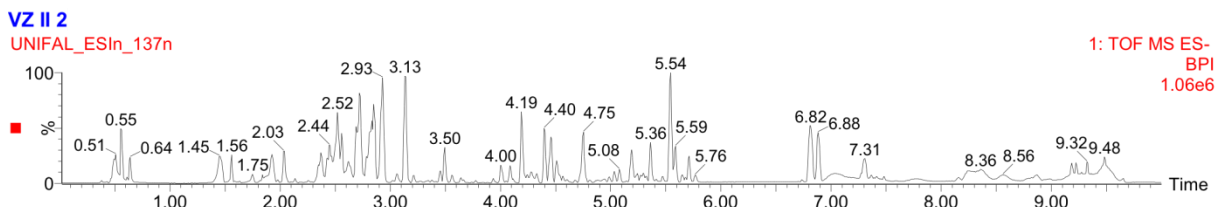
Source: From the author.

Figure S19 - VR I - *Ocotea variabilis* (UFOP), positive mode.

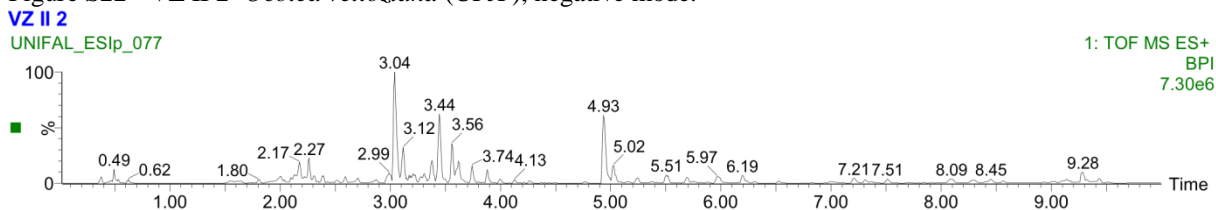
Source: From the author.

Figure S20 - VR I - *Ocotea variabilis* (UFOP), negative mode.

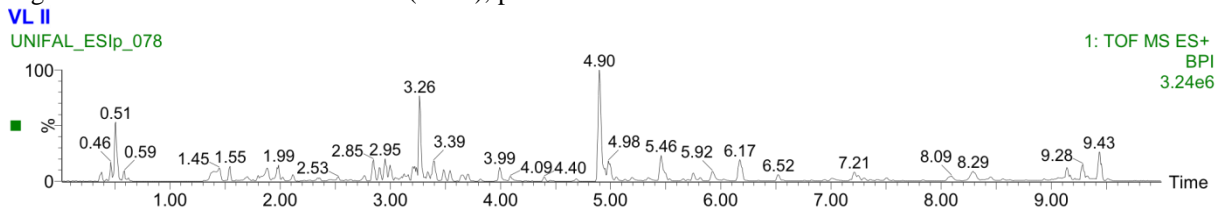
Source: From the author.

Figure S21 - VZ II 2 - *Ocotea velloziana* (UFJF), positive mode.

Source: From the author.

Figure S22 - VZ II 2 - *Ocotea velloziana* (UFJF), negative mode.

Source: From the author.

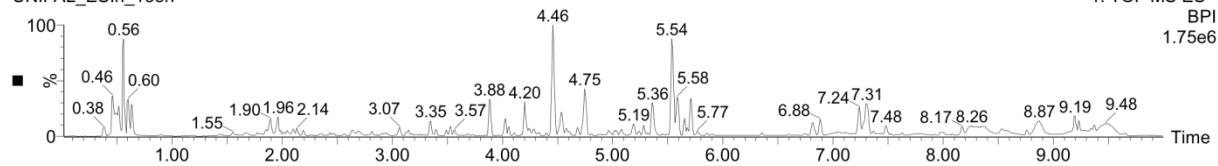
Figure S23 - VL II - *Ocotea velutina* (UFJF), positive mode.

Source: From the author.

Figure S24 - VL II - *Ocotea velutina* (UFJF), negative mode.

VL II

UNIFAL_ESIn_138n

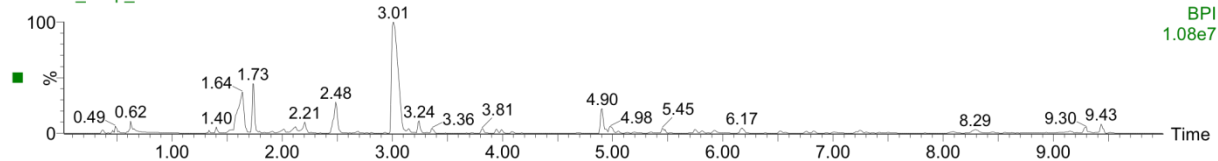


Source: From the author.

Figure S25 - VI II - *Ocotea villosa* (UFJF), positive mode.

VI II

UNIFAL_ESIp_079

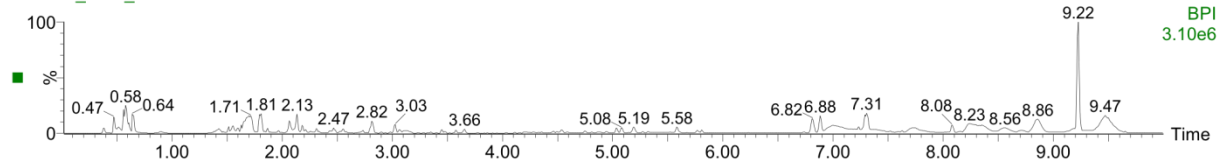


Source: From the author.

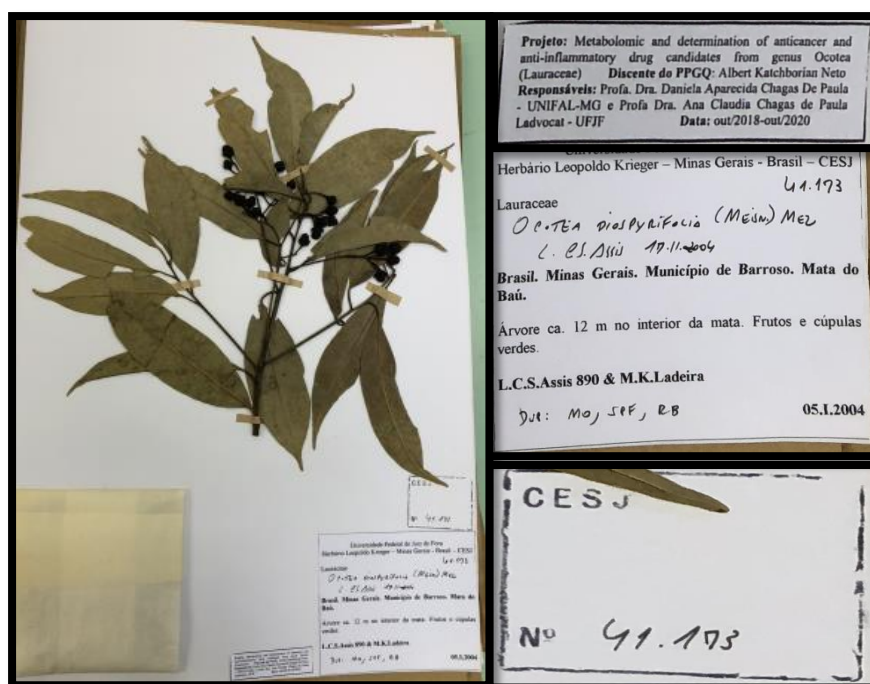
Figure S26 -VI II - *Ocotea villosa* (UFJF), negative mode.

VI II

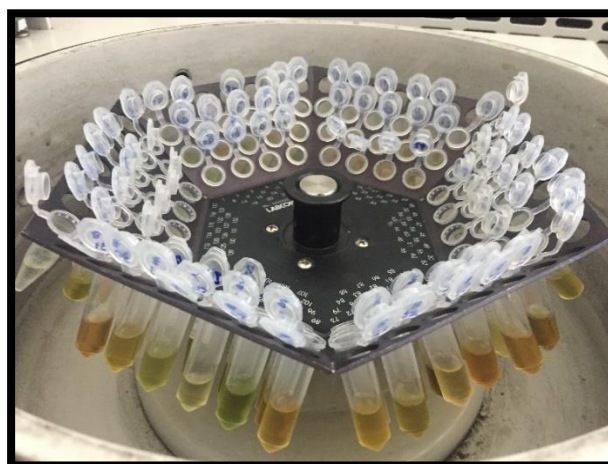
UNIFAL_ESIn_79hn



Source: From the author.

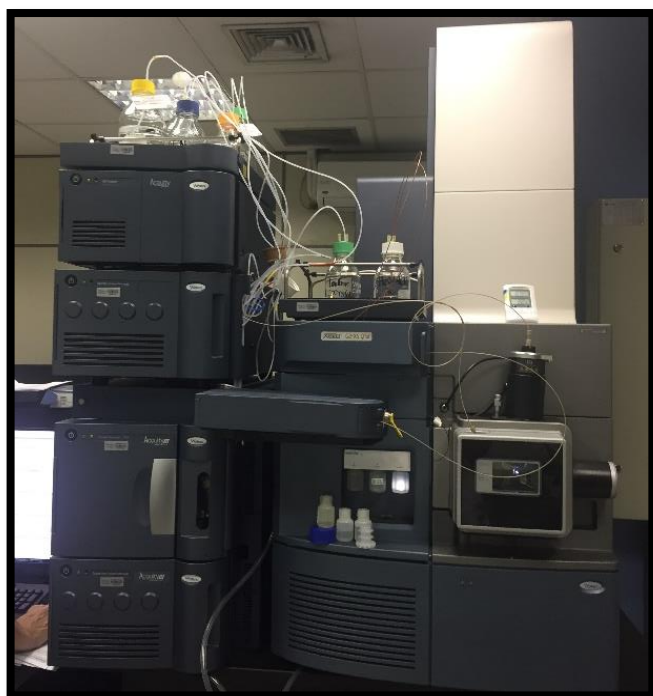
Figure S27 - *Ocotea diospyrifolia*, exsiccate #41173 from CESJ (Herbário Leopoldo Krieger- UFJF).

Source: From the author.

Figure S28 - The *Ocotea* extracts inside the speed vacuum during the drying stage.

Source: From the author.

Figure S29 -Waters mass spectrometer (UHPLC-TOF-MS/MS)



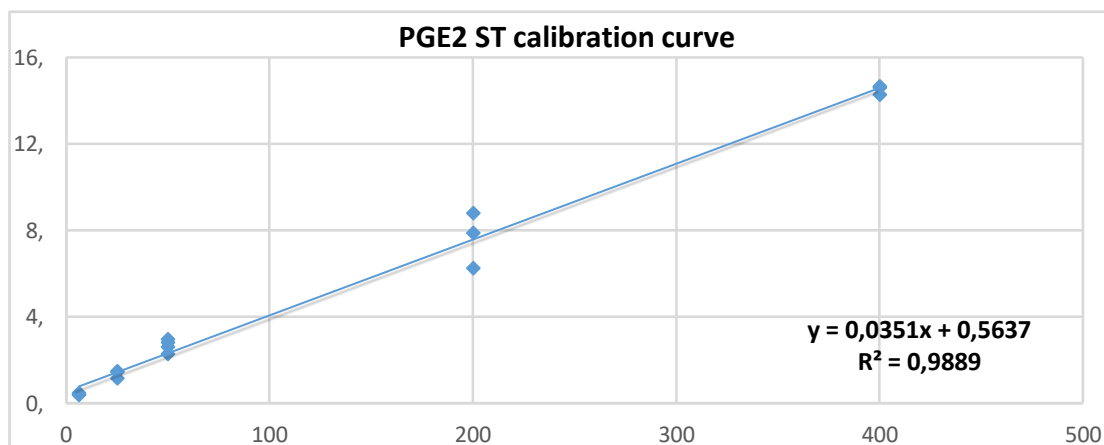
Source: From the author.

Figure S30 - Supelco (LC-18 Solid Phase Extraction -SPE 500mg, #57012).



Source: From the author.

Graph S1 - Calibration curve and equation of PGE2 quantification



Source: From the author.